

PEOPLE'S DEMOCRATIC REPUBLIC OF ALGERIA
MINISTRY OF HIGHER EDUCATION AND SCIENTIFIC RESEARCH
MOHAMED BOUDIAF UNIVERSITY - M'SILA

FACULTY OF TECHNOLOGY
DEPARTMENT OF ELECTRICAL ENGINEERING
N°:



FIELD: ELECTRICAL ENGINEERING
SECTOR: RENEWABLE ENERGIES
OPTION: GREEN HYDROGEN ENERGY
VECTOR

Thesis presented for obtaining
Academic Master's degree

By:

DJAIDJA NAZIH & CHEBLI SABER AYOUB

Titled by:

**Optimizing Green Hydrogen Production Using
MPPT Algorithms in a PV System**

Defended in front of the jury composed of:

First and last Name	Establishment	Quality
Dr.Salim DJERIOU	University of M'sila	President
Dr.Abderrahim ZEMMIT	University of M'sila	Supervisor
Dr.Abdeloudoud LOUKRIZ	Université STHB	Co-supervisor
Dr.Abdelghafour HERIZI	University of M'sila	Examiner
Dr.Mohamed Lakhdar NEBBAR	University of M'sila	Examiner

Academic year: 2024/ 2025

Acknowledgments

We are grateful to Allah for blessing us with good health and the strength to successfully accomplish this work.

Our sincere thanks go to Professor Pr. Abderrahim ZEMMOT for proposing an engaging master's topic and offering valuable guidance. We deeply appreciate Mr. Dr.

Abdelouadoud Loukriz for his insightful advice, shared knowledge, and unwavering support throughout this project. We also recognize the invaluable contributions of all the teachers who have shaped our academic journey. Finally, we express our heartfelt gratitude to our families, friends, and colleagues for their constant encouragement and support.

Dedications

We dedicate this master's thesis to our beloved family—our parents, grandparents, and dear friends—for their unwavering support throughout our academic journey. Their steadfast belief in us, their presence during challenging times, and their encouragement to pursue our dreams have been invaluable. This achievement is a testament to their love and dedication, which have been the driving force behind our success. We are endlessly grateful to have them in our lives.

[Nazih & Saber]

Table of contents

Table of Contents

GENERAL INTRODUCTION:	1
I.1 INTRODUCTION:	4
I.2 HISTORY OF HYDROGEN PRODUCTION:	4
I.3 TYPES OF HYDROGEN PRODUCTION METHODS:	5
I.3.1 Fossil Fuel-Based Methods:	5
I.3.1.1 Steam Methane Reforming (SMR):	5
I.3.1.2 Gasification:	5
I.3.1.3 Partial Oxidation (POX):	6
I.3.2 Electrolysis-Based Hydrogen Production:	6
I.3.2.1 Alkaline Electrolysis (AEL) :	6
I.3.2.2 Proton Exchange Membrane Electrolysis (PEM):	7
I.3.2.3 Solid Oxide Electrolysis (SOE):	8
I.4 INTRODUCTION TO GREEN HYDROGEN:	8
I.4.1 The Green Hydrogen:	8
I.4.2 Why Green Hydrogen:	9
I.4.3 Renewable Energy Sources for Green Hydrogen Production:	9
I.5 GREEN HYDROGEN PRODUCTION VIA ALKALINE ELECTROLYSIS POWERED BY SOLAR PV:	10
I.5.1 Solar PV System:	10
I.5.2 Control and Optimization:	10
I.5.3 Alkaline Electrolysis:	10
I.5.4 Hydrogen Storage and Utilization:	10
I.5.5 Alkaline Electrolysis Powered by Solar PV: A Controlled and Optimized System:	10
I.5.6 Role of MPPT Algorithm:	10
I.6 CONCLUSION:	11
II.1 INTRODUCTION:	13
II.2 PV SYSTEM:	13
II.2.1 Overview of PV System Operation:	13
II.2.2 Factors Affecting PV Performance:	14
II.2.3 PV System Output and Efficiency:	14

Table of contents

II.3 CONTROL ALGORITHM (MPPT):	15
II.3.1 Introduction to MPPT Algorithms:	15
II.2.3 Types of MPPT Algorithms:	16
II.2.3.1 Perturb and Observe (P&O):	16
II.3.2.2 Incremental Conductance (IC):	16
II.3.2.3 Artificial Neural Networks (ANN) MPPT:	17
II.3.2.4 Fuzzy Logic Control (FLC):	19
II.3.3 Role of MPPT in Hydrogen Production:	20
II.4 ALKALINE ELECTROLYZER:	20
II.4.1 Overview of Alkaline Electrolyzer:	20
II.4.2 Mathematical Modeling of Electrolyzer Performance:	21
II.5 LINK BETWEEN PV SYSTEM AND HYDROGEN PRODUCTION:	24
I.6 CONCLUSION:	24
III.1.INTRODUCTION:	26
III.2 SIMULATION OF PV SYSTEM :	26
III.2.1 PV Array Modeling:	26
III.2.1.1 Adding the PV Array:	26
III.2.1.2 Inputs to the PV Array:	26
III.2.1.3 Outputs of the PV Array:	27
III.2.1.4 Effect of Irradiance and Temperature:	27
III.2.2 Boost Converter Modeling:	27
III.2.3 MPPT: Perturb and Observe Method:	29
III.2.3.1 P&O Work:	29
III.2.3.2 Advantages of Using P&O in Green Hydrogen Production:	29
III.2.3.3 Challenges and Considerations:	29
III.2.3.4 Interaction of components :	30
III.2.4 Simulation in MATLAB/Simulink:	30
III.2.5 The MPPT control algorithm work:	32
III.3 SIMULATION OF ALKALINE ELECTROLYZER:	35
III.3.1 Hydrogen Production & Faraday Efficiency:	35

Table of contents

III.3.2 Simulation Approach:	36
III.3.3 Simulation Model:	37
III.3.4 Example to see the effects of irradiance and current on the hydrogen production:	38
III.4 CONCLUSION:	39
IV.1 INTRODUCTION:	41
IV.2 THE PARTIAL SHADING:	41
IV.2.1 How Partial Shading Happen:	41
IV.2.2 Effects of Partial Shading on the PV System:	42
IV.2.3 How to Simulate Partial Shading:	43
IV.3 SYSTEM CONFIGURATION:	44
IV.3.1 Power Curve Characteristics:	44
IV.3.2 Current-Voltage (I-V) Curve Behavior:	44
IV.3.3 Why Use Controlled Voltage Source with Ramp:	45
IV.3.4 Effects of Partial Shading on MPP Points:	47
IV.4 MPPT ALGORITHMS FOR PARTIAL SHADING CONDITIONS:	47
IV.4.1 Conventional MPPT Methods (Struggle with Partial Shading):	47
IV.4.2 Intelligent MPPT Algorithms (For Global MPP Tracking - GMPP):	48
IV.4.3 Using Intelligent Algorithms:	48
IV.4.4 The Reason of the failure P&O Under Partial Shading:	48
IV.4.5 P&O Power Output Characteristics:	49
IV.5 ELECTROLYZER IMPACT FROM P&O LIMITATIONS:	50
IV.6 CUCKOO SEARCH MPPT ALGORITHM FOR PV SYSTEMS UNDER PARTIAL SHADING:	51
IV.6.1 the Cuckoo Search Algorithm:	51
IV.6.2 Working Principle of the Cuckoo Search Algorithm:	52
IV.6.3 General Equations in Cuckoo Search Algorithm:	52
IV.6.4 Cuckoo Search Algorithm for PV System Optimization (Duty Cycle Control):	53
IV.6.4.1 Cuckoo Search Equations for Duty Cycle Optimization:	53
IV.6.5 How Cuckoo Search is Used for MPPT in PV Systems under Partial Shading:	54
IV.6.5.1 Advantages of Cuckoo Search for MPPT in Partial Shading:	54
IV.6.5.2 Key Steps & Working Principle:	55

Table of contents

IV.6.5.3 THE PURPOSE OF THESE VARIABLES IN THE SYSTEM :	55
IV.6.5.4 How to fit these variables into the cuckoo search algorithm:	56
IV.6.6 LEVY FLIGHT FUNCTION :	56
IV.6.7 Whole system:	57
IV.7 INTRODUCTION TO THE FDB-TLABC ALGORITHM FOR PV SYSTEMS UNDER PARTIAL SHADING :	62
IV.7.1 Teaching-Learning-based optimization (TLBO) in general use case:	63
IV.7.2 Artificial Bee Colony (ABC) Algorithm in general use case:	64
IV.7.3 the FDB-TLABC Algorithm:	65
IV.7.4 Artificial Bee Colony (ABC):	65
IV.7.4 Fitness-Distance Balance (FDB):	65
IV.7.6 How FDB-TLABC Algorithm Works in PV Systems for MPPT:	65
IV.7.7 Whole system:	66
IV.7.8 Fitness-Distance Balance (FDB) in the Algorithm:	68
IV.7.9 Key Steps & Working Principle:	69
IV.7.10 Outputs of the system (power current hydrogen production rate N_{H_2}):	69
IV.8 COMPARISON OF THE OUTPUTS OF THE THREE MPPT ALGORITHMS IN THE PV SYSTEM UNDER PSC:	71
IV.9 COMPARISON OF P&O, CUCKOO SEARCH, AND FDBTLABC FOR POWER CURRENT OUTPUTS & HYDROGEN PRODUCTION:	74
IV.10 CONCLUSION :	74
GENERAL CONCLUSION:	76
PERSPECTIVE:	77
BIBLIOGRAPHIC REFERENCES:	78
: ملخص	82
ABSTRACT:	82
RESUME :	83
THE ANNEXES:	84

List of Figures

List of figures:

Figure I.1 : the alkaline electrolyser diagram and operation chemical equations	7
Figure I.2 :the PEM electrolyser diagram and operation chemical equations	7
Figure I.3 :the SOE electrolyser diagram and operation chemical equations	8
Figure II.1 :The structure of the operation steps of the po algorithm	16
Figure II.2 :The structure of the operation steps of the IC algorithm.....	17
Figure II.3 :the structure of the pv system using ANN algorithm	18
Figure II.4 :the structure of the pv system using FLC algorithm	19
Figure II.5 :the alkaline electrolyser diagram.....	20
Figure II.6 :diagram showcasing the relation between the pv system voltage and current and the electrolyser system performance.....	22
Figure III.1 :The pv boost converter system simulation.....	30
Figure III.2 :the input boost converter voltage (from the pv system)	31
Figure III.3 :the output boost converter voltage	31
Figure III.4 :the output boost converter current	32
Figure III.5 :The effects of the po algorithm in the p-v curve (changing of power from changing the voltage	32
Figure III.6 :The MATLAB function script of the po algorithm.....	33
Figure III.7 :The whole MATLAB simulated p-v system mppt model	34
Figure III.8 :The pv system outputs(P, V) at 1000w/m2	34
Figure III.9 :The pv system outputs (P, V) when changing irradiance from 1000w/m2 to 500w/m2.....	35
figures III.10 :the simulation of the alkaline electrolyser system performance (n-h2 / n-f)	37
Figure III.11 :The whole MATLAB Simulink pv-electrolyser system simulation model.....	37
Figure III.12 : The faraday efficiency and hydrogen production rate Graph	38
Figure III.13 : Current at irradiance at 1000w/m2 vs 500w/m2.....	38
Figure III.14 : nh2 at irradiance at 1000w/m2 vs 500 w/m2	39
Figure IV.1 :the effects of partial shading on a pv system current and the job of bypass diodes.....	42
Figure IV.2 :the i-v / p-v curve showcasing the multiple power peaks effects due the PS	42
Figure IV.3 : the I-V curve showcasing the effects of full shading compared to partial shading the pv in series systems voltage and current	43
Figure IV.4 :the Simulation of a 3 identical panels in series pv system under partial shading	44
Figure IV.5 :Power output with multiple peaks under PSC.....	45
Figure IV.6 :Voltage output under PSC	45
Figure IV.7 :current output under PSC	45

List of Figures

Figure IV.8 :Simulation of a 3 panels in series in parallel with two identical 3 in series systems pv system under partial shading	46
Figure IV.9 :Power output with multiple peaks under PSC.....	46
Figure IV.10 :Voltage output under PSC	46
Figure IV.11 :current output under PSC	47
Figure IV.12 :the Whole pv-electrolyser system simulation with the pv system under partial shading using po mppt algorithm	48
Figure IV.13 :Simulation of a pv system under partial shading with a GMPP power of 400w we want to reach	49
Figure IV.14 :The po mppt pv system Power output.....	49
Figure IV.15 :The po mppt pv system current output.....	50
Figure IV.16 :The po mppt pv system n _{h2} output	50
figure IV.17 :The po mppt pv system n _F output	51
Figure IV.18 :The natural working of the cuckoo search algorithm.....	51
Figure IV.19 :The structure of the cuckoo search algorithm	52
Figure IV.20 :the levy flight equation in the cuckoo mppt algorithm	56
Figure IV.21 :the Whole pv-electrolyser system simulation with the pv system under partial shading using cuckoo search mppt algorithm.....	57
Figure IV.22 :The pv system with 3 identical panels one under partial shading with a lower irradiance compared to the other two with the whole system GMPP of 400w	57
Figure IV.23 :The simulation model of the boost converter.....	58
Figure IV.24 :The simulation model of the cuckoo search MPPT algorithm MATLAB function.....	58
Figure IV.25 :The whole MATLAB function script of the cuckoo search algorithm.....	59
Figure IV.26 :the CS optimized DUTY CYCLE output.....	60
Figure IV.27 :The Output power value converges near the 400w GMPP of the pv system under partial shading.....	60
Figure IV.28 :The Output faraday efficiency n-F of the electrolyser system	61
Figure IV.29 :The CS output Current	61
Figure IV.30 :The CS output hydrogen production rate	62
Figure IV.31 :The general structure of the TLBO algorithm in simulation.....	63
Figure IV.32 :The general structure of the TLBO algorithm in real life	63
Figure IV.33 :The natural behavior and flow chart of the artificial bee algorithm.....	64
Figure IV.34 :the Whole simulated pv-electrolyser system when using FDB-TLABC algorithm under partial shading	66

List of Figures

Figure IV.35 :The FDB_TLABC algorithm mppt script	67
Figure IV.36 :The FDB-TLABC output current of around 2.8 A.....	70
Figure IV.37 :The FDB-TLABC output power near the GMPP of the 400w.....	70
Figure IV.38 :the FDB-TLABC Hydrogen production rate n_h2 same value as CS algorithm.....	70
Figure IV.39 :The FDB-TLABC output value of N_F	71
Figure IV.40 : output power comparison	72
Figure IV.41 : output n_h2 comparison	72
Figure IV.42 : output current comparison.....	72
Figure IV.43 : output n_F comparison.....	73
Figure IV.44 :Table comparing the three algorithms in the pv-electrolyser system under partial shading	73

General Introduction:

The escalating challenges of climate change, environmental degradation, and energy insecurity have intensified the global pursuit of sustainable and renewable energy solutions. In this evolving energy landscape, hydrogen has emerged as a critical vector for decarbonization. Its versatility allows it to play a transformative role in power generation, transportation, industrial processes, and long-term energy storage. Unlike conventional fuels, hydrogen can be used in fuel cells or combustion engines to generate electricity without direct carbon dioxide (CO₂) emissions, making it a clean and promising energy carrier [1].

Despite its potential, current global hydrogen production remains heavily dependent on fossil fuels, with over 95% derived from carbon-intensive processes such as steam methane reforming (SMR), coal gasification, and partial oxidation [2][3]. These methods not only emit significant greenhouse gases but also perpetuate fossil fuel reliance. In response to growing environmental regulations and decarbonization targets, there is a pressing shift toward green hydrogen—produced through water electrolysis powered by renewable energy sources.

Green hydrogen, generated via electrolysis using solar, wind, or hydroelectric power, offers a zero-emission alternative with immense environmental and strategic benefits [4]. Among renewable sources, solar photovoltaic (PV) systems are particularly attractive due to their scalability, decreasing costs, and technical maturity. Countries with abundant solar resources, such as Algeria—which receives over 2000 kWh/m²/year of solar irradiation in southern regions—are uniquely positioned to capitalize on solar-powered hydrogen production [5]. This not only aids in meeting global carbon neutrality goals but also promotes national energy independence, industrial growth, and job creation.

However, the inherent intermittency of solar energy poses a major challenge. Variations in irradiance, temperature fluctuations, and partial shading can significantly impact PV output. Electrolyzers, especially alkaline types commonly used due to their cost-effectiveness and industrial maturity, require consistent power input for stable and efficient hydrogen production. Fluctuations in input power can degrade electrolyzer efficiency, reduce system lifespan, and lower hydrogen output [6].

General Introduction

To mitigate these issues, Maximum Power Point Tracking (MPPT) algorithms are employed in PV systems to ensure maximum energy extraction under dynamic environmental conditions. Traditional MPPT techniques like Perturb and Observe (P&O) and Incremental Conductance (IC) are widely used for their simplicity and real-time tracking capability . However, these methods often struggle under complex conditions such as partial shading, frequently locking onto local maxima instead of the global maximum power point (MPP), thereby limiting system performance .

In recent years, intelligent and metaheuristic MPPT algorithms have gained attention for their robustness and adaptability. Algorithms such as Cuckoo Search, Particle Swarm Optimization (PSO), and FDB-TLABC (Fitness-Distance Balance – Teaching-Learning-Based Artificial Bee Colony) have demonstrated superior tracking performance under non-linear and rapidly changing conditions . These nature-inspired methods offer higher convergence accuracy and improved energy harvesting, enhancing the overall efficiency of the PV-electrolyzer system.

This study focuses on modeling, simulating, and optimizing a PV–alkaline electrolyzer system using MATLAB/Simulink. The model includes a PV array, DC-DC boost converter, MPPT controller, and electrolyzer unit. Performance metrics such as PV output stability, electrolyzer input characteristics, Faraday efficiency (η_F), and hydrogen production rate (n_{H_2}) are analyzed. Simulation results show that advanced MPPT techniques, particularly Cuckoo Search and FDB-TLABC, can enhance hydrogen production by over 25% compared to conventional P&O methods under partial shading, while maintaining Faraday efficiencies above 90% .

In summary, this research provides a technical and analytical framework for integrating intelligent control strategies into green hydrogen production systems. It reinforces the viability of using Algeria’s solar potential to develop sustainable hydrogen infrastructure and supports global decarbonization efforts through innovative energy solutions.

Chapter I

The Art of Green Hydrogen Production

I.1 Introduction:

We explore in this chapter Hydrogen, the most abundant element in the universe, has long been a cornerstone of industrial and energy systems. Its journey from early scientific discovery to modern production methods reflects humanity's quest for cleaner energy solutions.

This chapter explores the history of hydrogen production, tracing its evolution from simple laboratory experiments to large-scale industrial processes. We then examine the key production methods :

Steam Methane Reforming (SMR) – The dominant method today, extracting hydrogen from natural gas.

Gasification & Partial Oxidation (POX) – Converting coal or biomass into hydrogen.

Electrolysis – Using electricity to split water, a pathway gaining momentum.

Finally, we focus on green hydrogen—the sustainable future of hydrogen production. By harnessing renewable energy (solar, wind, hydro) to power electrolyzers, we can produce hydrogen with near-zero emissions. This section highlights the technology, benefits, and potential of green hydrogen in the global energy transition.

I.2 HISTORY OF HYDROGEN PRODUCTION:

Hydrogen has received increased attention as an environmentally friendly option to help meet today's energy needs. The road leading to an understanding of hydrogen's energy potential presents a fascinating tour through scientific discovery and industrial ingenuity[7].

→ **Early Discoveries and Uses (1766-1800):**

Hydrogen was first identified by Henry Cavendish in 1766, who called it "flammable air."

Antoine Lavoisier later named it "hydrogen" (water-former) after demonstrating its role in water formation.

→ **Industrial Revolution and Early Applications (1800-1900):**

Hydrogen gained industrial importance as a lifting gas for airships and balloons in the 19th century.

It was also used in early lighting systems and as a chemical feedstock for ammonia production.

→ **Fossil Fuel Era (1900-2000):**

Steam Methane Reforming (SMR) emerged as the dominant method for hydrogen production, leveraging natural gas.

Hydrogen became critical in refining, fertilizer production, and the space race (e.g., rocket fuel).

→ **Shift Toward Sustainability (2000-Present):**

Growing environmental concerns led to research into cleaner hydrogen production methods.

Electrolysis powered by renewables gained traction, marking the beginning of the green hydrogen era [8].

I.3 Types of Hydrogen Production Methods:

I.3.1 Fossil Fuel-Based Methods:

I.3.1.1 Steam Methane Reforming (SMR):

→ **How It Work:**

Natural gas (methane) is reacted with high-temperature steam (700–1000°C) in the presence of a catalyst. The process produces syngas (a mix of hydrogen and carbon monoxide).

A secondary water-gas shift reaction converts CO into additional hydrogen and CO₂.

→ **Chemical Equations:**

Primary Reaction: $\text{CH}_4 + \text{H}_2\text{O} \rightarrow \text{CO} + 3\text{H}_2$

Water-Gas Shift: $\text{CO} + \text{H}_2\text{O} \rightarrow \text{CO}_2 + \text{H}_2$

→ **Benefits:**

High efficiency and large-scale hydrogen production.

Well-established and cost-effective technology.

→ **Negatives:**

High CO₂ emissions, contributing to climate change.

Relies on non-renewable natural gas[10][11].

I.3.1.2 Gasification:

→ **How It Works:**

Carbon-rich materials (coal, biomass, or waste) are heated with limited oxygen to produce syngas (H₂, CO, CO₂).

The syngas is then purified, and hydrogen is separated through additional processes like the water-gas shift reaction.

→ **Chemical Equations:**

Coal Gasification: $\text{C} + \text{H}_2\text{O} \rightarrow \text{CO} + \text{H}_2$

Water-Gas Shift: $\text{CO} + \text{H}_2\text{O} \rightarrow \text{CO}_2 + \text{H}_2$

→ **Benefits:**

Can use low-cost feedstocks like coal or biomass.

Potential for partial sustainability with biomass.

→ **Negatives:**

High CO₂ emissions, especially with coal.

Complex and energy-intensive process[10][11].

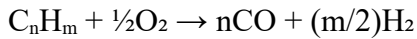
I.3.1.3 Partial Oxidation (POX):

→ **How It Works:**

Hydrocarbons (e.g., heavy oils or natural gas) are reacted with limited oxygen to produce syngas (H₂, CO, and CO₂).

The process is exothermic, meaning it releases heat, which can be utilized for other industrial processes.

→ **Chemical Equation:**



→ **Benefits:**

Suitable for heavy feedstocks like crude oil or refinery residues.

Can operate at high temperatures without requiring external heat.

→ **Negatives:**

Lower efficiency compared to SMR.

Produces CO₂ and other pollutants[9][10].

I.3.2 Electrolysis-Based Hydrogen Production:

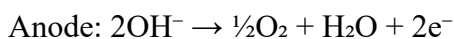
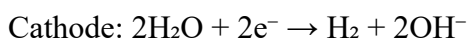
I.3.2.1 Alkaline Electrolysis (AEL) :

→ **How It Works:**

Uses an alkaline solution (e.g., potassium hydroxide) as the electrolyte.

Water is split into hydrogen and oxygen at two electrodes (cathode and anode).

→ **Chemical Equations:**



→ **Benefits:**

Mature and well-established technology.

Lower cost compared to other electrolysis methods.

Long operational lifespan.

→ **Negatives:**

Lower efficiency (60–70%).

Slow response to variable energy inputs (e.g., renewables).

Requires corrosive electrolytes, increasing maintenance needs[11].

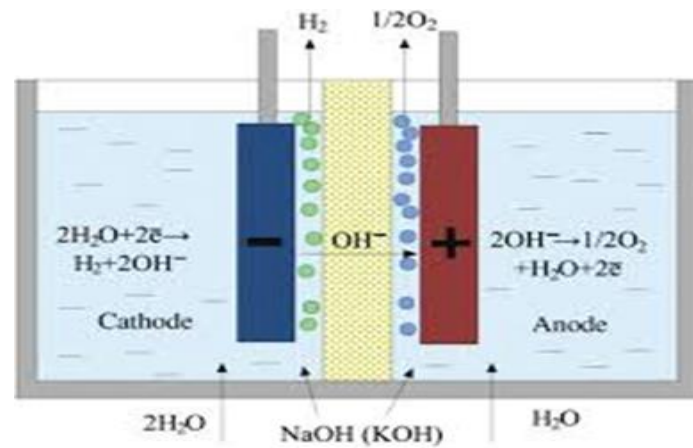


Figure I.1 : the alkaline electrolyser diagram and operation chemical equations [1]

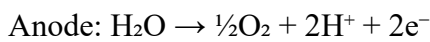
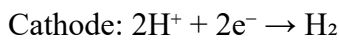
I.3.2.2 Proton Exchange Membrane Electrolysis (PEM):

→ **How It Works:**

Uses a solid polymer electrolyte (PEM) to conduct protons.

Water is split into hydrogen and oxygen at two electrodes.

→ **Chemical Equations:**



→ **Benefits:**

High efficiency (70–80%).

Compact design and fast response to variable energy inputs.

Produces high-purity hydrogen.

→ **Negatives:**

High cost due to expensive materials (e.g., platinum catalysts).

Shorter lifespan compared to alkaline systems.

Sensitive to impurities in water [12].

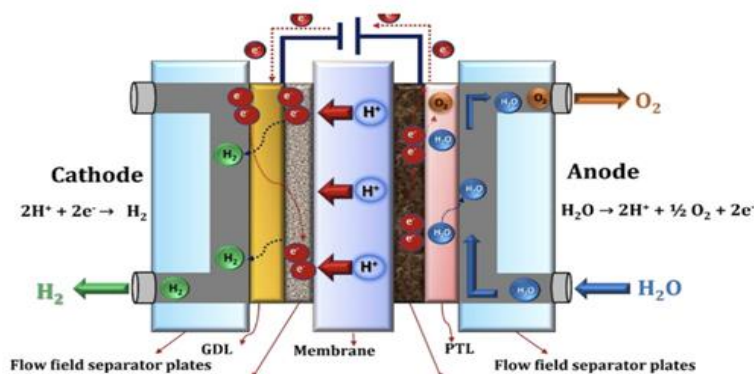


Figure I.2 :the PEM electrolyser diagram and operation chemical equations [2]

I.3.2.3 Solid Oxide Electrolysis (SOE):

→ How It Works:

Uses a ceramic electrolyte that conducts oxygen ions at high temperatures (700–1000°C).

Steam is split into hydrogen and oxygen at two electrodes.

→ Chemical Equations:

Cathode: $\text{H}_2\text{O} + 2\text{e}^- \rightarrow \text{H}_2 + \text{O}^{2-}$

Anode: $\text{O}^{2-} \rightarrow \frac{1}{2}\text{O}_2 + 2\text{e}^-$

→ Benefits:

Highest efficiency (80–90%) due to high-temperature operation.

Can utilize waste heat from industrial processes.

No need for expensive catalysts.

→ Negatives:

Requires high operating temperatures, increasing energy demand.

Longer startup times and slower response to load changes.

Durability and material degradation issues over time[12][13].

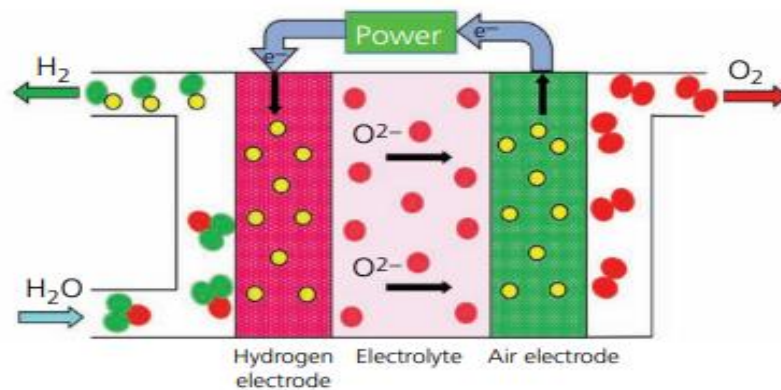


Figure I.3 :the SOE electrolyser diagram and operation chemical equations [3]

I.4 Introduction to Green Hydrogen:

I.4.1 The Green Hydrogen:

→ Definition:

Green hydrogen is hydrogen produced through the electrolysis of water using electricity generated from 100% renewable energy sources.

→ How It Works:

Electrolysis splits water (H₂O) into hydrogen (H₂) and oxygen (O₂) using an electric current.

The electricity used comes from renewable sources like solar, wind, or hydropower, ensuring zero carbon emissions.

→ Purpose:

Provides a clean, sustainable energy carrier for industries, transportation, and energy storage.

Helps decarbonize sectors that are hard to electrify directly[14].

I.4.2 Why Green Hydrogen:**→ Environmental Benefits:**

Zero greenhouse gas emissions during production.

Reduces reliance on fossil fuels and mitigates climate change.

→ Energy Transition Role:

Enables large-scale renewable energy storage and grid balancing.

Supports global net-zero emissions goals[15].

I.4.3 Renewable Energy Sources for Green Hydrogen Production:**→ Solar Energy:**

Photovoltaic (PV) panels convert sunlight into electricity, which powers electrolyzers.

Ideal for sunny regions and decentralized hydrogen production.

→ Wind Energy:

Wind turbines generate electricity from wind, which is used for electrolysis.

Suitable for onshore and offshore wind farms, especially in windy regions.

→ Hydropower:

Uses flowing or falling water to generate electricity for electrolysis.

Provides a stable and reliable energy source for large-scale hydrogen production.

→ Geothermal Energy:

Harnesses heat from the Earth's core to generate electricity for electrolysis.

Limited to regions with geothermal activity but offers consistent energy output.

→ Biomass Energy:

Converts organic materials into electricity or biogas, which can power electrolyzers.

Provides a renewable option but is less common for green hydrogen due to emissions during biomass processing.

I.5 Green Hydrogen Production via Alkaline Electrolysis Powered by Solar PV:

I.5.1 Solar PV System:

Photovoltaic (PV) panels convert sunlight into direct current (DC) electricity.

The system includes an MPPT (Maximum Power Point Tracking) algorithm to optimize energy extraction from the solar panels under varying sunlight conditions.

I.5.2 Control and Optimization:

The MPPT algorithm ensures the solar panels operate at their maximum power point, improving efficiency. A power conditioning unit (inverter) converts DC electricity to alternating current (AC) if required by the electrolyzer[16].

I.5.3 Alkaline Electrolysis:

The optimized electricity powers the alkaline electrolyzer, which splits water (H_2O) into hydrogen (H_2) and oxygen (O_2).

Electrolyte: An alkaline solution (e.g., potassium hydroxide) facilitates ion conduction.

Electrodes: Hydrogen is produced at the cathode, and oxygen is released at the anode.

I.5.4 Hydrogen Storage and Utilization:

The produced hydrogen is purified, compressed, and stored for use in industries, transportation, or energy storage[16].

I.5.5 Alkaline Electrolysis Powered by Solar PV: A Controlled and Optimized System:

→ Objective:

To design and implement a PV-Electrolyzer System that maximizes hydrogen production efficiency using advanced control and optimization techniques.

→ Key Components:

Solar PV System: Converts sunlight into electricity.

MPPT Algorithm: Optimizes power extraction from PV panels under varying conditions.

Alkaline Electrolyzer: Splits water into hydrogen and oxygen using the optimized electricity.

Control System: Ensures seamless integration and operation of the PV and electrolyzer systems[17].

I.5.6 Role of MPPT Algorithm:

→ Maximizes Energy Extraction:

Ensures the PV system operates at its maximum power point, even under partial shading or changing weather conditions.

→ Improves Efficiency:

Reduces energy losses and enhances the overall hydrogen production rate.

→ Ensures System Stability:

Maintains a stable power supply to the electrolyzer, preventing disruptions in hydrogen production[17].

I.6 CONCLUSION:

To design and demonstrate an integrated PV-Electrolyzer System controlled and optimized via an MPPT algorithm, ensuring maximum hydrogen production efficiency.

The system combines solar PV energy with alkaline electrolysis, creating a fully renewable and sustainable hydrogen production process.

Advanced control techniques, including MPPT, ensure optimal energy extraction and stable operation under varying conditions.

Chapter II

Modeling of PV- Electrolyzer system

II.1 Introduction:

This chapter shows that Renewable-powered hydrogen production relies on seamlessly integrating solar energy with electrolysis. This chapter explores the design, optimization, and performance of a PV-electrolyzer system, bridging photovoltaics (PV) and hydrogen generation.

We begin with an overview of PV solar systems, examining how sunlight is converted into electrical energy and the critical factors—irradiance and temperature—that influence efficiency. Next, we break down the key components of a PV system, from solar cells to inverters, that enable effective energy harvesting. A major challenge in PV systems is maximizing power output under varying conditions. Thus, we analyze Maximum Power Point Tracking (MPPT) algorithms, including:

- Perturb & Observe (P&O) and Incremental Conductance (IC) – Classic, widely used methods.
- Artificial Neural Networks (ANN) and Fuzzy Logic – Intelligent, adaptive approaches for dynamic conditions.

Finally, we shift focus to the alkaline electrolyzer, the heart of hydrogen production. We discuss its working principles and how its performance is evaluated using two key parameters:

- Hydrogen production rate ($n\text{H}_2$, mol/s) – Quantifying output efficiency.
- Faraday efficiency (0–1 or %) – Measuring charge transfer effectiveness.

By modeling the interaction between the PV system's optimized power and the electrolyzer's hydrogen output, this chapter lays the foundation for sustainable, solar-driven hydrogen production.

II.2 PV System:

II.2.1 Overview of PV System Operation:

→ Solar Energy Capture:

Photovoltaic (PV) panels absorb sunlight, which excites electrons in the semiconductor material (e.g., silicon), generating direct current (DC) electricity[18].

→ Energy Conversion:

The DC electricity is converted into alternating current (AC) using an inverter, making it compatible with most electrical systems and devices[18].

→ System Components:

Includes PV panels, inverters, mounting structures, and balance of system (BOS) components like wiring and connectors[19].

→ Output Characteristics:

The system produces electricity proportional to solar irradiance, with voltage and current depending on panel configuration and environmental conditions[20].

→ **Role in Hydrogen Production:**

The electricity generated powers the electrolyzer, enabling water splitting into hydrogen and oxygen[21].

→ **Efficiency Factors:**

Performance depends on solar irradiance, temperature, shading, and panel orientation, which must be optimized for maximum energy output[22].

II.2.2 Factors Affecting PV Performance:

→ **Solar Irradiance:**

Effect: Higher irradiance increases the energy absorbed by PV panels, leading to higher power output.

Example: A PV panel produces more electricity on a sunny day (1000 W/m² irradiance) compared to a cloudy day (300 W/m²) [23].

→ **Temperature:**

Effect: PV panels are less efficient at higher temperatures. For every 1°C rise above 25°C, efficiency drops by about 0.3–0.5%.

Example: A panel operating at 45°C may produce 6–10% less power than at 25°C, even under the same irradiance[23].

→ **Shading and Orientation:**

Effect: Shading (e.g., from trees or buildings) reduces energy output, and improper panel orientation (angle or direction) decreases sunlight capture.

Example: A shaded panel may lose 20–30% of its potential output, while optimal orientation (e.g., south-facing at a tilt angle equal to the latitude) maximizes energy production.

II.2.3 PV System Output and Efficiency:

→ **Energy Output:**

The power output of a PV system depends on solar irradiance, panel efficiency, and environmental conditions. It is calculated as:

$P = A \times \eta \times G$, where:

P = Power output (W),

A = Panel area (m²),

η = Panel efficiency (%),

G = Solar irradiance (W/m²).

→ **Efficiency Factors:**

Panel Efficiency: Ranges from 15–22% for commercial panels, depending on technology.

System Losses: Inverter efficiency (95–98%), wiring losses, and shading reduce overall system efficiency.

Example:

A 10 m² PV panel with 20% efficiency under 1000 W/m² irradiance produces:

$$P = 10 \times 0.20 \times 1000 = 2000 \text{ W (2 kW)}.$$

→ **Role in Hydrogen Production:**

Higher PV output directly increases the energy available for electrolysis, improving hydrogen production rates[24].

II.3 Control Algorithm (MPPT):

II.3.1 Introduction to MPPT Algorithms:

→ **Definition:**

Maximum Power Point Tracking (MPPT) algorithms are control techniques used to optimize the power output of photovoltaic (PV) systems by ensuring they operate at their maximum power point (MPP).

→ **Purpose:**

They dynamically adjust the electrical operating point of the PV panels to extract the maximum available power under varying environmental conditions (e.g., solar irradiance, temperature)[25].

→ **Tracking Mechanism:**

MPPT algorithms continuously monitor the voltage and current output of the PV system and adjust the load or operating point to maximize power ($P = V \times I$).

→ **Key Components:**

Sensors to measure voltage and current.

A controller (e.g., microcontroller) to implement the algorithm.

A DC-DC converter to adjust the operating point[26].

→ **Role in Hydrogen Production:**

Optimizing Energy Input: By maximizing the power extracted from the PV system, MPPT algorithms ensure the electrolyzer receives a stable and optimal energy supply[27].

Improving Efficiency: Higher energy extraction increases the hydrogen production rate and overall system efficiency.

Adaptability: MPPT algorithms adjust to changing conditions (e.g., cloud cover, shading), ensuring consistent hydrogen production even in suboptimal environments.

II.2.3 Types of MPPT Algorithms:

II.2.3.1 Perturb and Observe (P&O):

→ **How It Works:**

Perturbs the operating voltage and observes the change in power.

Adjusts voltage based on whether power increases or decreases[28].

→ **Mathematical Model:**

Power Calculation: $P(k) = V(k) \times I(k)$

Voltage Update:

If $P(k) > P(k-1)$, $V(k+1) = V(k) + \Delta V$

If $P(k) < P(k-1)$, $V(k+1) = V(k) - \Delta V$

→ **Benefits:** Simple and low cost.

→ **Negatives:** Oscillates around MPP [29][30].

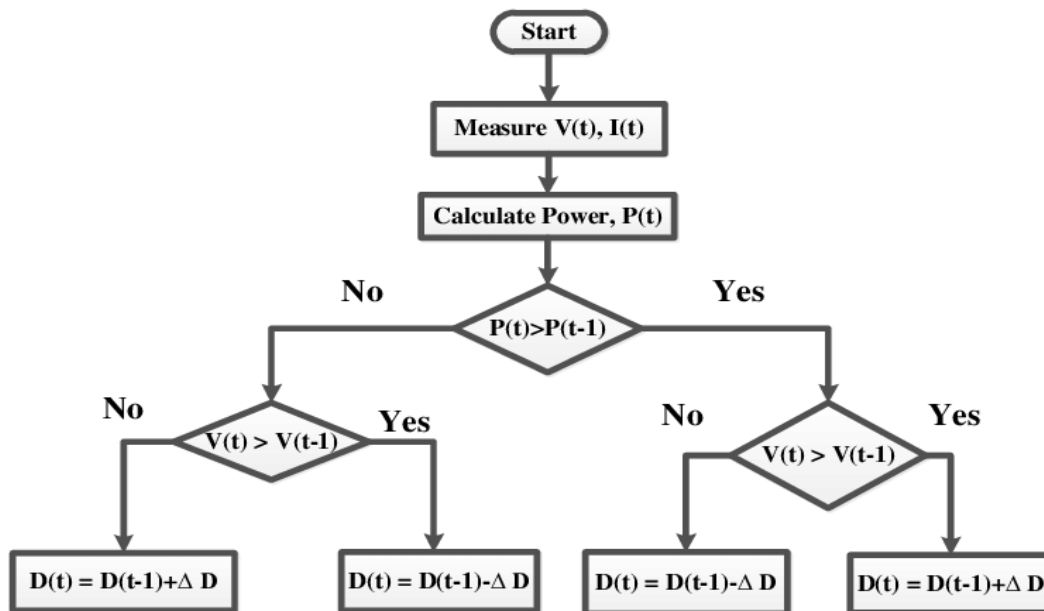


Figure II.1 :The structure of the operation steps of the po algorithm [4]

II.3.2.2 Incremental Conductance (IC):

The IC algorithm adjusts the voltage of the PV array to reach the MPP by comparing the incremental conductance (dI/dV) to the instantaneous conductance (I/V). The key idea is to use the relationship between the change in current (ΔI) and the change in voltage (ΔV) to determine the direction of the MPP[30].

→ **Incremental Conductance Condition:**

If $dI/dV > -I/V$, the operating point is to the left of the MPP, and the voltage should be increased.

If $dI/dV < -I/V$, the operating point is to the right of the MPP, and the voltage should be decreased.

If $dI/dV = -I/V$, the operating point is at the MPP, and no adjustment is needed.

→ **Relationship Between Output and Input:**

The IC algorithm does not directly provide a simple equation like $V_{out}=V_{in}/1-D$ (as in the Perturb and Observe (P&O) method with a DC-DC converter). Instead, it dynamically adjusts the voltage reference V_{ref} based on the incremental conductance condition. The output voltage V_{out} is controlled by the duty cycle D of the DC-DC converter, which is adjusted to track the MPP.

in the IC algorithm, the duty cycle D is adjusted based on the incremental conductance condition rather than a fixed relationship.

→ **Benefits:** Accurate and stable.

→ **Negatives:** Computationally intensive[31].

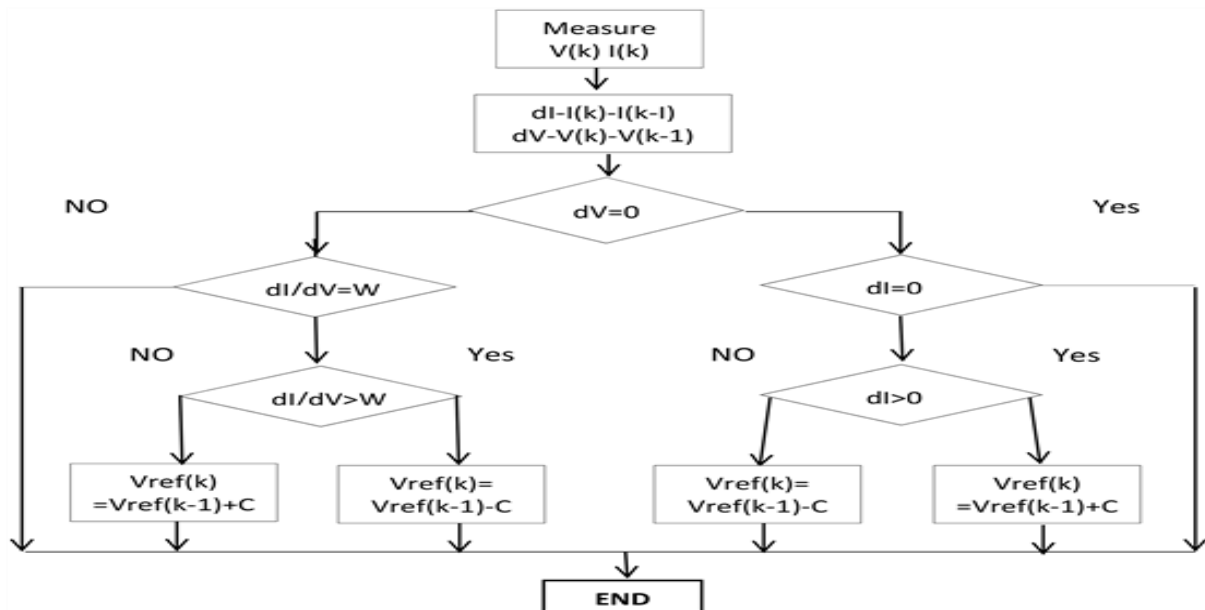


Figure II.2 :The structure of the operation steps of the IC algorithm[5]

II.3.2.3 Artificial Neural Networks (ANN) MPPT:

An ANN-based MPPT controller uses a trained neural network to predict the optimal voltage or duty cycle for the PV system to operate at the MPP. The ANN is trained using historical data or simulated data that includes various environmental conditions and the corresponding MPP[32][33].

→ **How ANN-Based MPPT Works:**

Inputs:

Environmental data (solar irradiance G , temperature T) and/or PV array measurements (voltage V , current I).

ANN Structure:

Input layer: Receives data.

Hidden layers: Process data using weights, biases, and activation functions.

Output layer: Predicts the optimal voltage (V_{mpp}) or duty cycle (D).

Training:

Train the ANN using historical or simulated data (irradiance, temperature, and corresponding MPP).
Minimize prediction error (e.g., Mean Squared Error) during training.

Operation:

Measure G , T , V , and I .

Feed inputs into the trained ANN to predict V_{mpp} or D .

Adjust the DC-DC converter's duty cycle to track the MPP.

→ **Relationship Between Input and Output:**

The ANN learns a complex mapping between inputs (environmental conditions) and outputs (optimal V_{mpp} or D).

For a boost converter, the output voltage is:

$V_{out} = V_{in} / (1 - D)$ where D is predicted by the ANN.

→ **Benefits:** Highly adaptive.

→ **Negatives:** Requires training data and resources.

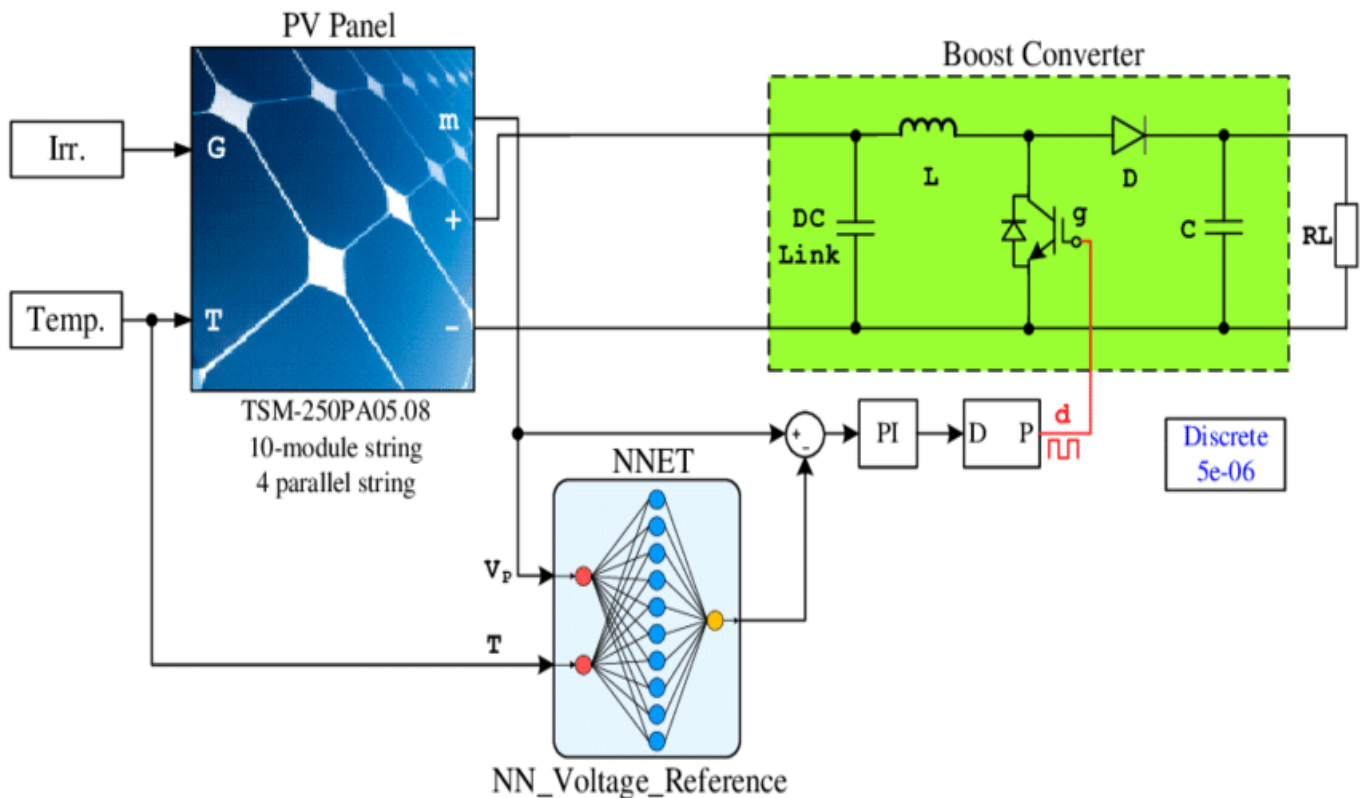


Figure II.3 :the structure of the pv system using ANN algorithm[6]

II.3.2.4 Fuzzy Logic Control (FLC):

Fuzzy Logic Control is a rule-based control method that handles imprecise or uncertain inputs. Instead of using strict binary logic (true/false), it uses degrees of truth (e.g., "partially true") to make decisions, making it ideal for complex, non-linear systems like PV MPPT.

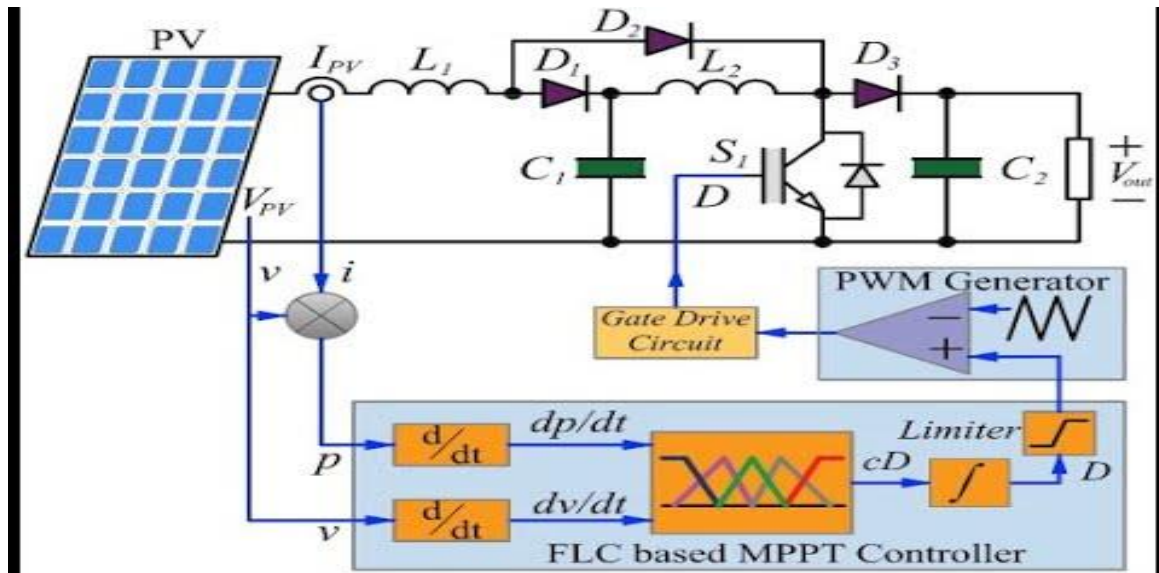


Figure II.4 :the structure of the pv system using FLC algorithm[7]

→ How FLC-Based MPPT Works:

Inputs:

Error (E): Difference between current and desired power.

Change in error (ΔE): Rate of change of E .

Fuzzification:

Convert crisp inputs ($E, \Delta E$) into fuzzy values using membership functions (e.g., "Negative," "Zero," "Positive").

Fuzzy Rules:

Apply IF-THEN rules (e.g., IF E is Negative AND ΔE is Negative, THEN increase duty cycle D).

Inference Engine:

Combine rules to determine the fuzzy output (e.g., "Increase D slightly").

Defuzzification:

Convert fuzzy output into a crisp duty cycle (D).

Control:

Adjust the DC-DC converter's D to track the MPP[34].

→ Relationship Between Input and Output:

FLC dynamically adjusts D based on fuzzy rules, not a fixed equation.

For a boost converter:

$$V_{out} = V_{in} / (1 - D) \text{ where } D \text{ is determined by FLC.}$$

Benefits: Handles uncertainty well.

Negatives: Requires expert knowledge.

In short, FLC uses fuzzy logic to make decisions based on imprecise inputs, dynamically adjusting the duty cycle (DD) to keep the PV system at the MPP. It's a powerful tool for complex, real-world systems[35].

II.3.3 Role of MPPT in Hydrogen Production:

→ Maximizing Energy Extraction:

MPPT algorithms ensure the PV system operates at its maximum power point (MPP), extracting the highest possible energy from sunlight.

This maximizes the electricity available for the electrolyzer, directly increasing hydrogen production[36].

→ Stable Power Supply:

MPPT adapts to changing environmental conditions (e.g., cloud cover, shading, temperature), providing a stable and consistent power supply to the electrolyzer.

This prevents disruptions in hydrogen production caused by fluctuating energy input.

→ Improving System Efficiency:

By optimizing the PV system's performance, MPPT reduces energy losses and improves the overall efficiency of the hydrogen production process.

Higher efficiency means more hydrogen is produced per unit of solar energy[36].

II.4 Alkaline Electrolyzer:

II.4.1 Overview of Alkaline Electrolyzer:

→ The Alkaline Electrolyzer :

An alkaline electrolyzer is a device that splits water (H_2O) into hydrogen (H_2) and oxygen (O_2) using an alkaline electrolyte (e.g., potassium hydroxide, KOH).

It is one of the most mature and widely used electrolysis technologies for hydrogen production[37].

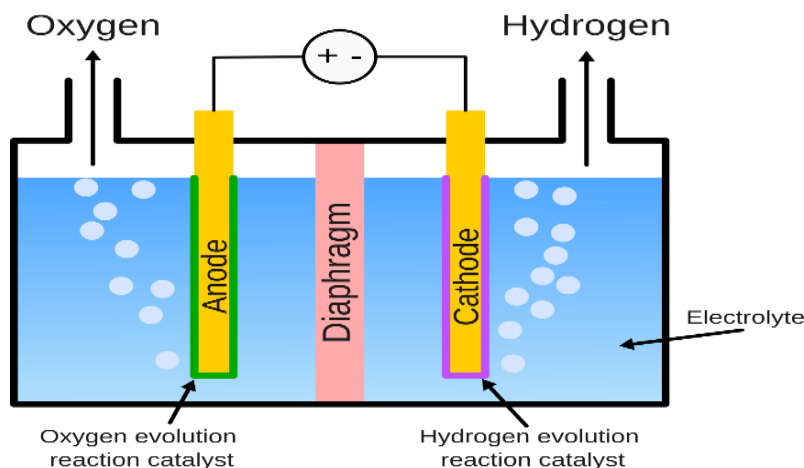


Figure II.5 :the alkaline electrolyser diagram[8]

→ **Key Components:**

Electrolyte: A concentrated alkaline solution (e.g., 20–30% KOH) that facilitates ion conduction between the electrodes.

Electrodes:

Cathode: Where hydrogen is produced.

Anode: Where oxygen is produced.

Typically made of nickel or nickel-based alloys for durability and conductivity.

Separator (Diaphragm): A porous membrane that allows ion transport but prevents mixing of hydrogen and oxygen gases.

Power Supply: Provides the direct current (DC) required for the electrolysis process[37].

→ **How It Works:**

Electrolysis Process:

When DC electricity is applied, water molecules are split into hydrogen and oxygen at the electrodes.

The alkaline electrolyte facilitates the movement of hydroxide ions (OH^-) between the electrodes.

Chemical Reactions:

Cathode (Hydrogen Production): $2\text{H}_2\text{O} + 2\text{e}^- \rightarrow \text{H}_2 + 2\text{OH}^-$

Anode (Oxygen Production): $2\text{OH}^- \rightarrow \frac{1}{2}\text{O}_2 + \text{H}_2\text{O} + 2\text{e}^-$

Overall Reaction: $2\text{H}_2\text{O} \rightarrow 2\text{H}_2 + \text{O}_2$

Gas Separation:

Hydrogen and oxygen gases are collected separately at the cathode and anode, respectively.

The separator ensures the gases do not mix, preventing safety hazards[37].

→ **Advantages of Alkaline Electrolyzers:**

Mature Technology: Well-established and commercially available for decades.

Cost-Effective: Lower capital costs compared to other electrolyzer types (e.g., PEM).

Durability: Long operational lifespan with proper maintenance[38].

→ **Challenges of Alkaline Electrolyzers:**

Slow Response Time: Less suitable for dynamic operation with variable renewable energy sources.

Corrosive Electrolyte: Requires careful handling and maintenance.

Lower Efficiency: Typically 60–70%, lower than PEM electrolyzers.

II.4.2 Mathematical Modeling of Electrolyzer Performance:

The electrolyzer represents the load of the system. Its operating point is defined according to its connection with the energy source which is in our case the PV system. The equivalent diagram of electrolyzer is showed in figure

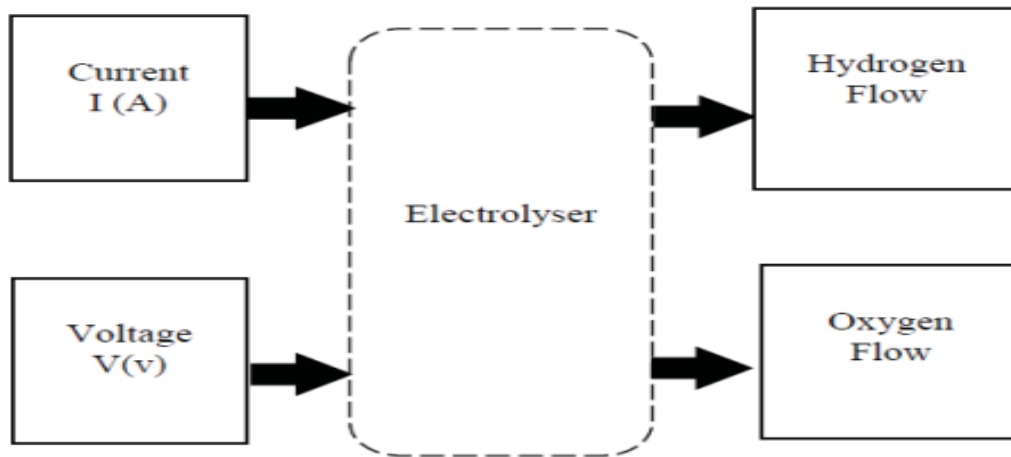


Figure II.6 :diagram showcasing the relation between the pv system voltage and current and the electrolyser system performance

The cell voltage of an electrolyzer is expressed according to four terms

$$U_{el} = U_{cathode} + U_{anode} + U_{hom} + U_{th}$$

Theoretical Voltage (U_{th})

Minimum voltage required to split water (thermodynamic limit): $U_{th}=1.23 \text{ V}$ (at 25°C)

Represents the energy needed to overcome Gibbs free energy of water dissociation.

Derived from Gibbs free energy of water dissociation:

$$\Delta G^{\circ} = 237.1 \text{ kJ/mol} \quad U_{th} = \Delta G / n \times F = 237 \times 10^3 / 2 \times 96485 = 1.23 \text{ V}$$

Dependence on I

Independent of current (fundamental property).

Temperature effect: Decreases by $\sim 0.9 \text{ mV}/^{\circ}\text{C}$ rise:

$$U_{th}(T) = 1.23 - 0.9 \times 10^{-3} (T - 298)$$

Ohmic Losses (U_{ohm})

Voltage drop due to ionic resistance in the electrolyte and electrical resistance in electrodes: $U_{ohm} = I \cdot R_{int}$

Increases linearly with current (I), where R_{int} is the electrolyzer's internal resistance.

Physics:

Voltage drop due to:

Ionic resistance (electrolyte, e.g., KOH or PEM).

Electrical resistance (electrodes, contacts).

Dependence on I

Linear with current (Ohm's Law).

R_{int} decreases with temperature (faster ion mobility).

Anodic Overvoltage (U_{anode})

Extra voltage needed to drive the oxygen evolution reaction (OER) at the anode due to kinetic barriers.

Dominated by activation overpotential (non-linear with current).

Equation (Butler-Volmer Kinetics):

$$U_{\text{anode}} = \frac{RT}{\alpha nF} \times \ln(I/I_0)$$

Physics:

Extra voltage to drive the oxygen evolution reaction (OER).

Dominated by activation overpotential (slow OER kinetics).

Key Terms:

I_0 : Exchange current density (material-dependent, e.g., low for Ni anodes).

α : Charge transfer coefficient (typically 0.5 for OER).

Dependence on I

Non-linear (logarithmic).

Dominates at low currents, flattens at high I (mass transport limits).

Cathodic Overvoltage (U_{cathode})

Additional voltage for hydrogen evolution reaction at the cathode.

Equation (Butler-Volmer Kinetics):

$$U_{\text{anode}} = \frac{RT}{\alpha nF} \times \ln(I/I_0)$$

Physics:

Extra voltage for hydrogen evolution reaction (HER).

HER is faster than OER (higher I_0 , e.g., Pt cathodes).

Dependence on I Similar logarithmic form but smaller magnitude than U_{anode}

→ **Hydrogen Production Rate (n_{H₂}):**

$$n_{\text{H}_2} = (\text{current} * \text{faraday_efficiency} * n_{\text{cells}}) / (z * F)$$

Where:

n_{H_2} = Hydrogen production rate (mol/s),

I = Current supplied to the electrolyzer (A),

η_F = Faraday efficiency (dimensionless, $0 < \eta_F \leq 1$),

F = Faraday constant (96485 C/mol).

z = Number of electrons per water molecule

n_{cells} = Number of electrolyzer cells

→ **Faraday Efficiency (η_F):**

Faraday Efficiency Equation:

$$\text{faraday_efficiency} = (i_1/i_2)^2 / (1 + (i_1/i_2)^2)$$

Where:

η_F = Faraday efficiency (dimensionless, $0 < \eta_F \leq 1$)

i_1 = Empirical parameter (A/m²)

i_2 = current_density

II.5 Link Between PV System and Hydrogen Production:

→ **Role of PV System:**

The PV system supplies the current (I) and voltage required for the electrolyzer to produce hydrogen.

The hydrogen production rate (n_{H_2}) depends on the current (I) supplied by the PV system

→ **Impact of MPPT (Perturb and Observe):**

The P&O algorithm ensures the PV system operates at its maximum power point (MPP), maximizing the current (I) supplied to the electrolyzer.

By optimizing I, the MPPT algorithm directly increases the hydrogen production rate (n_{H_2}).

Additionally, a stable and optimized power supply improves the Faraday efficiency (η_F) by reducing fluctuations and inefficiencies in the electrolyzer's operation[39].

I.6 Conclusion:

This chapter presents a modular framework for integrating photovoltaic systems with alkaline electrolyzers to optimize green hydrogen production. The PV system analysis covers operational principles, performance factors (irradiance, temperature), and efficiency enhancements through maximum power point tracking (MPPT) algorithms - including conventional (P&O, IC) and intelligent (ANN-based) methods, comparing their trade-offs in hydrogen applications. The electrolyzer section details alkaline system components, working principles, and mathematical modeling using Faraday's laws to quantify hydrogen output, with emphasis on the critical voltage-current relationship between PV generation and electrolyzer demand. The integrated model establishes how MPPT optimization directly impacts electrolyzer efficiency, creating a foundation for simulating renewable hydrogen systems under variable conditions in subsequent chapters.

Chapter III

Simulation of PV- Electrolyzer System

III.1.Introduction:

This chapter focuses on the dynamic simulation of a PV-electrolyzer system, demonstrating how solar energy is efficiently converted into hydrogen through modeling and control.

We begin by simulating the PV array, which takes real-world inputs of irradiance and temperature to generate electrical power. The PV output is then fed into a boost converter, which steps up the voltage to match the electrolyzer's requirements.

A critical component of this system is the Perturb & Observe (P&O) MPPT algorithm, which continuously adjusts the duty cycle of the boost converter's MOSFET to maximize power extraction. The algorithm processes the PV system's voltage and current, dynamically optimizing the operating point to ensure the maximum power point (MPP) is maintained under varying environmental conditions.

Next, we simulate the alkaline electrolyzer, which receives the PV system's current and produces hydrogen. The electrolyzer's performance is evaluated using two key outputs:

Hydrogen production rate (nH₂, mol/s) – Shows how efficiently current is converted into hydrogen gas.

Faraday efficiency (nF, 0–1 or %) – Indicates the electrolyzer's charge utilization effectiveness.

By analyzing these outputs, we observe how fluctuations in PV power (due to changing irradiance/temperature) impact the electrolyzer's hydrogen yield and efficiency. This simulation provides critical insights into the real-world behavior of solar-powered green hydrogen systems.

III.2 Simulation of PV System :

III.2.1 PV Array Modeling:

III.2.1.1 Adding the PV Array:

→ The PV array is modeled as a collection of solar cells connected in series and parallel to achieve the desired voltage and current output.

→ Key parameters of the PV array include:

Open-circuit voltage (V_{oc}): Voltage when no current is flowing.

Short-circuit current (I_{sc}): Current when the voltage is zero.

Maximum power point (MPP): Voltage (V_{mp}) and current (I_{mp}) at which the array delivers maximum power.

Number of series and parallel cells: Determines the total voltage and current output.

III.2.1.2 Inputs to the PV Array:

→ **Solar Irradiance (G):** Directly affects the current output of the PV array. Higher irradiance increases the current.

→ **Temperature (T):** Affects the voltage output. Higher temperatures reduce the voltage.

→ These inputs are modeled as variables that can be adjusted during simulation to study their impact on performance.

III.2.1.3 Outputs of the PV Array:

→ **VPV**: Voltage output of the PV array, which varies with temperature and irradiance.

→ **IPV**: Current output of the PV array, which is primarily influenced by irradiance.

III.2.1.4 Effect of Irradiance and Temperature:

→ **Irradiance (G)**:

Proportional to the current output: $IPV \propto G$.

Example: At 1000 W/m², the PV array produces its rated current; at 500 W/m², the current is halved.

→ **Temperature (T)**:

Inversely proportional to the voltage output: VPV decreases as T increases.

Example: At 25°C, the PV array produces its rated voltage; at 50°C, the voltage drops by ~10%.

III.2.2 Boost Converter Modeling:

→ **Definition**:

A DC-DC converter that steps up the input voltage from the PV array to a higher output voltage.

Essential for matching the PV array voltage to the required input voltage of the electrolyzer[40][41].

→ **Working Principle**:

Switching Operation:

A semiconductor switch (e.g., MOSFET) turns on and off at a high frequency, controlled by the duty cycle (D).

When the switch is ON, energy is stored in an inductor.

When the switch is OFF, the stored energy is released, boosting the output voltage[42].

Voltage Relationship:

The output voltage (V_{out}) is related to the input voltage (V_{in}) and duty cycle (D) by: $V_{out} = V_{in} / (1 - D)$

Example: If $V_{in} = 20$ V and $D = 0.5$, then $V_{out} = 40$ V [42].

→ **Key Components**:

Inductor (L): Stores and releases energy during switching.

Capacitor (C): Smooths the output voltage.

Diode: Ensures one-way current flow during the switch-OFF phase.

Semiconductor Switch (e.g., MOSFET): Controls the energy flow[42].

→ **Designing boost converter for photovoltaic system**:

In a simple pv system where we just have a pv array and a boost converter there are no conventional way to design a boost converter since the voltage of the pv array isn't constant and changes from 0 to V_{oc}

so its output voltage V_{out} is also not constant and also where we track the MPP the duty cycle value is always changing with the change in the pv array conditions that's why usually engineers design them by hit-and-error method we can though with these equations size the parameters values of the boost converter (L , C , D , R_{load} ...) following these steps:

we take the pv array specifications at STC ($1000\text{w}/\text{m}^2$ 25°C) and worst case ($50\text{w}/\text{m}^2$ 25°C) conditions let's say for example: at STC we have $V_{mp}=106.5\text{v}$ and $I_{mp}=16.9\text{A}$ and $P_{mp}=1800\text{w}$

At worst case -10% we have $V_{mp}=0.9 \times 106.5 = 95.85\text{v}$ and $P_{mp}=0.05 \times 1800 = 90\text{w}$ and $I_{mp}=P_{mp}/V_{mp}=0.94\text{A}$

we define the switching frequency at 25kHz

define current and voltage ripples at $\Delta v=0.2\%$ and $\Delta I=40\%$

calculate the internal resistance of the pv array at MPP at STC and worst case : $R_{mp}=V_{mp}/I_{mp}$ at STC $R_{mp}=6.3\text{ohm}$ at worst case $R_{mp}=102\text{ohm}$

calculate the load resistance $R_o=2.5 \times R_{mp}$ at worst case $R_o=2.5 \times 102 = 255\text{ohm}$

calculate the value of the duty cycle at MPP $D_{mp} = 1 - \sqrt{R_{mp}/R_o}$

At STC $D_{mp}=0.843$ and at worst case $D_{mp}=0.368$

calculate the load voltage and load current (the output boost converter voltage and current V_o and I_o)[38].

We know that V_i is V_{mp} and $V_{out}=V_{input}/(1-D)$ and $I_o=V_o/R_o$

so at STC $V_o=678.3\text{v}$ and $I_o=2.66\text{A}$ and at worst case $V_o=152\text{V}$ and $I_o=0.6\text{A}$

calculate the values of ripple voltage and current ΔV at STC and ΔI at worst case

$\Delta V_i=0.002 \times V_i=0.002 \times 106.5=0.213\text{v}$ and $\Delta V_o=0.002 \times V_o=0.002 \times 678.3=1.36\text{v}$ and

$\Delta I_o=0.4 \times I_o=0.4 \times 0.6=0.24\text{A}$

Calculate reflected output resistance of the pv array input at STC

$R_i=R_o(1-D^2)=255(1-0.843^2)=73.78\text{ohm}$

use all these found values in the following equations to calculate C_{in} C_{out} L (C_{in} and C_o at STC and L at worst case)

$C_i = \frac{4V_{mp} \times D_{mp}}{\Delta V_i \times R_i \times f_s}$, $C_o = \frac{2V_o \times D_{mp}}{\Delta V_o \times R_o \times f_s}$, $L = \frac{V_{mp} \times D_{mp}}{2\Delta I_o \times f_s}$ we get $C_i=914\mu\text{F}$ and $C_o=131\mu\text{F}$ and $L=2.94\text{mH}$

So at the end the final designed parameters of the boost converter are :

$C_i=1000\mu\text{F}$

$C_o=150\mu\text{F}$

$L=3\text{mH}$

$R_o=255\text{ohm}$

$f_s=25\text{kHz}$ [43].

III.2.3 MPPT: Perturb and Observe Method:

Maximum Power Point Tracking (MPPT) is a technique used in photovoltaic (PV) systems to maximize the power output from solar panels under varying conditions such as sunlight intensity, temperature, and load. The **Perturb and Observe (P&O)** method is one of the most commonly used MPPT algorithms due to its simplicity and effectiveness[44].

III.2.3.1 P&O Work:

→ **Perturbation:**

The algorithm slightly adjusts (perturbs) the operating voltage or current of the PV system. For example, it increases or decreases the voltage by a small amount.

→ **Observation:**

After the perturbation, the algorithm measures the resulting change in power output from the solar panel. Power is calculated as $P=V \times I$, where V is voltage and I is current.

→ **Decision:**

If the power increases after the perturbation, the algorithm continues to perturb the system in the same direction (e.g., increasing voltage further).

If the power decreases, the algorithm reverses the direction of the perturbation (e.g., decreases the voltage).

→ **Repetition:**

This process is repeated continuously, causing the system to oscillate around the Maximum Power Point (MPP), where the solar panel produces the maximum possible power[45].

III.2.3.2 Advantages of Using P&O in Green Hydrogen Production:

→ **Maximized Energy Harvest:** The P&O algorithm ensures the solar panels operate at their maximum efficiency, increasing the overall energy available for hydrogen production.

→ **Cost Efficiency:** By optimizing power output, the system reduces the need for additional solar panels or energy storage, lowering costs.

→ **Scalability:** The P&O method is simple and can be easily implemented in small- or large-scale hydrogen production systems[46].

III.2.3.3 Challenges and Considerations:

→ **Rapid Environmental Changes:** The P&O method may struggle to track the MPP accurately under rapidly changing conditions (e.g., sudden cloud cover). Advanced MPPT algorithms or hybrid methods may be needed in such cases.

→ **Electrolyzer Efficiency:** The electrolyzer's efficiency curve must be considered when designing the system to ensure the MPPT algorithm aligns with the electrolyzer's optimal operating conditions.

→ **System Stability:** The oscillations inherent in the P&O method must be minimized to avoid instability in the electrolyzer's operation.

III.2.3.4 Interaction of components :

→ **Solar Panels:**

Generate voltage and current based on the input irradiance and temperature. These values are fed into the boost converter and the P&O controller.

→ **P&O Controller:**

Measures the PV voltage and current to calculate power. Perturbs the duty cycle of the boost converter and observes the change in power. Adjusts the duty cycle to maximize power output.

→ **Boost Converter:**

Receives the duty cycle from the P&O controller. Steps up the PV voltage to the required level for the electrolyzer. Delivers the boosted voltage and current to the electrolyzer.

→ **Electrolyzer:**

Receives the boosted voltage and current. Converts the electrical energy into hydrogen gas. Outputs the hydrogen production rate.

III.2.4 Simulation in MATLAB/Simulink:

Components and Interaction with PV Array:

This one is a pv system with a boost converter boosting the voltage from around 348 to 476v with a duty cycle and a frequency of 27% [47].

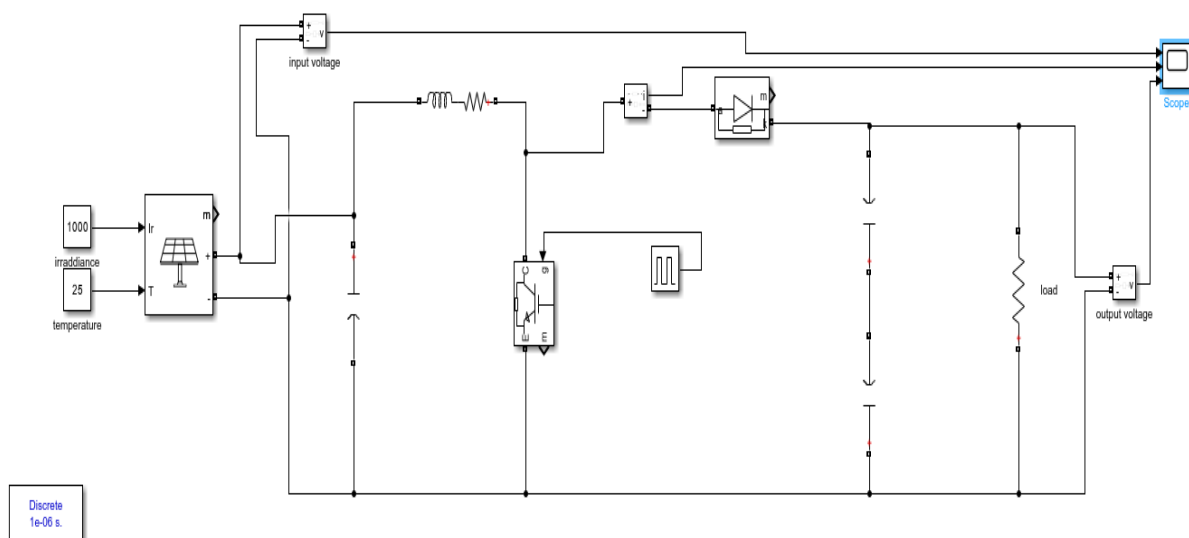


Figure III.1 :The pv boost converter system simulation

→ **PV Array Block:**

Provides the input voltage (VPV) and current (IPV) to the boost converter.

→ **Boost Converter Block:**

Simulates the inductor, capacitor, diode, and switch.

Takes VPV and IPV as inputs and produces a higher output voltage (Vout).

→ **Duty Cycle Control:**

The duty cycle (D) is controlled by the P&O MPPT algorithm to optimize power transfer.

→ **Interaction:**

The boost converter adjusts its output voltage based on the PV array’s operating point, ensuring maximum power extraction[47].

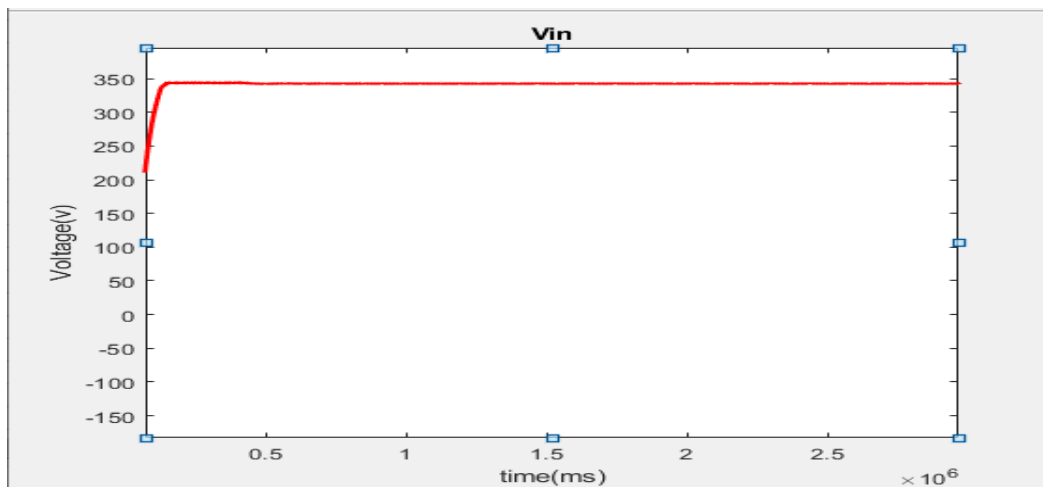


Figure III.2 :the input boost converter voltage (from the pv system)

The pv boost converter system output voltage that is boosted from 348v to 476v where $V_{out}=V_{in}/(1-d)$

Where the duty cycle (pulse width) value $d=1-(V_{in}/V_{out})$

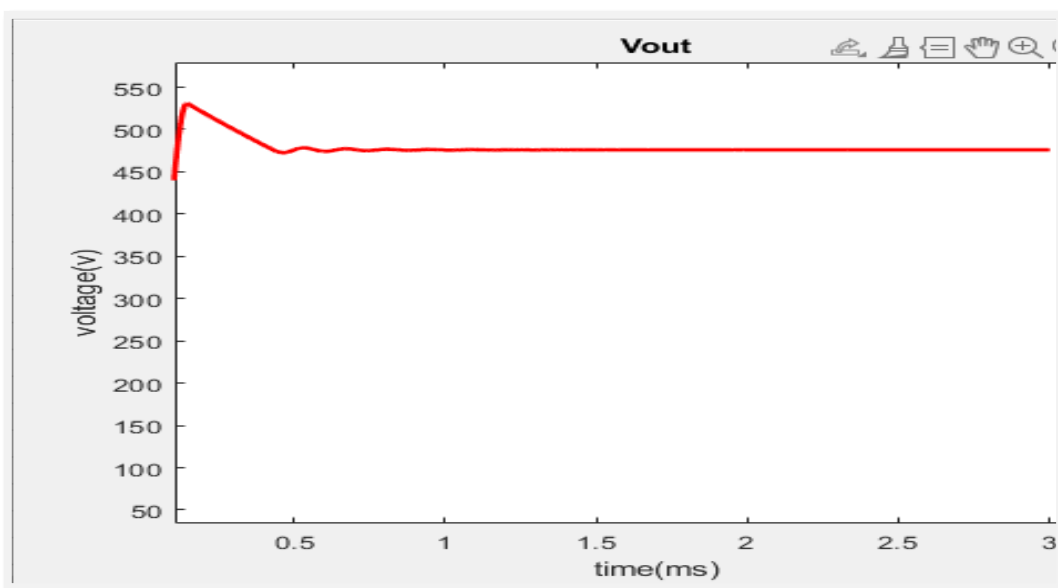


Figure III.3 :the output boost converter voltage

The current oscillates between 0 to 15A

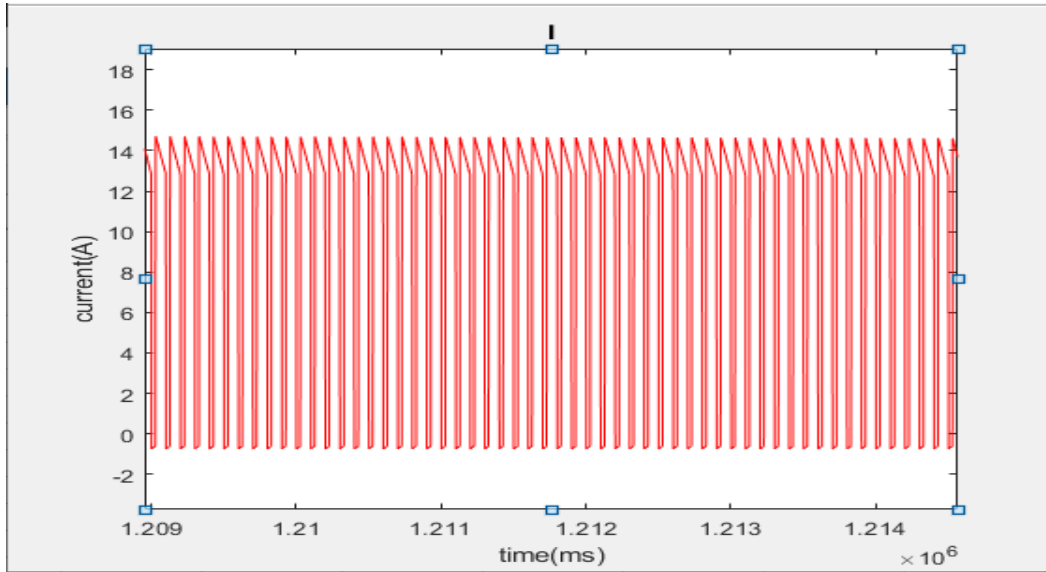


Figure III.4 :the output boost converter current

III.2.5 The MPPT control algorithm work:

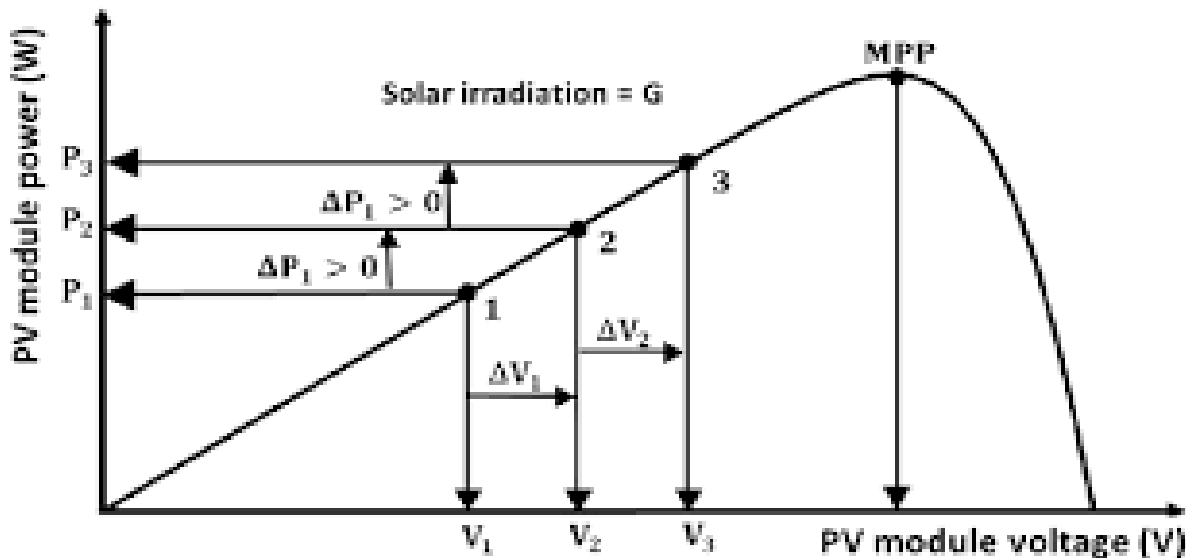


Figure III.5 :The effects of the po algorithm in the p-v curve (changing of power from changing the voltage [9])

→ First to add it we add a MATLAB function from the library to system where :

The inputs are Vpv and Ipv from the solar panel.

the output is the duty cycle alpha that we control.

→ Now we set the duty cycle maximum and minimum limit Aswell as the delta (alpha) D which is the change of the duty cycle either increase or decrees at each time

→ We set values that are constant in the function throughout it operation which are VOLD POLD DOLD

→ Use if conditions with empty so that only during first time values are assigned

→ Calculate the power P and the change of the voltage delta v and change of power delat P

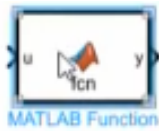
→ check the change of p if it is not equal to zero we have 4 possibilities :

$D_p < 0$ and $dV < 0$ then decrease D

$D_p < 0$ and $dV > 0$ then increase D

$D_p > 0$ and $dV < 0$ then increase D

$D_p > 0$ and $dV > 0$ then decrease D [48].



```
function D = fcn(vpv,ipv)

Dinit=0.4;
Dmax=0.9;
Dmin=0.1;
deltaD=20e-6;

persistent Vold Pold Dold;

dataType="double";

if isempty(Vold)
    Vold=0;
    Pold=0;
    Dold=Dinit;
end

P=vpv*ipv;
dV=vpv-Vold;
dP=P-Pold;

if dP~=0
    if dP<0
        if dV<0
            D=Dold-deltaD;
        else
            D=Dold+deltaD;
        end
    else
        if dV<0
            D=Dold+deltaD;
        else
            D=Dold-deltaD;
        end
    end
else D=Dold;
end
if D>=Dmax||D<=Dmin
    D=Dold;
end

Dold=D;
Vold=vpv;
Pold=P;
```

Figure III.6 :The MATLAB function script of the po algorithm

→ if D value surpasses the maximum or minimum limit we fix it by $D=OLD$

→ We update the values of $Vold$ $pold$ $dold$

→ Now we have po mppt algorithm for the pv array

→ we connect the mppt function to vpv and ipv as it inputs and connect it output the duty cycle D to a pwm generator that connects to the IGBT diode instead of the normal pulse generator in the case of a simple boost generator pv system where we just put the duty cycle value without mppt control for optimization.

→ now we collect the data from the array side where we monitor vpv ipv power p and on the load (output side) we monitor $vload$ $iload$ $pload$ where we can see the effect of the boost generator that amplifies the power output to the level we desire and the effect of the mppt function that controls the boost converter by the duty cycle value it gives to it

→ Now after we obtain optimized output values from pv array we connect it to the electrolyzer system for hydrogen production[48].

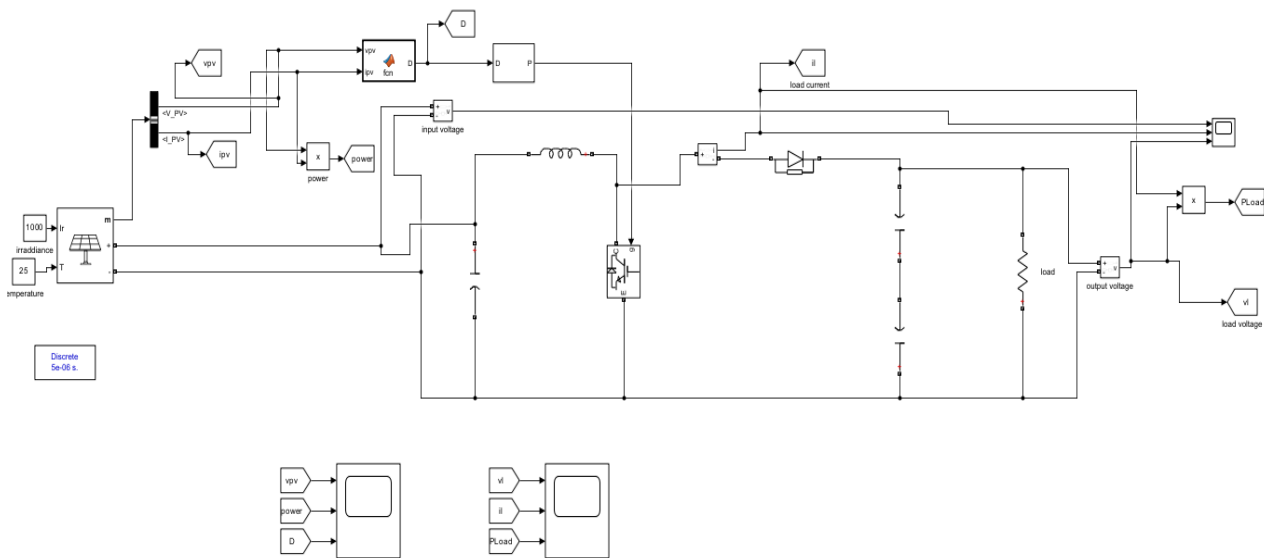


Figure III.7 :The whole MATLAB simulated p-v system mppt model

The system where we take the outputs from the pv system the voltage and the current that are effected by the changes in irradiance and temperature and inputting them to the po mppt algorithm that takes them and optimizes the system by giving the duty cycle value as an output then connecting the pv system to the boost converter system that is controlled from the misfit diode by the input from the output of the po algorithm to give us an optimized power output that converges to MPP point.

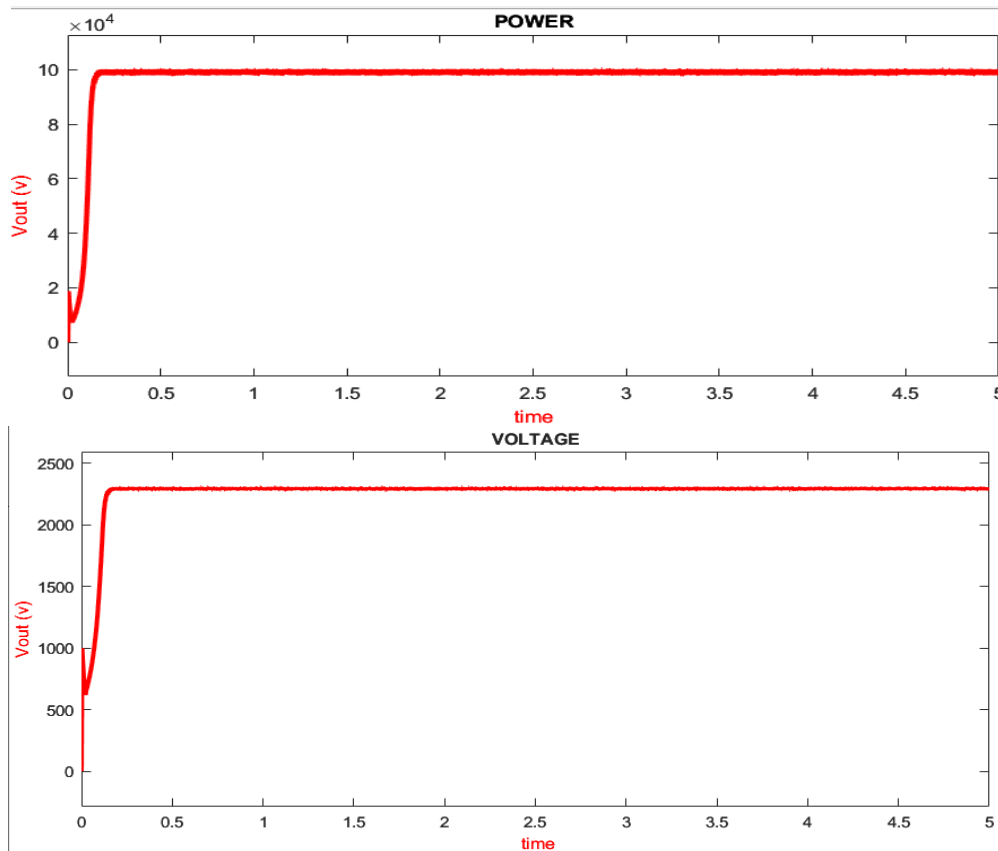


Figure III.8 :The pv system outputs(P, V) at 1000w/m2

See how the change in irradiance effects the power voltage where we see the power output value drop from 10×10^4 to 4.8×10^4 and the output voltage from 2300 to 1600:

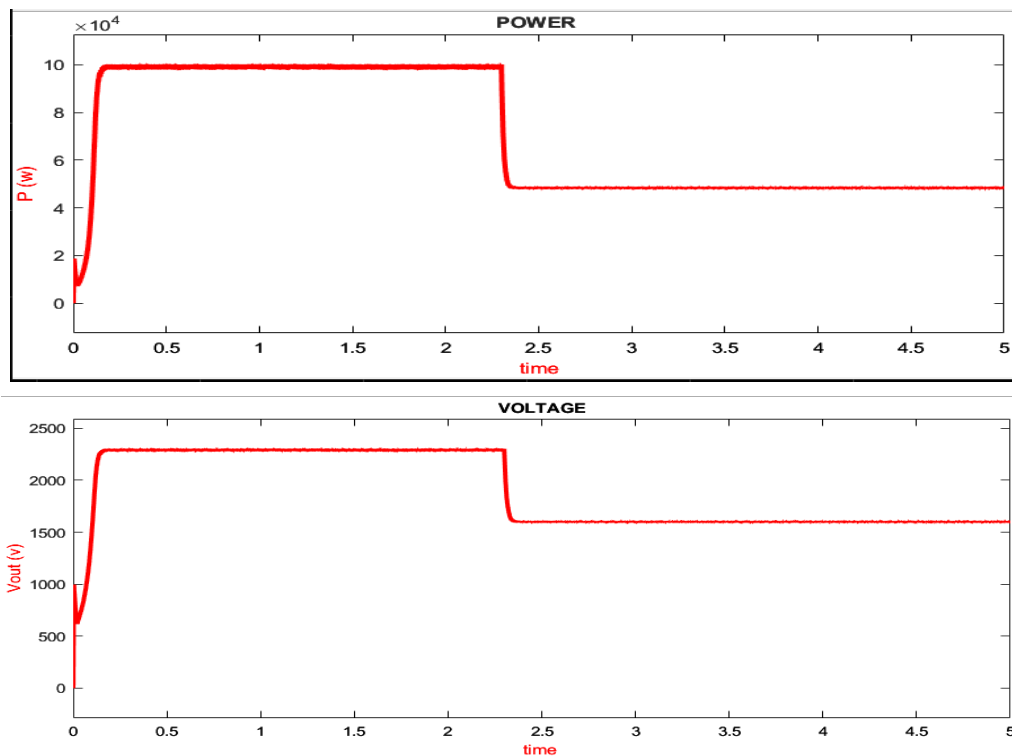


Figure III.9 :The pv system outputs (P, V) when changing irradiance from 1000w/m2 to 500w/m2

III.3 Simulation of Alkaline Electrolyzer:

III.3.1 Hydrogen Production & Faraday Efficiency:

→ Hydrogen Production Rate (nH₂):

Represents the amount of hydrogen gas produced per second (mol/s).

Depends on:

Current input (A) – Higher current → more H₂.

Faraday efficiency – How effectively electrons split water.

Number of electrolyzer cells – More cells → higher production.

Equation: $nH_2 = \text{Current} \times \text{Faraday Efficiency} / 2 \times \text{Faraday Constant}$.

→ Faraday Efficiency:

Measures how efficiently electrons are used in electrolysis (0-100%).

Decreases at very high currents due to energy losses.

Equation: $\eta F = (i_1/i_2)^2 / 1 + (i_1/i_2)^2$

$i_1 = 200 \text{ A/m}^2$ (efficiency parameter).

$i_2 = \text{Current density (A/m}^2\text{)}$.

Bounded between 70% and 99% for realistic operation[49].

→ **How Current Affects the Electrolyzer:**

Impact on Hydrogen Production

Higher current → More H₂ (linear relationship).

But at very high currents, efficiency drops, reducing gains.

Impact on Faraday Efficiency

Low current density → High efficiency (~99%)

High current density → Lower efficiency (≥70%) [49].

→ **PV System Effects on Electrolyzer Performance:**

Solar Irradiance Changes

More sunlight → Higher PV current → Increased H₂.

Cloudy/weak light → Lower current → Reduced H₂.

Temperature Effects

PV panels lose efficiency when hot → Reduced current.

Electrolyzer efficiency also varies with temperature (not modeled here).

Shading or Degradation

Partial shading → Lower PV output → Less H₂.

Panel aging → Gradual current reduction.

III.3.2 Simulation Approach:

→ **Define Physical Constants**

Faraday's constant (charge per mole of electrons)

Number of electrons needed to produce one H₂ molecule ($z = 2$)

Number of electrolyzer cells (scalable for larger systems).

→ **Calculate Current Density**

Divide input current by cell active area (0.25 m² default)

Current density determines efficiency behavior.

→ **Compute Faraday Efficiency**

Empirical formula relates efficiency to current density

Efficiency decreases at high current densities

Constrained between 70% and 99% for realistic operation.

→ **Calculate Hydrogen Production**

Apply Faraday's law using: Input current

Computed efficiency

Number of cells

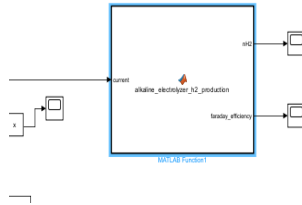
Output is moles of H₂ produced per second

→ Key Relationships

Higher PV current → More H₂ but lower efficiency

Current density directly affects system performance

Model helps optimize PV-electrolyzer pairing.



```

function [nH2, faraday_efficiency] = alkaline_electrolyzer_h2_production(current)
% ALKALINE_ELECTROLYZER_H2_PRODUCTION - Calculates hydrogen production rate and Faraday efficiency
% Inputs:
% current - Current from the system (A)
% Outputs:
% nH2 - Hydrogen production rate (mol/s)
% faraday_efficiency - Faraday efficiency (0-1)

% Constants
F = 96485.3329; % Faraday constant (C/mol)
z = 2; % Number of electrons per water molecule
n_cells = 1; % Number of electrolyzer cells (can be adjusted)

% Current density calculation (A/m2)
% Assuming a standard cell area of 0.25 m2 (can be adjusted)
A_cell = 0.25; % Cell active area (m2)
current_density = current / (n_cells * A_cell);

% Faraday efficiency calculation (based on current density)
% Using a common empirical model for alkaline electrolyzers:
% η_F = (i1/i2)^2 / (1 + (i1/i2)^2)
i1 = 200; % Empirical parameter (A/m2)
i2 = current_density;

faraday_efficiency = (i1/i2)^2 / (1 + (i1/i2)^2);

% Ensure efficiency stays within reasonable bounds
faraday_efficiency = max(0.7, min(0.99, faraday_efficiency));

% Hydrogen production rate (mol/s)
nH2 = (current * faraday_efficiency * n_cells) / (z * F);
end
    
```

figures III.10 :the simulation of the alkaline electrolyser system performance (n-h2 / n-f)

Simulating the performance of the electrolyser that has both the faraday efficiency with the current coming from the pv system and the other constant parameters then the other subsystem is the hydrogen production rate that monitors the performance of the electrolyser that has both the n-f and the pv system current as inputs the current constant here is replaced by the current from the pv system so we can monitor the effects of the irradiance to the electrolyser and see how we can optimize it .

III.3.3 Simulation Model:

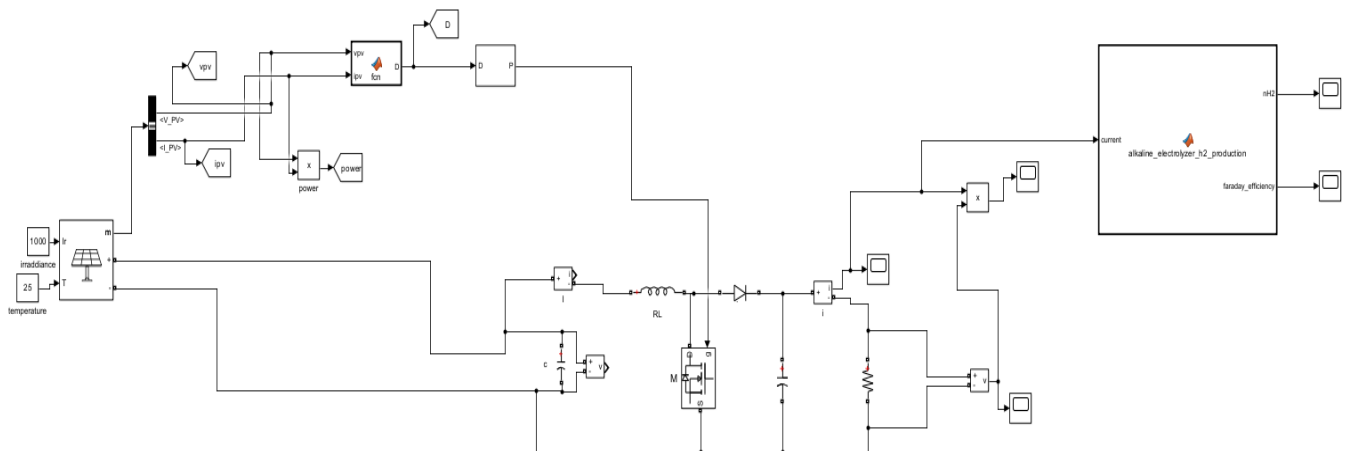


Figure III.11 :The whole MATLAB Simulink pv-electrolyser system simulation model

Pv system connected via output current to the electrolyser system to the faraday efficiency and the hydrogen production rate subsystems.

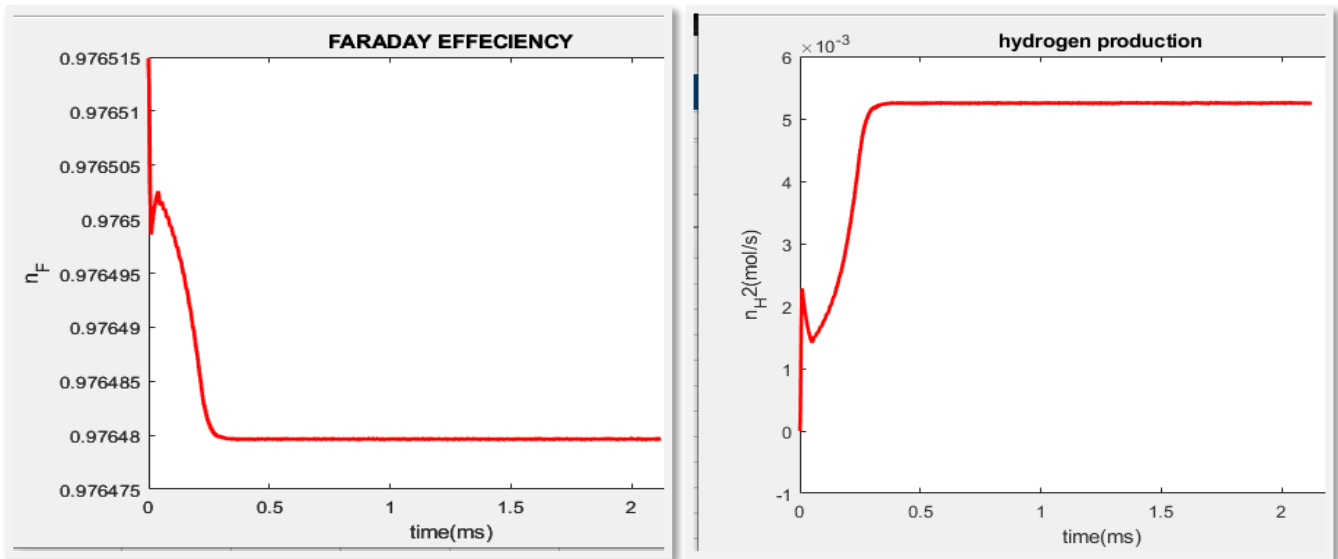


Figure III.12 : The faraday efficiency and hydrogen production rate Graph

The modeling of the PV system with electrolyser have been simulated by using MATLAB-Simulink environment. This system was assembled to present the system depicted in Figure .

The Equations of n_{H_2} and n_f described the functioning of the electrolyser was illustrated by subsystem 1 and subsystem 2 ,who is presented into the previous section. This subsystems were assembled to modeled the electrolyseur system. An electric current generated from a power photovoltaic array is used as an input signal changing in time with solar radiation.

III.3.4 Example to see the effects of irradiance and current on the hydrogen production:

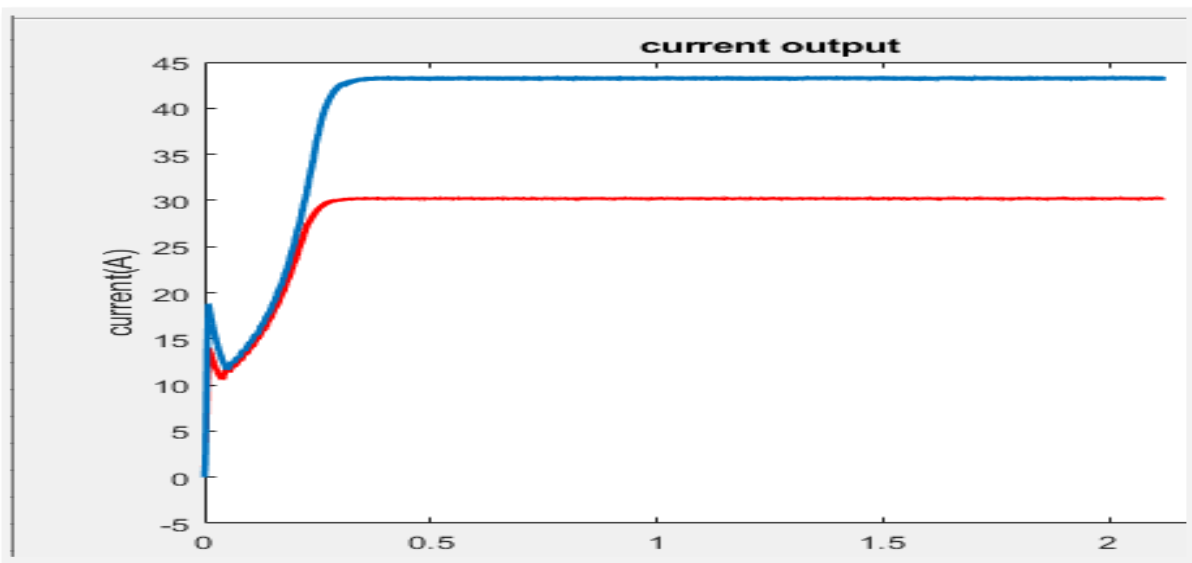


Figure III.13 : Current at irradiance at 1000w/m2 vs 500w/m2

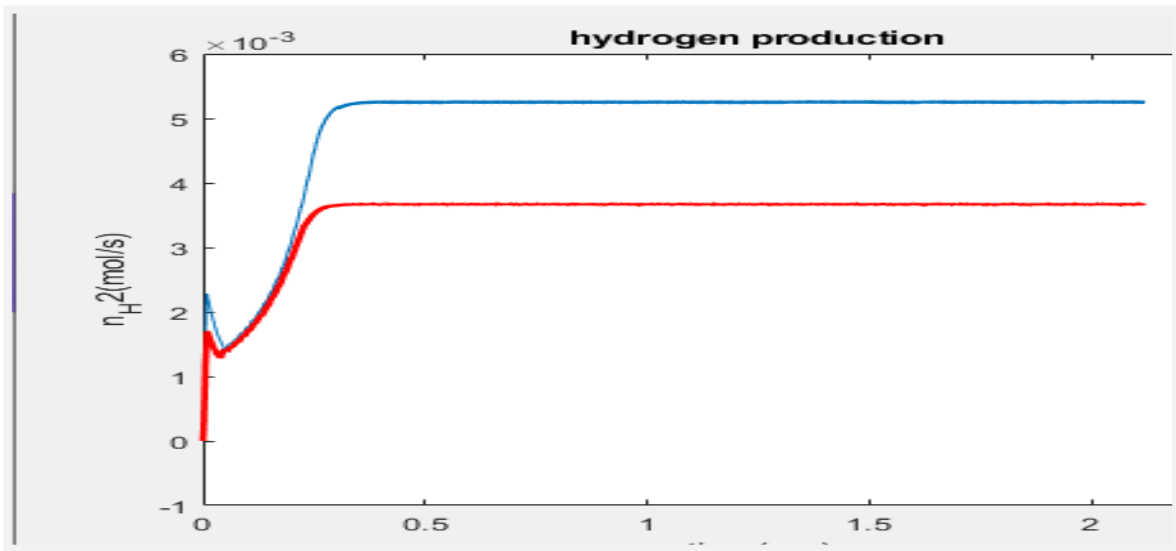


Figure III.14 : n_{H_2} at irradiance at 1000w/m² vs 500 w/m²

Figures 13 and 14 illustrate the proportional relationship between PV system performance and alkaline electrolyzer efficiency. As the available solar irradiance decreases from 1000 W/m² to 500 W/m², the PV system's output current exhibits a corresponding decline from 44.5 A to 30 A. This reduction in current directly impacts hydrogen production, with the generation rate dropping from 5.4×10^{-3} (mol/s) to 3.5×10^{-3} . The data underscores the electrolyzer's dependency on consistent solar input, highlighting the challenges of intermittent renewable energy sources in sustaining optimal hydrogen output.

III.4 Conclusion:

This chapter details the simulation framework for the integrated PV-electrolyzer system, beginning with the PV model coupled to a DC-DC boost converter controlled by a Perturb & Observe (P&O) MPPT algorithm to maximize power extraction under varying irradiance conditions. The alkaline electrolyzer is simulated using electrochemical equations that convert the PV's DC output into hydrogen flow rates, with dynamic models accounting for temperature effects and Faraday efficiency. Key interactions are analyzed, particularly how PV voltage-current characteristics directly determine the electrolyzer's operational range and hydrogen production rate. The simulation reveals critical linkages - PV power fluctuations from MPPT tracking directly impact electrolyzer efficiency, demonstrating why stable maximum power point maintenance is essential for optimal hydrogen yield. This virtual prototyping validates the system's real-world performance potential before experimental implementation.

Chapter IV

**Optimization of hydrogen
production under unfavorable
condition (partial shading)**

IV.1 Introduction:

In this chapter we see that Green hydrogen production relies on consistent and efficient solar energy conversion—but real-world conditions are often imperfect. This chapter examines how partial shading and other challenges impact PV-electrolyzer systems and explores intelligent optimization techniques to maximize hydrogen output even under adverse scenarios.

We begin by analyzing partial shading, a common issue where uneven sunlight distribution (due to clouds, dust, or obstructions) creates multiple power peaks in the PV system's output. Traditional MPPT algorithms like Perturb & Observe (P&O) struggle in these conditions, often getting trapped in local maxima and failing to extract the global maximum power point (GMPP).

To overcome this, we turn to intelligent optimization algorithms, such as:

Cuckoo Search Algorithm (CSA) – A bio-inspired method that efficiently tracks the GMPP even under complex shading patterns.

Hybrid FDB-TLABC Algorithm – A more advanced approach combining Fitness-Distance Balance (FDB) and Teaching-Learning-Based Artificial Bee Colony (TLABC) for faster convergence, higher stability, and superior tracking accuracy compared to standalone algorithms.

By integrating these AI-driven MPPT techniques, we ensure that the PV system operates at peak efficiency, delivering stable power to the electrolyzer. This optimization directly enhances hydrogen production rates (nH₂) and Faraday efficiency (nF), making green hydrogen systems more resilient and economically viable even in suboptimal environments.

IV.2 The Partial Shading:

Partial shading occurs when some parts of a solar PV array are shaded (e.g., by trees, buildings, dust, or clouds) while other parts remain exposed to sunlight. This creates non-uniform irradiance across the PV array, leading to mismatched operating conditions among the PV modules.

IV.2.1 How Partial Shading Happen:

Partial shading can occur due to:

Obstacles: Trees, buildings, or poles casting shadows on the PV array.

Dust or Dirt: Accumulation on certain parts of the PV modules.

Clouds: Passing clouds that partially cover the PV array.

Bird Droppings: Droppings that block sunlight on specific areas of the modules[50].

System IV curve is built from individual substring IV curves in series and parallel.

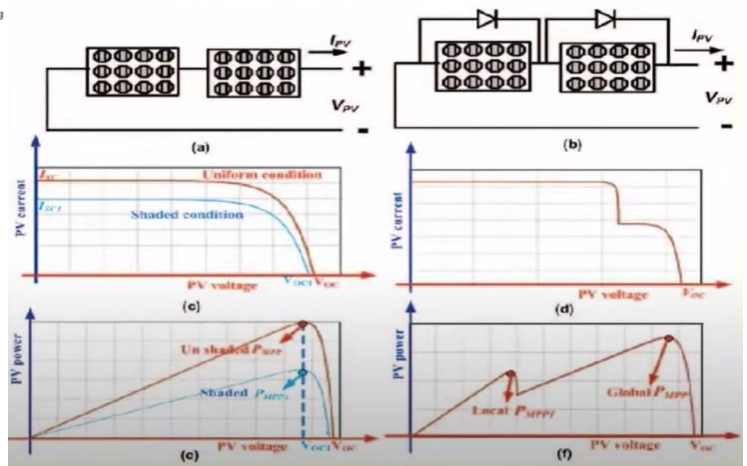
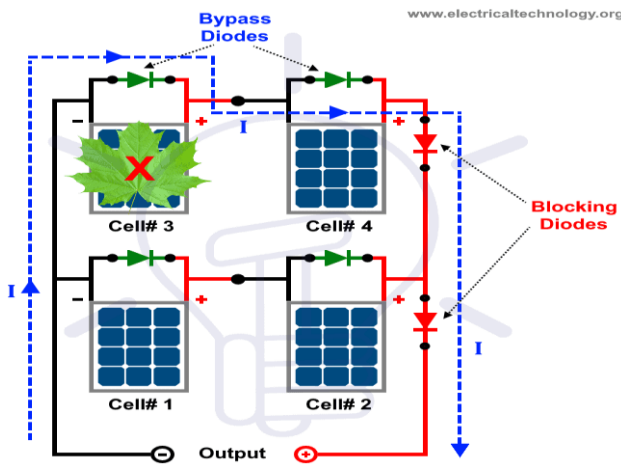
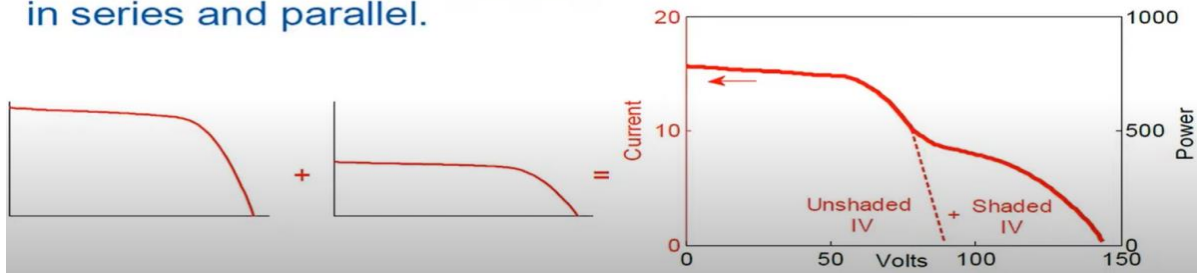


Figure IV.1 :the effects of partial shading on a pv system current and the job of bypass diodes[10][11]

IV.2.2 Effects of Partial Shading on the PV System:

→ On the P-V power Curve

Under uniform irradiance, the P-V power curve of a PV array has a single peak (one MPP).

However, under partial shading, the P-V curve becomes multi-modal, meaning it has multiple peaks:

Global Maximum Power Point (**GMPP**): The highest peak, representing the maximum power the PV array can produce under the given shading conditions.

Local Maximum Power Points (**LMPPs**): Lower peaks that represent suboptimal operating points[50][51].

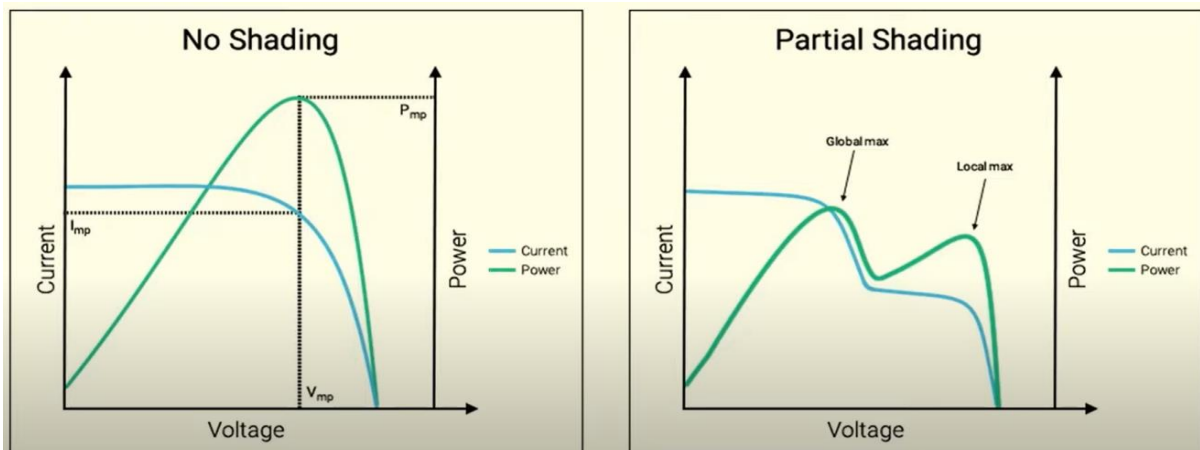


Figure IV.2 :the i-v / p-v curve showcasing the multiple power peaks effects due the PS[12]

→ **On the I-V Curve**

The I-V curve also changes under partial shading:

Steps or kinks: The I-V curve develops steps or kinks due to the activation of bypass diodes in shaded modules.

Reduced current: The overall current output of the PV array decreases because shaded modules produce less current.

→ **On Power Output**

Power loss: Partial shading significantly reduces the total power output of the PV array.

Hotspots: Shaded cells can dissipate power as heat, leading to hotspots and potential damage to the PV modules[51].

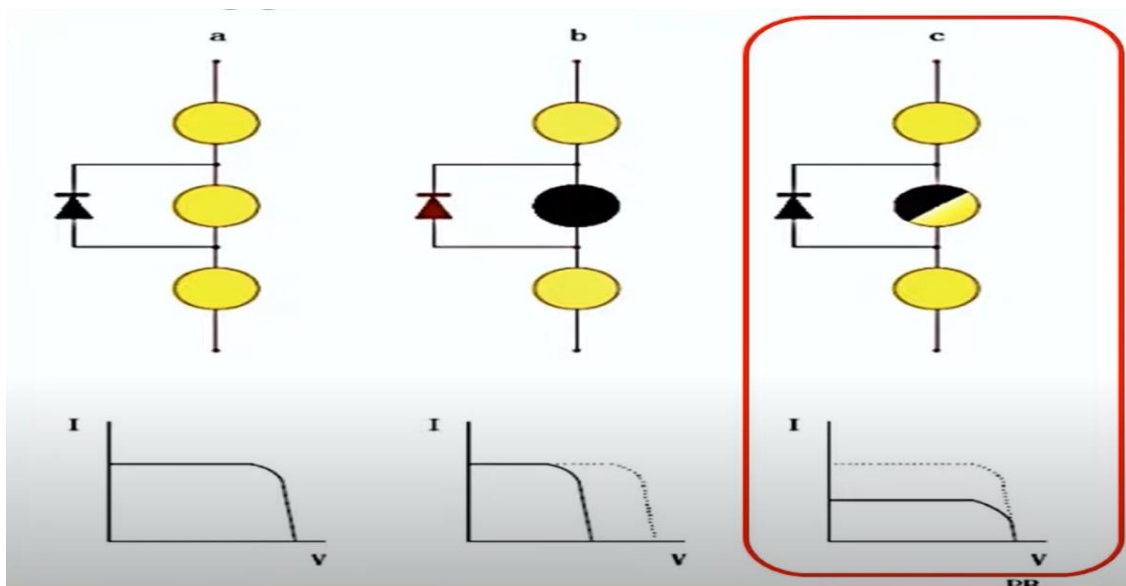


Figure IV.3 : the I-V curve showcasing the effects of full shading compared to partial shading the pv in series systems voltage and current[13]

IV.2.3 How to Simulate Partial Shading:

To study the effects of partial shading, we simulate it in software tools like MATLAB/Simulink, PSIM, or PVsyst. Here's how it's done:

→ **Modeling the PV Array**

The PV array is modeled as a combination of series and parallel-connected PV modules.

Each module is represented by its equivalent circuit (e.g., a single-diode or double-diode model)[52][53].

→ **Introducing Shading**

Shading is simulated by reducing the irradiance on specific modules in the array.

For example, if one module in a series string is shaded, its irradiance is set to a lower value (e.g., 200 W/m² instead of 1000 W/m²)[52][53].

→ **Bypass Diodes**

Bypass diodes are added across each module or group of modules to prevent reverse bias and hotspot formation[50].

When a module is shaded, its bypass diode activates, allowing current to flow around the shaded module.

→ **Simulation Setup**

The PV array is connected to a load or DC-DC converter (e.g., a buck or boost converter).

The system is simulated under different shading patterns to observe the effects on the P-V and I-V curves.

IV.3 System Configuration:

- 3 PV panels in series
- Uneven irradiance (e.g., 1000/500/1000 W/m²)
- Each panel has bypass diodes.

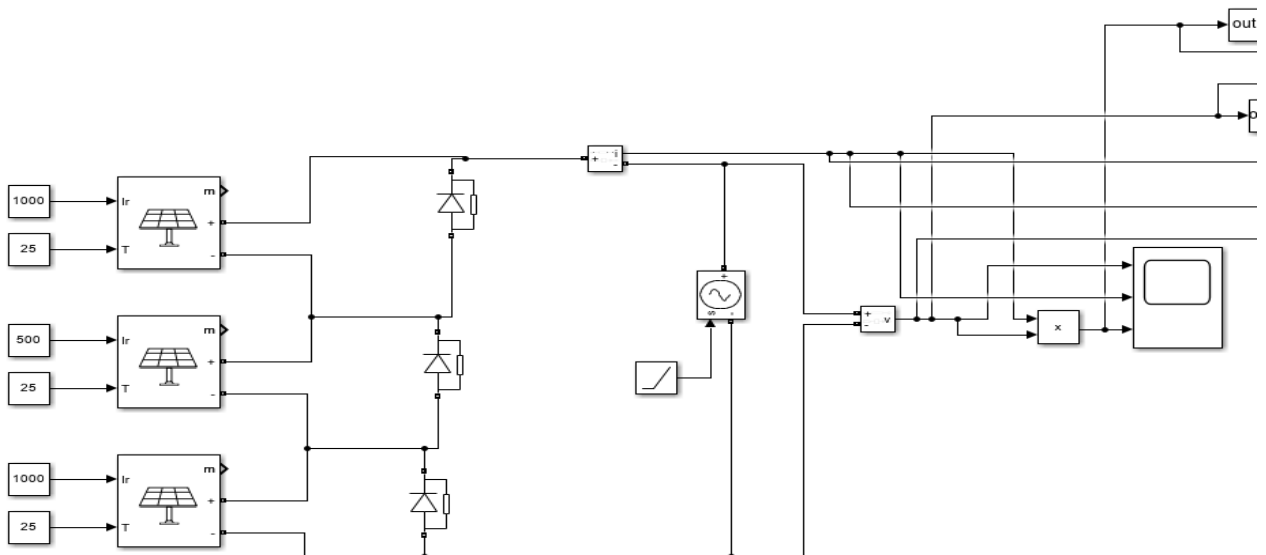


Figure IV.4 :the Simulation of a 3 identical panels in series pv system under partial shading

IV.3.1 Power Curve Characteristics:

Shows multiple peaks due to partial shading:

- Global MPP (highest power point)
- Local MPPs (lower power peaks)

Steps in curve occur when bypass diodes activate.

Power drops sharply at panel-specific V_{mp} points.

IV.3.2 Current-Voltage (I-V) Curve Behavior:

- Current "steps" correspond to bypass diode activation
- Flat current regions until each panel reaches its I_{sc}
- Multiple inflection points visible

IV.3.3 Why Use Controlled Voltage Source with Ramp:

Sweeps voltage from 0V to $V_{oc} \times N$ (N=series panels)

Ensures full curve characterization:

- Captures all operating points
- Reveals all possible MPPs
- Shows bypass diode effects clearly

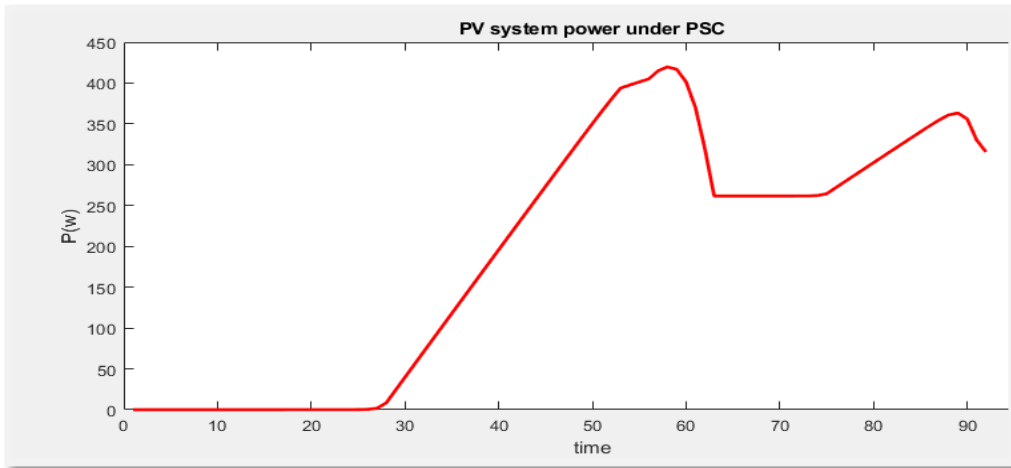


Figure IV.5 :Power output with multiple peaks under PSC

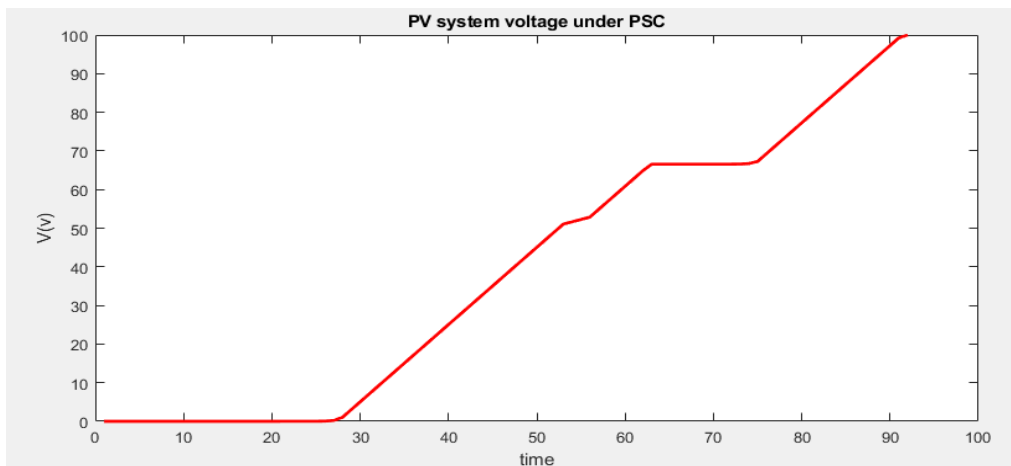


Figure IV.6 :Voltage output under PSC

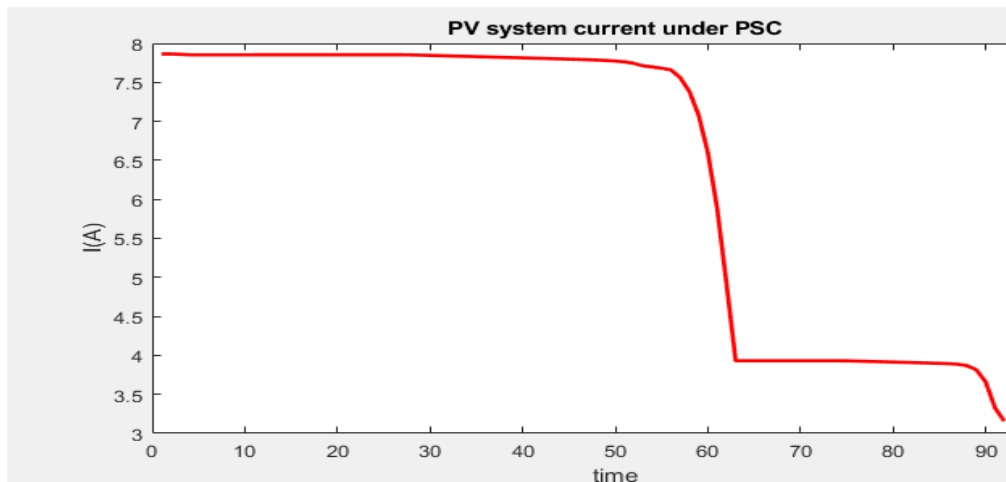


Figure IV.7 :current output under PSC

A more complex system with 3by3 pv system with different ones under partial shading

Showing the same effects with multiple power peaks

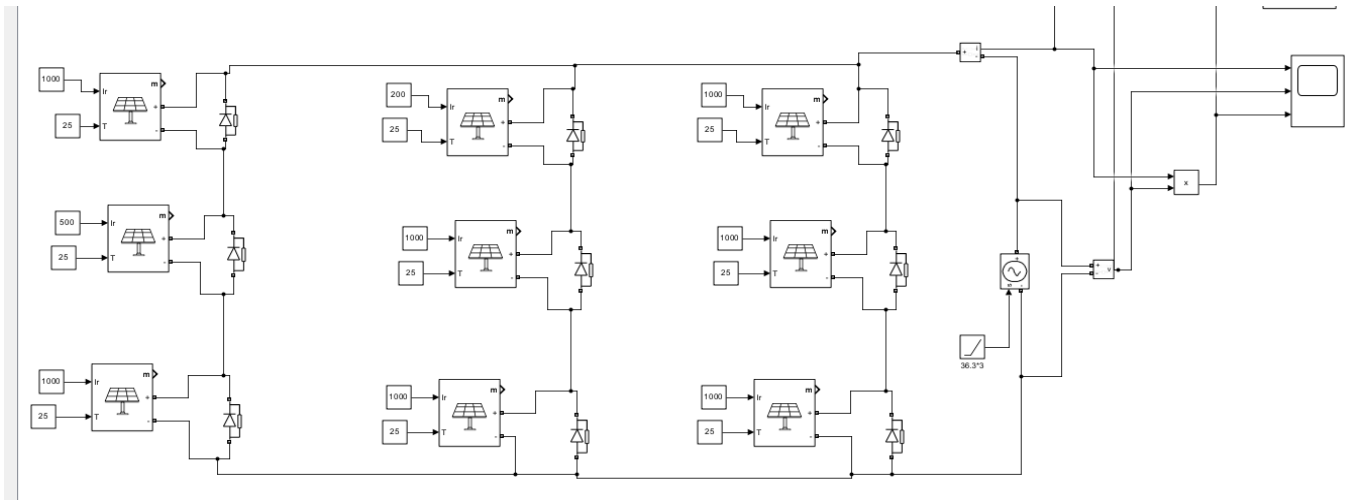


Figure IV.8 :Simulation of a 3 panels in series in parallel with two identical 3 in series systems pv system under partial shading

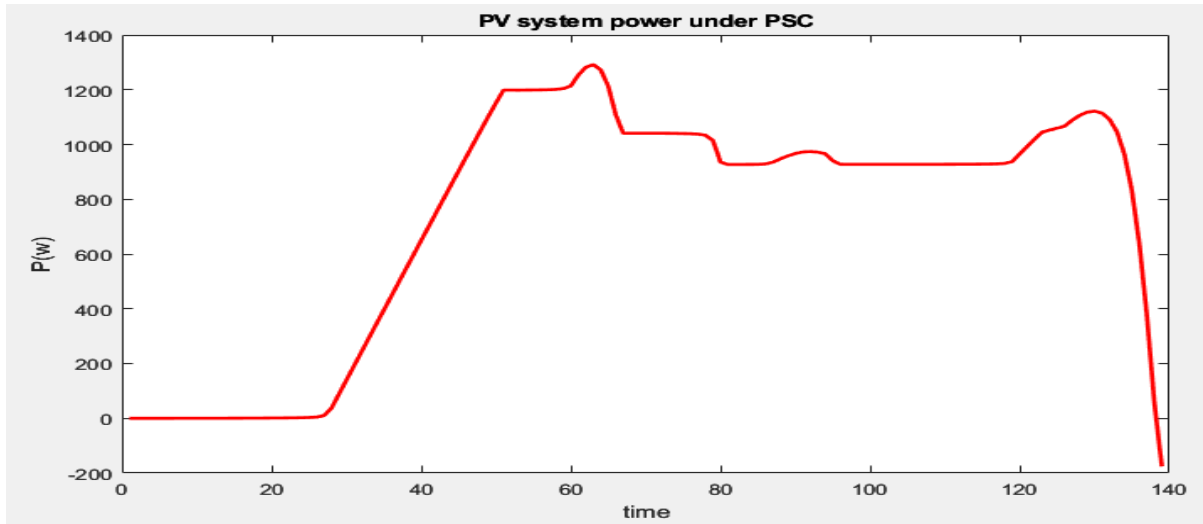


Figure IV.9 :Power output with multiple peaks under PSC

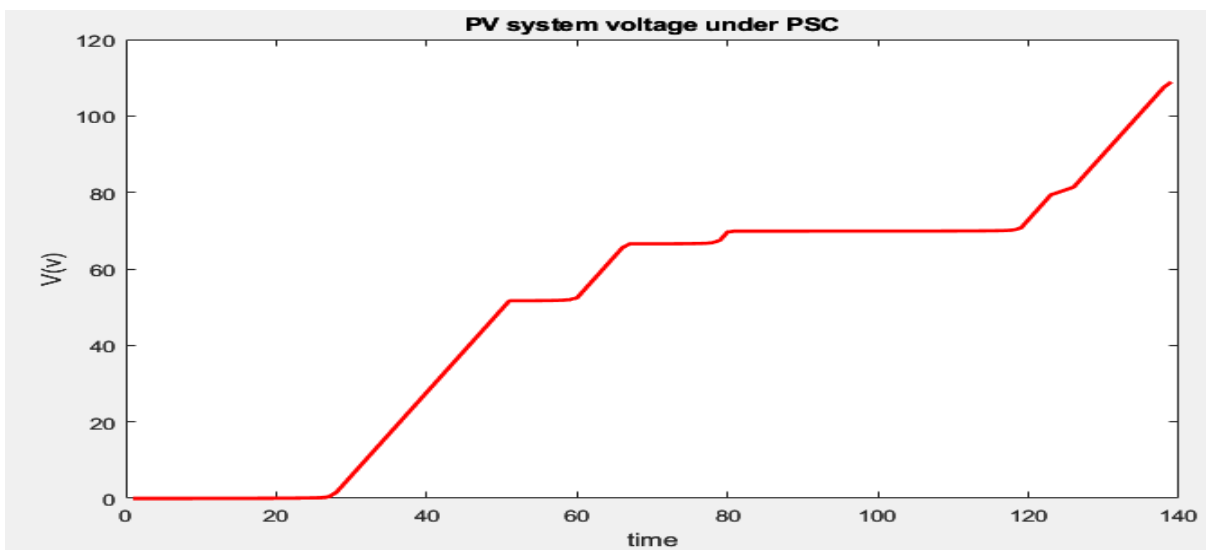


Figure IV.10 :Voltage output under PSC

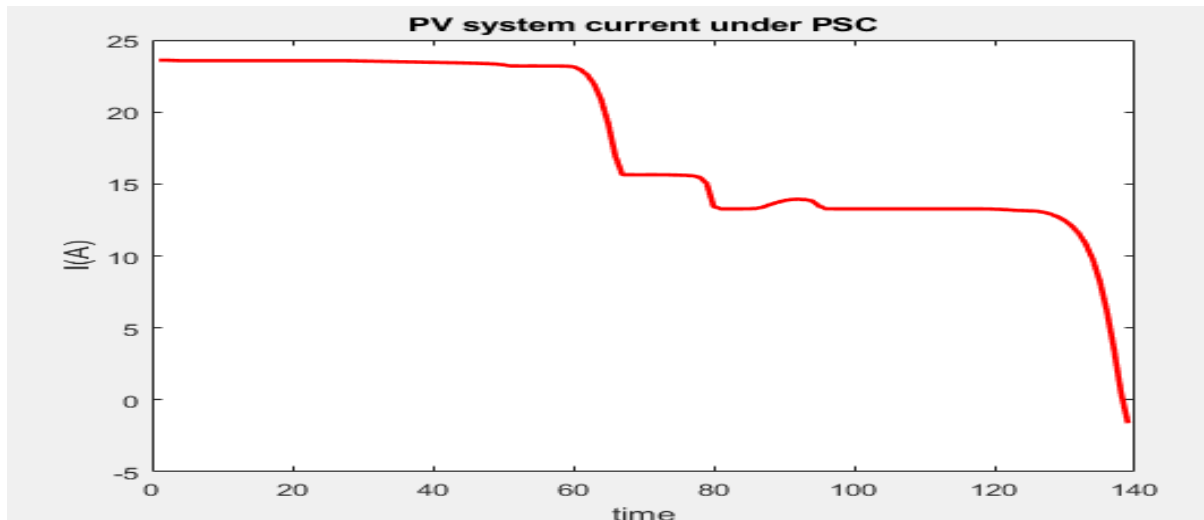


Figure IV.11 :current output under PSC

IV.3.4 Effects of Partial Shading on MPP Points:

Multiple Peaks in the Power Curve

Under partial shading, the Power curve develops multiple peaks due to the mismatch in current and voltage among the modules.

The GMPP is the highest peak, while the LMPPs are lower peaks.

Challenges for MPPT Algorithms

Traditional MPPT algorithms like Perturb and Observe (P&O) and Incremental Conductance (IncCond) may get stuck in a local maximum and fail to find the GMPP.

Advanced algorithms are needed to locate the GMPP.

Power Loss

The power output at the LMPPs is significantly lower than at the GMPP.

If the MPPT algorithm fails to find the GMPP, the system operates at a suboptimal point, leading to energy losses.

IV.4 MPPT Algorithms for Partial Shading Conditions:

IV.4.1 Conventional MPPT Methods (Struggle with Partial Shading):

Perturb & Observe (P&O) – Tracks MPP by perturbing voltage but gets stuck at local peaks.

Incremental Conductance (INC) – Better than P&O but still fails under shading.

IV.4.2 Intelligent MPPT Algorithms (For Global MPP Tracking - GMPP):**→ Nature-Inspired Metaheuristic Algorithms (Single-Method)**

Cuckoo Search Algorithm (CS)

- Inspired by bird behavior (egg-laying strategy).
- Efficiently explores multiple peaks to find GMPP.

→ Hybrid Intelligent Algorithms (Combined Techniques)

Fitness-Distance Balance based TLABC (FDB-TLABC)

- Hybrid of Teaching-Learning-Based Optimization (TLBO) and Artificial Bee Colony (ABC).
- Uses fitness-distance balance for better exploration.

IV.4.3 Using Intelligent Algorithms:

Partial shading creates multiple power peaks (local & global).

Traditional methods get stuck at local maxima.

Metaheuristic (CS) & Hybrid (FDB-TLABC) algorithms ensure reliable GMPP tracking under shading.

IV.4.4 The Reason of the failure P&O Under Partial Shading:**→ Problem with P&O Algorithm:**

Gets trapped at local power peaks (LMPP) instead of finding the true Global MPP (GMPP)

Causes power loss (typically 10-30% lower than possible in our case it has around 22% less power and current and hydrogen production rate)

Produces steady-state oscillations (ripples) around MPP

Slow response to shading changes.

→ Result:

- Suboptimal power extraction
- Wasted solar energy

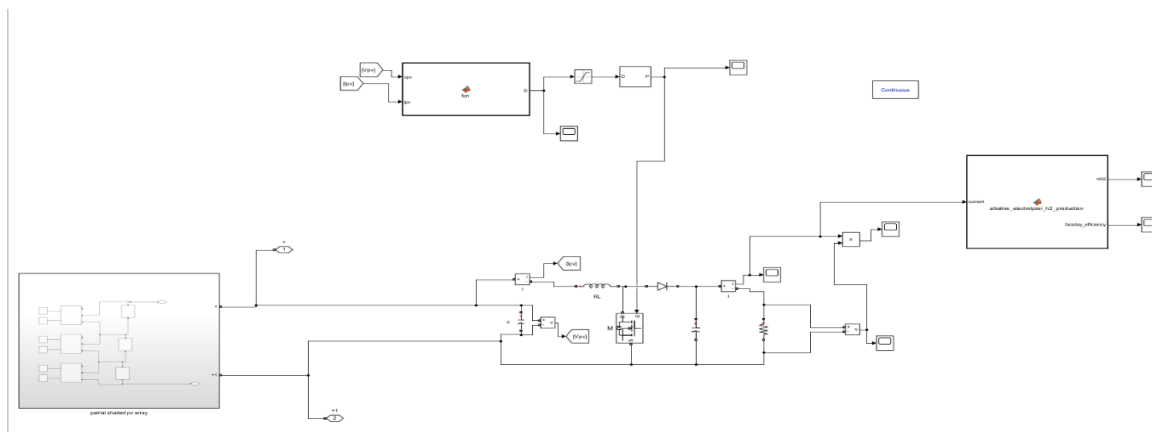


Figure IV.12 :the Whole pv-electrolyser system simulation with the pv system under partial shading using po mppt algorithm

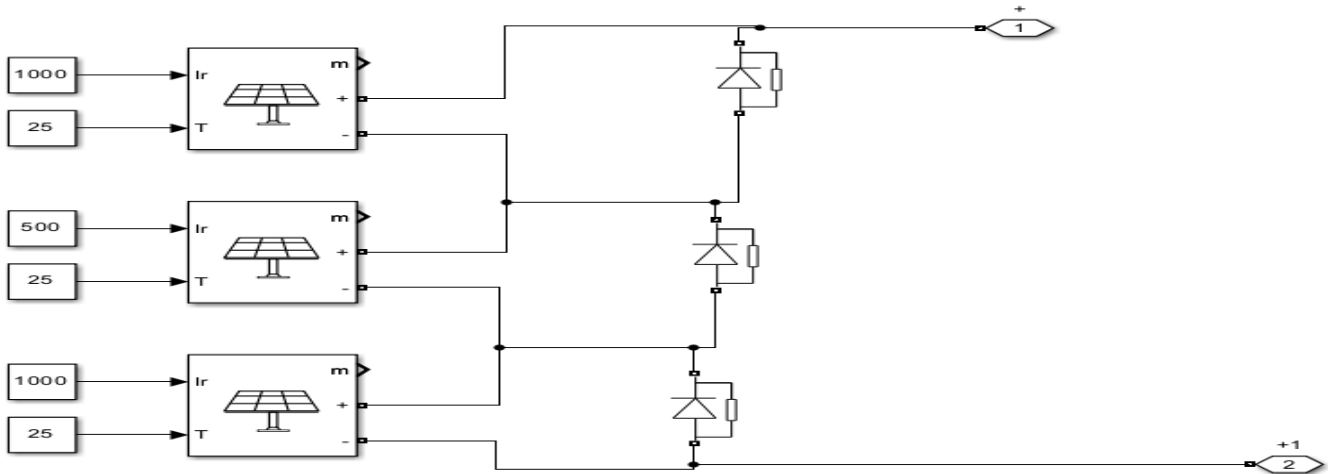


Figure IV.13 :Simulation of a pv system under partial shading with a GMPP power of 400w we want to reach

IV.4.5 P&O Power Output Characteristics:

Observed Behavior:

→ **Reduced Power Level**

Typically extracts only 70-90% of available GMPP power it has around 22% less power output compared to the intelligent algorithms in our case

→ **Ripple Effects**

Visible oscillations in power output

Amplitude depends on step size (typically ±3% of power)

→ **Step Artifacts**

Sudden jumps when shading pattern changes

Temporary power drops during re-tracking

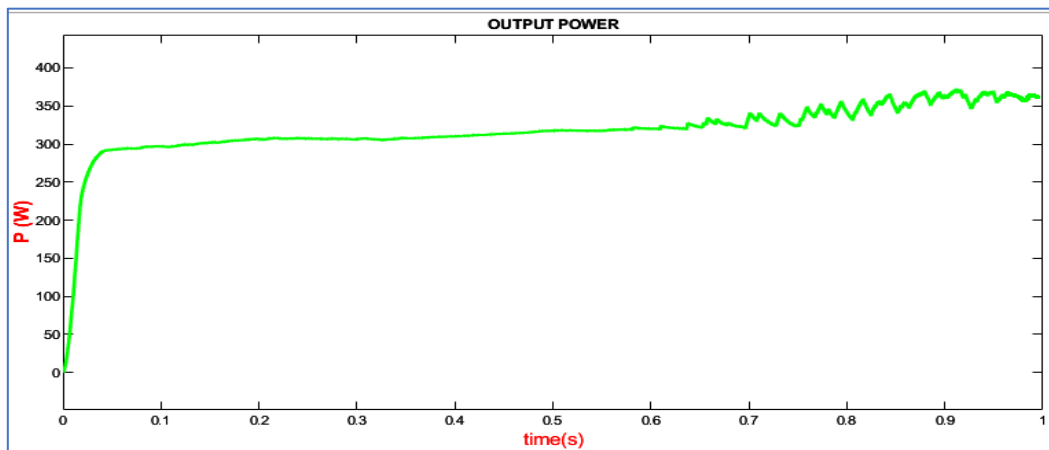


Figure IV.14 :The po mppt pv system Power output

IV.5 Electrolyzer Impact from P&O Limitations:

Current Feed Effects:

→ **Reduced Hydrogen Production**

Faraday efficiency drops further at lower currents

→ **Ripple Propagation**

Current fluctuations cause:

→ 2-3% variation in Faraday efficiency

→ Mechanical stress on electrolyzer membranes

→ **System Inefficiency**

Energy wasted as heat during oscillations

Accelerated component aging

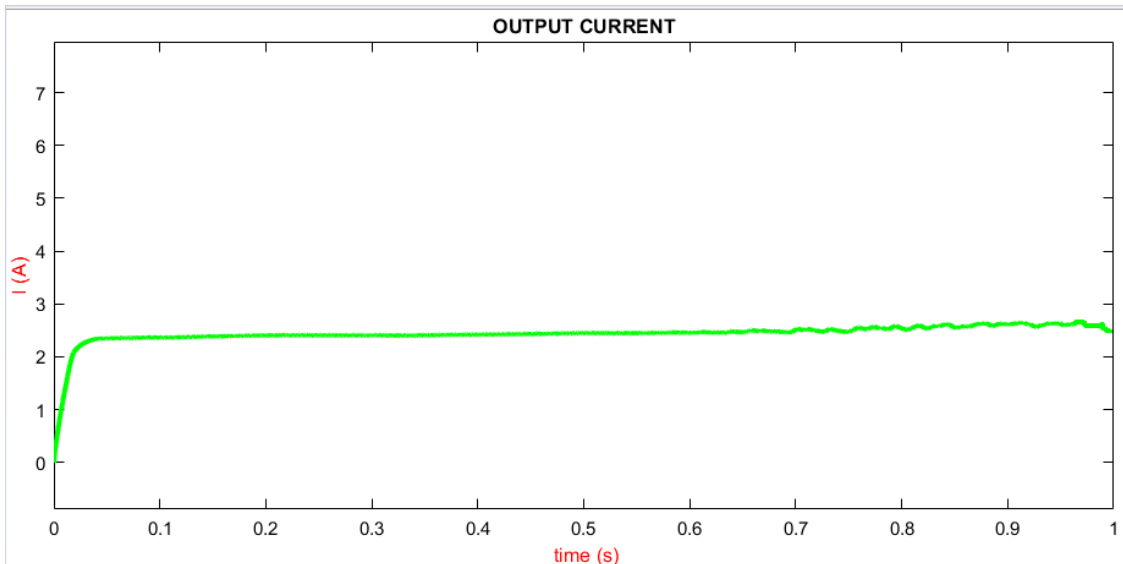


Figure IV.15 :The po mppt pv system current output

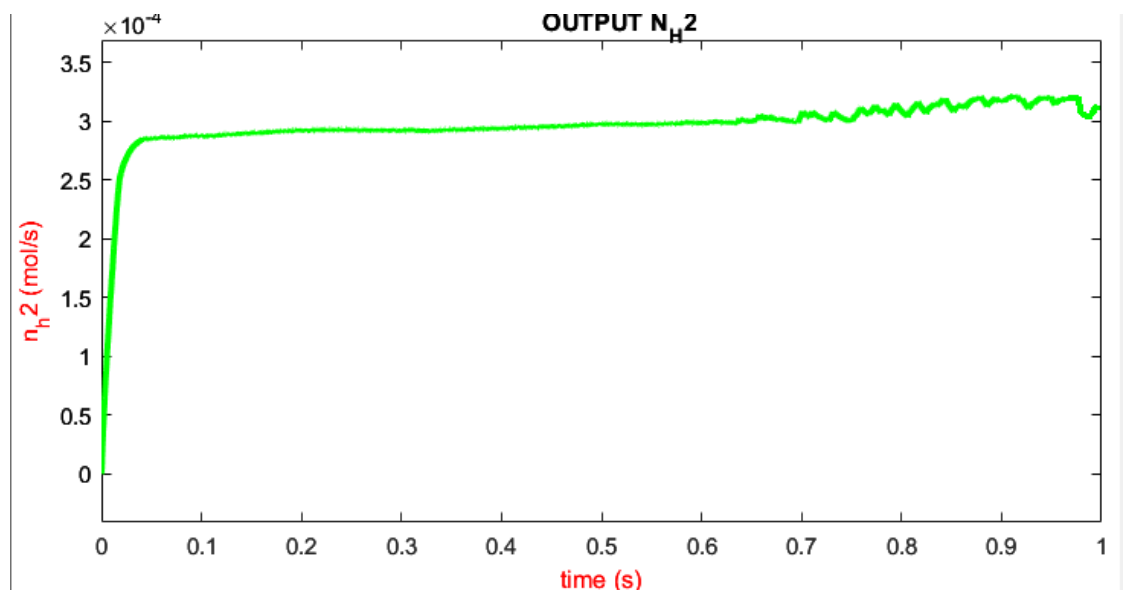


Figure IV.16 :The po mppt pv system n_h2 output

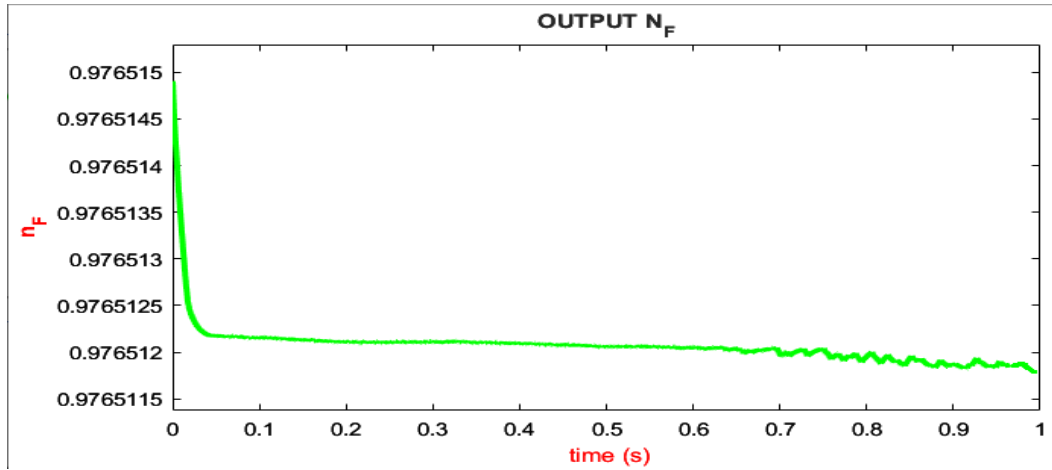


figure IV.17 :The po mppt pv system n_F output

From looking at the Figure IV.14 we see that the use of traditional p&o MPPT algorithm leads to a lower and more unstable power outputs of around the 350w LMPP same goes for the Figure IV.15 the current output and since the performance of the electrolyser system is directly proportional to the pv system output current where we see in Figure IV.16 and Figure IV.17 the same lower value and being more unstable which shows the limitations of traditional mppt algorithms such as the p&o under PSC .

IV.6 cuckoo Search MPPT Algorithm for PV Systems under Partial Shading:

IV.6.1 the Cuckoo Search Algorithm:

The Cuckoo Search (CS) algorithm is a nature-inspired metaheuristic optimization algorithm developed by Xin-She Yang and Suash Deb in 2009. It is inspired by the brood parasitism behavior of cuckoo birds, where cuckoos lay their eggs in the nests of other host birds. If the host bird discovers the foreign eggs, it may either throw them out or abandon the nest. This behavior is mimicked in the algorithm to solve optimization problems[54] .

The algorithm also incorporates Lévy flights, which are a type of random walk that allows for both local and global search capabilities. Lévy flights are inspired by the foraging behavior of animals and insects, enabling the algorithm to explore the search space efficiently.

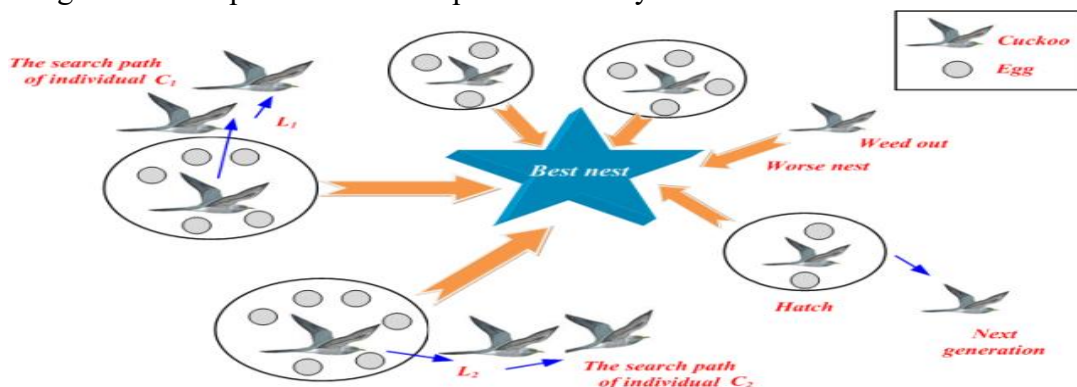


Figure IV.18 :The natural working of the cuckoo search algorithm[14]

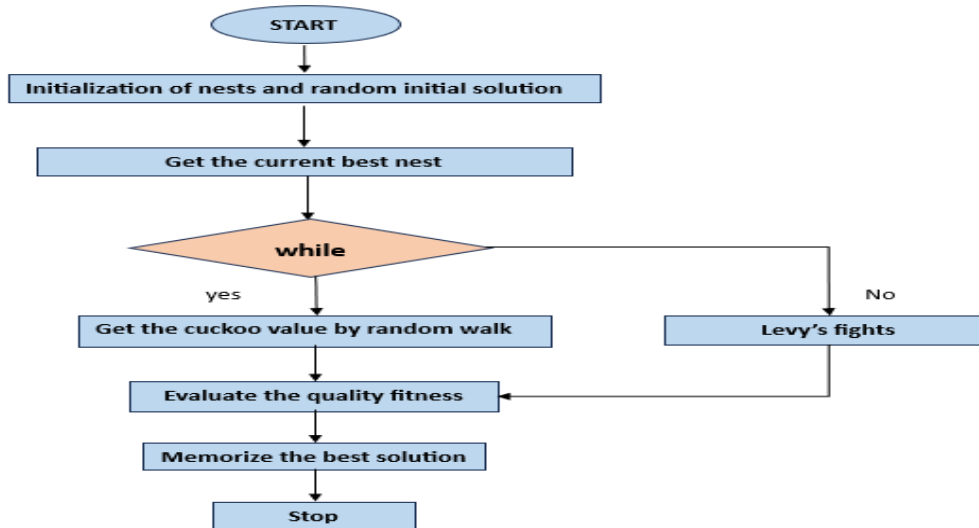


Figure IV.19 :The structure of the cuckoo search algorithm [15]

IV.6.2 Working Principle of the Cuckoo Search Algorithm:

The Cuckoo Search algorithm operates based on the following principles:

→ Cuckoo Breeding Behavior:

Each cuckoo lays one egg (solution) in a randomly chosen nest (search space).

The best nests (solutions) are carried forward to the next generation.

If a host bird discovers a cuckoo egg, it abandons the nest, and the cuckoo must find a new nest (solution).

→ Lévy Flights:

Lévy flights are used to generate new solutions by taking random steps with a heavy-tailed probability distribution.

This allows the algorithm to explore the search space effectively, balancing between local and global search[54].

→ Randomization and Selection:

Randomization ensures diversity in the search process.

Selection ensures that the best solutions are retained.

IV.6.3 General Equations in Cuckoo Search Algorithm:

→ Lévy Flight for Generating New Solutions

A new solution (cuckoo) $x_i(t+1)$ is generated using Lévy flights:

$$x_i(t+1) = x_i(t) + \alpha \oplus \text{Levy}(\lambda) \quad \text{where :}$$

$x_i(t)$ = current solution at iteration t ,

α = step size (usually $\alpha=1$),

\oplus = entry-wise multiplication,

$\text{Levy}(\lambda)$ = random step drawn from a Lévy distribution (heavy-tailed)[54].

→ Lévy Distribution

The step length s is calculated as:

$$s = u / |v|^{1/\beta} \quad \text{where:}$$

$$u \sim N(0, \sigma_u^2)$$

$$v \sim N(0, \sigma_v^2)$$

$$\beta = 3/2 \text{ (typically)}$$

Γ = Gamma function.

→ Host Nest Replacement (Abandonment)

A fraction pa of the worst nests is abandoned, and new ones are generated:

$$x_{\text{worst}}(t+1) = x_{\text{worst}}(t) + r \cdot (x_{\text{rand1}}(t) - x_{\text{rand2}}(t)) \quad \text{where:}$$

r = random number $\in [0, 1]$

$x_{\text{rand1}}, x_{\text{rand2}}$ = randomly selected solutions.

IV.6.4 Cuckoo Search Algorithm for PV System Optimization (Duty Cycle Control):

In a PV system, we often need to optimize the duty cycle (D) of a DC-DC converter (e.g., buck, boost, or buck-boost) to extract the Maximum Power Point (MPP) under varying irradiance and temperature.

The Cuckoo Search Algorithm (CSA) can be applied to dynamically adjust D such that the PV system operates at its highest efficiency.

Objective: Maximize PV power $P = V_{pv} \times I_{pv}$ by optimizing D .

Control Variable: Duty cycle D (where $0 \leq D \leq 1$).

IV.6.4.1 Cuckoo Search Equations for Duty Cycle Optimization:

→ Lévy Flight-Based Duty Cycle Update

A new candidate duty cycle $D_i(t+1)$ is generated using Lévy flights:

$$D_i(t+1) = D_i(t) + \alpha \oplus \text{Levy}(\lambda) \quad \text{where:}$$

$D_i(t)$ = current duty cycle at iteration t ,

α = step size (e.g., $\alpha = 0.01$),

$\text{Levy}(\lambda)$ = random step from Lévy distribution (encourages both small and large jumps)[54].

→ Power Calculation (Fitness Function)

For each D_i , measure V_{pv} and I_{pv} , then compute:

$$P_i = V_{pv} \times I_{pv} \quad \text{The goal is to maximize } P_i$$

→ Host Nest Replacement (Abandoning Poor Solutions)

A fraction pa (e.g., $pa = 0.2$) of the worst-performing duty cycles (lowest P_i) are discarded and replaced with new random values:

$$D_{\text{worst}}(t+1) = D_{\text{rand1}}(t) + r \cdot (D_{\text{rand2}}(t) - D_{\text{rand3}}(t)) \quad \text{where:}$$

$r =$ random number $\in [0,1] \in [0,1]$,

Drand1, Drand2, Drand3 = randomly selected duty cycles.

IV.6.5 How Cuckoo Search is Used for MPPT in PV Systems under Partial Shading:

In a photovoltaic (PV) system, partial shading occurs when some parts of the PV array receive less sunlight due to obstructions like clouds, trees, or buildings. This creates multiple local maxima in the power-voltage (P-V) curve, making it challenging for traditional MPPT algorithms (like Perturb and Observe or Incremental Conductance) to find the global maximum power point (GMPP).

The Cuckoo Search MPPT algorithm is well-suited for this problem because of its ability to explore the search space efficiently and avoid getting trapped in local maxima. Here's how it works in a PV system:

→ **Initialization:**

Initialize a population of "nests" (candidate solutions), where each nest represents a possible voltage or duty cycle value for the PV system.

Define the search space (e.g., the range of possible voltage or duty cycle values).

→ **Fitness Evaluation:**

For each nest, calculate the corresponding power output of the PV system.

The power output is the fitness value, and the goal is to maximize it.

→ **Lévy Flight Exploration:**

Generate new solutions (nests) using Lévy flights to explore the search space.

This helps the algorithm escape local maxima and explore the global search space.

→ **Nest Replacement:**

Compare the new solutions with the existing ones.

Replace inferior nests with better ones based on their fitness values.

→ **Convergence to GMPP:**

Repeat the process until the algorithm converges to the global maximum power point (GMPP).

The algorithm dynamically adjusts the voltage or duty cycle to track the GMPP even under partial shading conditions.

IV.6.5.1 Advantages of Cuckoo Search for MPPT in Partial Shading:

Global Search Capability: The Lévy flight mechanism allows the algorithm to explore the entire search space, making it effective in finding the GMPP under partial shading.

Robustness: The algorithm is less likely to get stuck in local maxima compared to traditional MPPT methods.

Simplicity: The algorithm has few parameters to tune, making it easy to implement.

Adaptability: It can adapt to changing environmental conditions (e.g., varying irradiance and temperature).

IV.6.5.2 Key Steps & Working Principle:→ **Initialization**

Starts with 4 fixed duty cycles (0, 0.3, 0.5, 0.9) as initial "nests."

Measures PV voltage and current to compute power for each duty cycle.

Identifies the best-performing duty cycle (dbest) based on maximum power.

→ **Exploration via Lévy Flights**

Random Walk: Uses Lévy flight distribution to generate new duty cycles, enabling large jumps for global search.

Dynamic Adjustment: Updates nests (duty cycles) based on:

Best solution (dbest) for guided search.

Randomized Lévy steps to escape local optima.

→ **Nest Replacement & Discovery**

Abandonment: If a duty cycle underperforms, it is replaced via:

Discovery Probability (25% chance): Replaces the worst nest with a new Lévy-adjusted value.

Elitism: Keeps the best solution while perturbing others.

Power Re-evaluation: Measures new power after each adjustment.

→ **Convergence to GMPP**

Continuously refines duty cycles, favoring those that extract higher power.

Returns the best duty cycle (dbest) for DC-DC converter control.

IV.6.5.3 THE PURPOSE OF THESE VARIABLES IN THE SYSTEM :

→ **U**: used to cycle through different steps or states of the algorithm for example it might control which duty cycle is being evaluated or updated

→ **Dcurrent**: represents the current duty cycle being tested the algorithm evaluates the pv power at this duty cycle the determine if it is better that previous solutions

→ **P**: stores the power values corresponding to different duty cycles this helps the algorithm compare and identify the best solution

→ **Dc** : stores the duty cycles being explored these are the NESTS in the cuckoo search algorithm

→ **Dbest** : tracks the best duty cycle found so far (the one that maximizes the power)

→ **Counter** : used to control the timing or iteration steps for example it might delay updates to the duty cycle to allow the system to stabilize

→ **Iworst** : identifies the worst performing duty cycle (lowest power) this is used to replace poor solutions with new ones

→ **Discover** : a flag that indicates whether a new solution has been discovered this is part of the cuckoo search mechanism for replacing poor solutions .

IV.6.5.4 How to fit these variables into the cuckoo search algorithm:

The cuckoo search algorithm works by:

exploring solutions: testing different duty cycles (dc) and evaluating their corresponding power values (p).

identifying the best solution: tracking the best duty cycle (dbest) that maximizes the power .

replacing poor solutions: using the LEVY FLIGHT MECHANISM to replace the worst performing duty cycle (iworst) with a new solution.

iterating: repeating the process until the algorithm converges to the MPP.

The variables mentioned before are used for :

- Initialize the algorithm
- Store and update the state of the system
- Control the flow of the algorithm

IV.6.6 LEVY FLIGHT FUNCTION :

This function implements the LEVY FLIGHT mechanism which is used to generate new solutions (duty cycles) in the cuckoo search algorithm

What each part does :

Beta : a parameter controlling the SHAPE OF LEVY DISTRIBUTION (set to 3/2)

Kcoeff : a scaling factor for the STEP SIZE (set to 0.8)

Sigmau and sigmav : parameters for the levy distribution calculated using GAMMA function

u and v : random numbers generated from normal distribution

dup : is the new duty cycle generated using the LEVY FLIGHT FORMULA :

$$dup = d + (kcoeff \cdot \frac{|u|}{|v|^{1/b}}) \cdot (dbest - d)$$

boundary handling: - If dup>1 it is clamped to 1

- If dup<0 it is clamped to 0

- Otherwise dup is returned as the new duty cycle

```
function dfinal=levyflight(dbest,d)
beta=3/2;
kcoeff=0.8;
sigmau=(gamma(1+beta)*sin(pi*beta/2)/(gamma((1+beta)/2)*beta*2^((beta-1)/2)))^(1/beta);
sigmav=1;
u=normrnd(0,(sigmau)^2);
v=normrnd(0,(sigmav)^2);
dup=d+(kcoeff*(abs(u)/((abs(v))^(1/beta)))*(dbest-d));

if(dup>1)
    dfinal=1;
elseif(dup<0)
    dfinal=0;
else
    dfinal=dup;
end
end
```

Figure IV.20 :the levy flight equation in the cuckoo mppt algorithm

IV.6.7 Whole system:

This algorithm implements Maximum Power Point Tracking (MPPT) for photovoltaic (PV) systems using Cuckoo Search Optimization, inspired by the brood parasitism behavior of cuckoo birds. It dynamically adjusts the duty cycle (D) of a DC-DC converter to maximize power extraction from the solar panel under varying conditions (e.g., partial shading, irradiance changes).

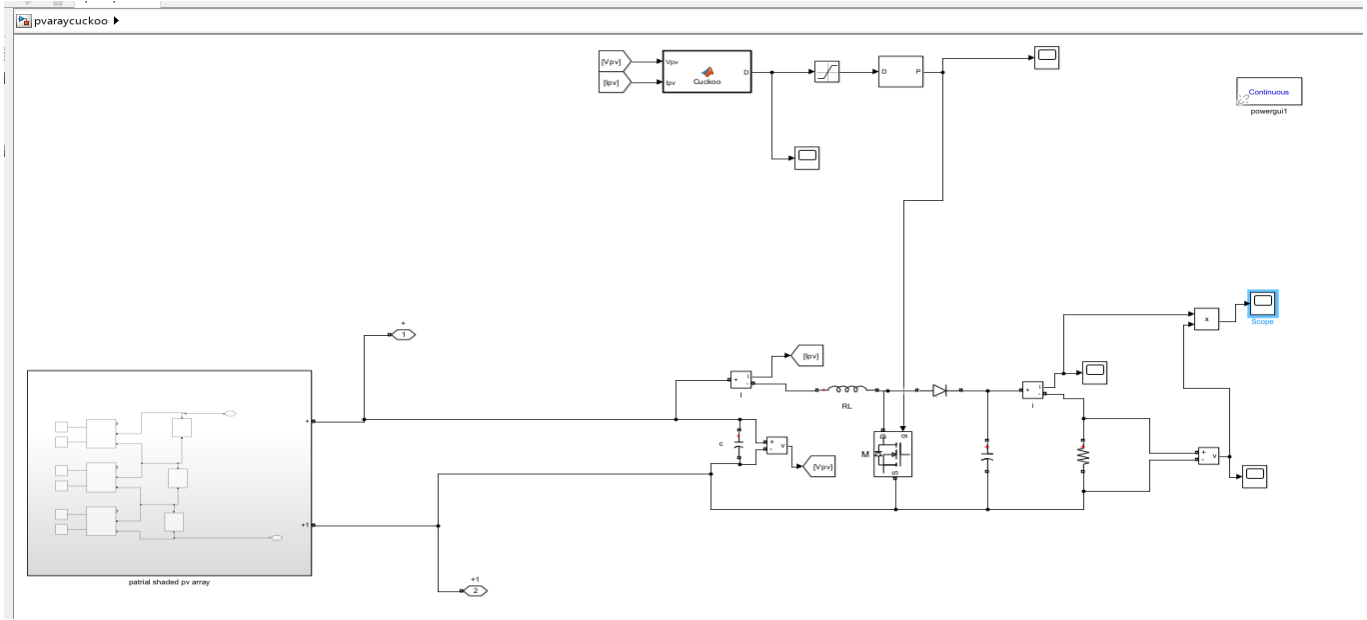


Figure IV.21 :the Whole pv-electrolyser system simulation with the pv system under partial shading using cuckoo search mppt algorithm

Pv system under partial shading with a GMPP of 400w

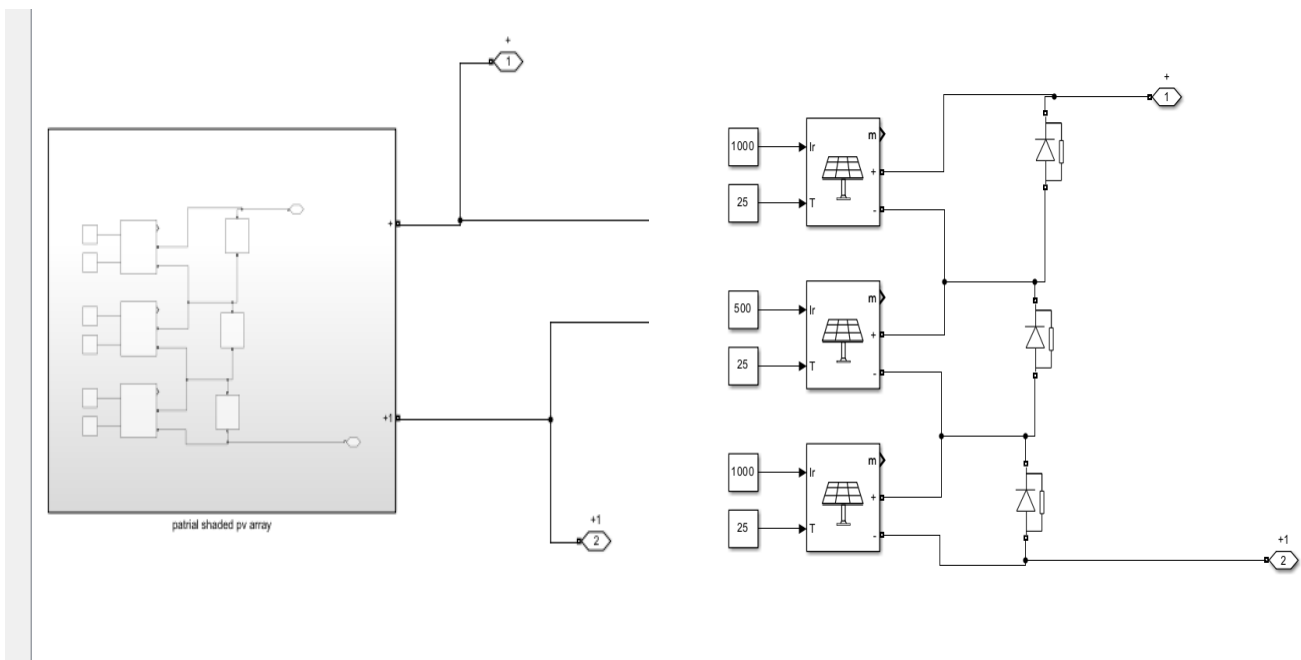


Figure IV.22 :The pv system with 3 identical panels one under partial shading with a lower irradiance compared to the other two with the whole system GMPP of 400w

Cuckoo search algorithm with VPV and IPV as inputs and DUTY CYCLE as the output connected to saturation so I won't go past 1 and pwm generator then connected to IGBT rapid switching diode as a controlled optimized duty cycle .

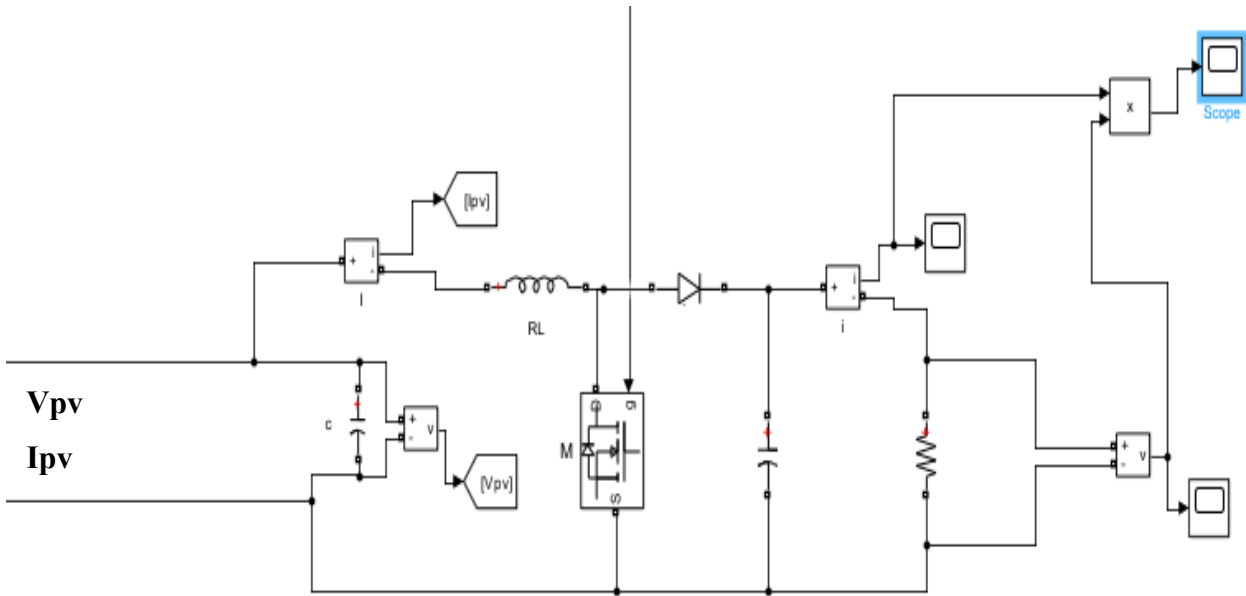


Figure IV.23 :The simulation model of the boost converter

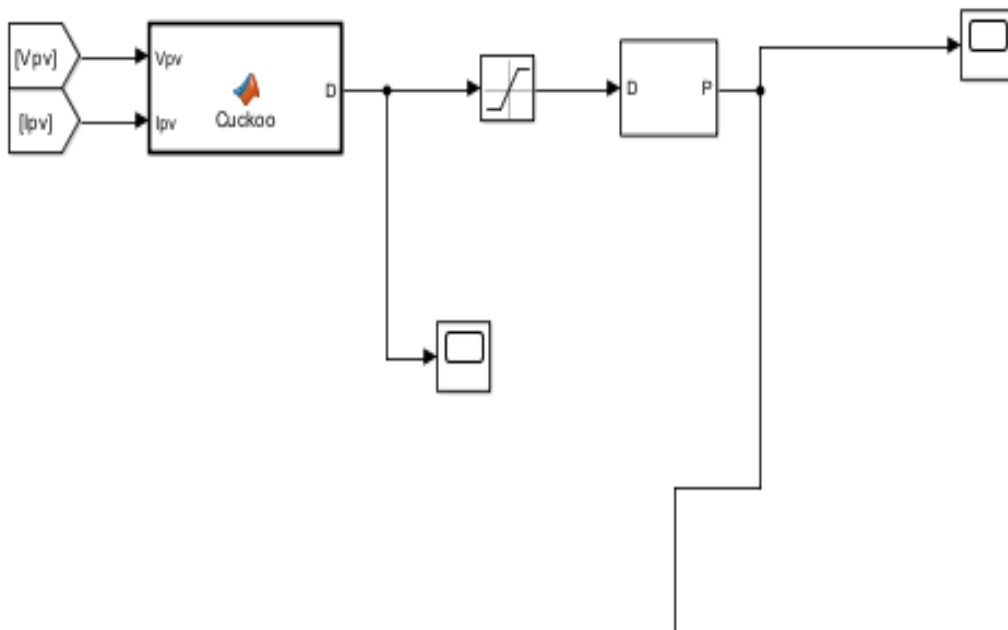


Figure IV.24 :The simulation model of the cuckoo search MPPT algorithm MATLAB function

```

function D = Cuckoo(Vpv,Ipv)
%#codegen
persistent u;
persistent dcurrent;
persistent p;
persistent dc;
persistent dbest;
persistent counter;
persistent iworst;
persistent discover;
if isempty(discover)
    discover=0;
end
if isempty(counter)
    counter=0;
end
if isempty(dcurrent)
    dcurrent=0.5;
end
if isempty(iworst)
    iworst=0;
end

if isempty(dbest)
    dbest=0;
end
if isempty(p)
    p=zeros(4,1);
end
if isempty(u)
    u=0;
end
if isempty(dc)
    dc=zeros(4,1);
    dc(1)=0;
    dc(2)=0.3;
    dc(3)=0.5;
    dc(4)=0.9;
end
if counter>=1 && counter<150)
    D=dcurrent;
    counter=counter+1;
    return;
end
counter=0;

if u>=1 && u<=4)
    p(u)=Vpv*Ipv;
end

u=1;
end
if(u==1)
    D=dc(u);
    dcurrent=D;
    counter=1;
    return;
elseif(u==2)
    D=dc(u);
    dcurrent=D;
    counter=1;
    return;
elseif(u==3)
    D=dc(u);
    dcurrent=D;
    counter=1;
    return;
elseif(u==4)
    D=dc(u);
    dcurrent=D;
    counter=1;
    return;
elseif(u==5 || u==6 )
    if(u==5)
        if(rand(1)>0.25)
            discover=1;
            [m,i]=max(p);
            dbest=dc(i);
            %determine the worst nest
            [m,iworst]=min(p);
            %build new nest
            %dc(iworst)=dbest;
            dc(iworst)=levyflight(dbest,dc(iworst));
            %dc(iworst)=withinlimits(dc(iworst));
            D=dc(iworst);
            dcurrent=D;
            counter=1;
            return;
        else
            u=u+1;
            [m,i]=max(p);
            dbest=dc(i);
            D=dbest;
            dcurrent=D;
            counter=1;
            dc(1)=levyflight(dbest,dc(1))
            % dc(1)=withinlimits(dc(1))
            dc(2)=levyflight(dbest,dc(2))
            %dc(2)=withinlimits(dc(2))
            dc(3)=levyflight(dbest,dc(3))
            %dc(3)=withinlimits(dc(3))
            dc(4)=levyflight(dbest,dc(4))
            %dc(4)=withinlimits(dc(4))
            discover=0;
            return;
        end
    else
        %calculate new power of new nest
        p(iworst)=Vpv*Ipv;
        %determine the best nest
        [m,i]=max(p);
        dbest=dc(i);
        D=dbest;
        dcurrent=D;
        counter=1;

        dc(1)=levyflight(dbest,dc(1))
        % dc(1)=withinlimits(dc(1))
        dc(2)=levyflight(dbest,dc(2))
        %dc(2)=withinlimits(dc(2))
        dc(3)=levyflight(dbest,dc(3))
        % dc(3)=withinlimits(dc(3))
        dc(4)=levyflight(dbest,dc(4))
        % dc(4)=withinlimits(dc(4))
        discover=0;
        return;
    end
end
else
    u
    y='hello'
    D=0.1
end

end
function dfinal=levyflight(dbest,d)
beta=3/2;
kcoeff=0.8;
sigmau=(gamma(1+beta)*sin(pi*beta/2)/(gamma((1+beta)/2)*beta*2^((beta-1)/2)))^(1/beta);
sigmav=1;
u=normrnd(0,(sigmau)^2);
v=normrnd(0,(sigmav)^2);
dup=d+(kcoeff*(abs(u)/(abs(v))^(1/beta)))*(dbest-d);

if(dup>1)
    dfinal=1;
elseif(dup<0)
    dfinal=0;
else
    dfinal=dup;
end
end

```

Figure IV.25 :The whole MATLAB function script of the cuckoo search algorithm

The optimized Output duty cycle value

Where it searches for the best duty cycle value and when it finds it converges the system to GMPP here in this case it found that a duty cycle value of around 0.65 as the optimal duty cycle value it feeds to the system

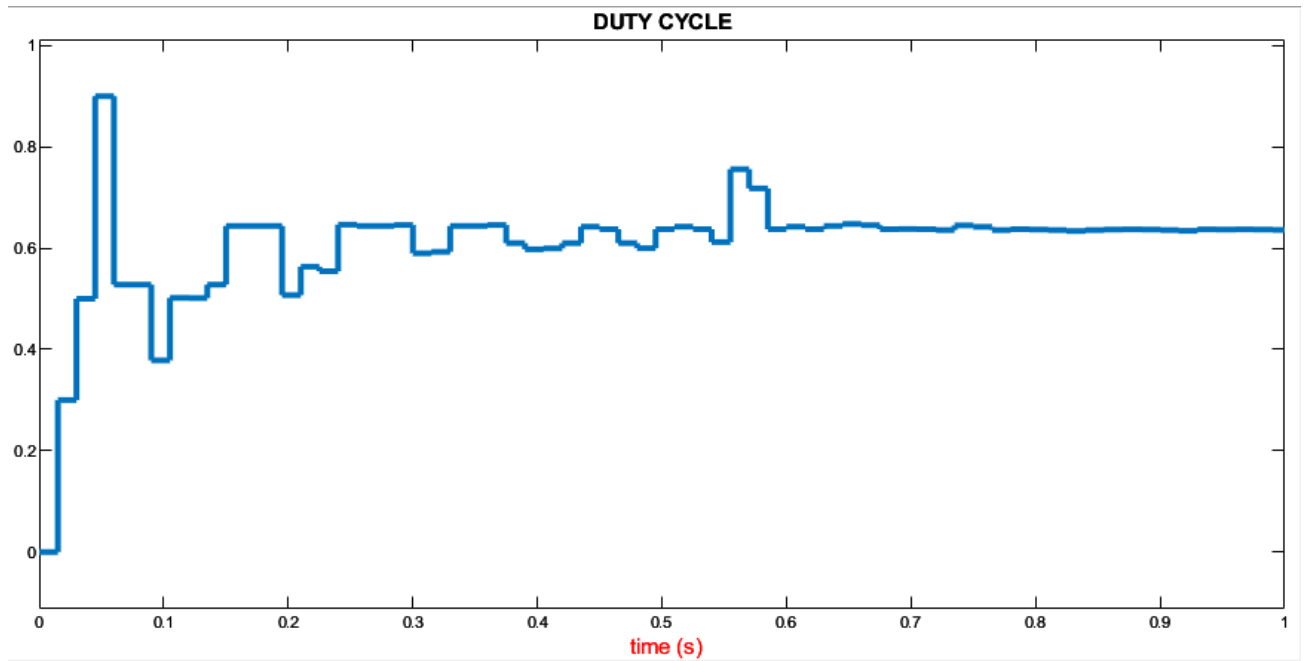


Figure IV.26 :the CS optimized DUTY CYCLE output

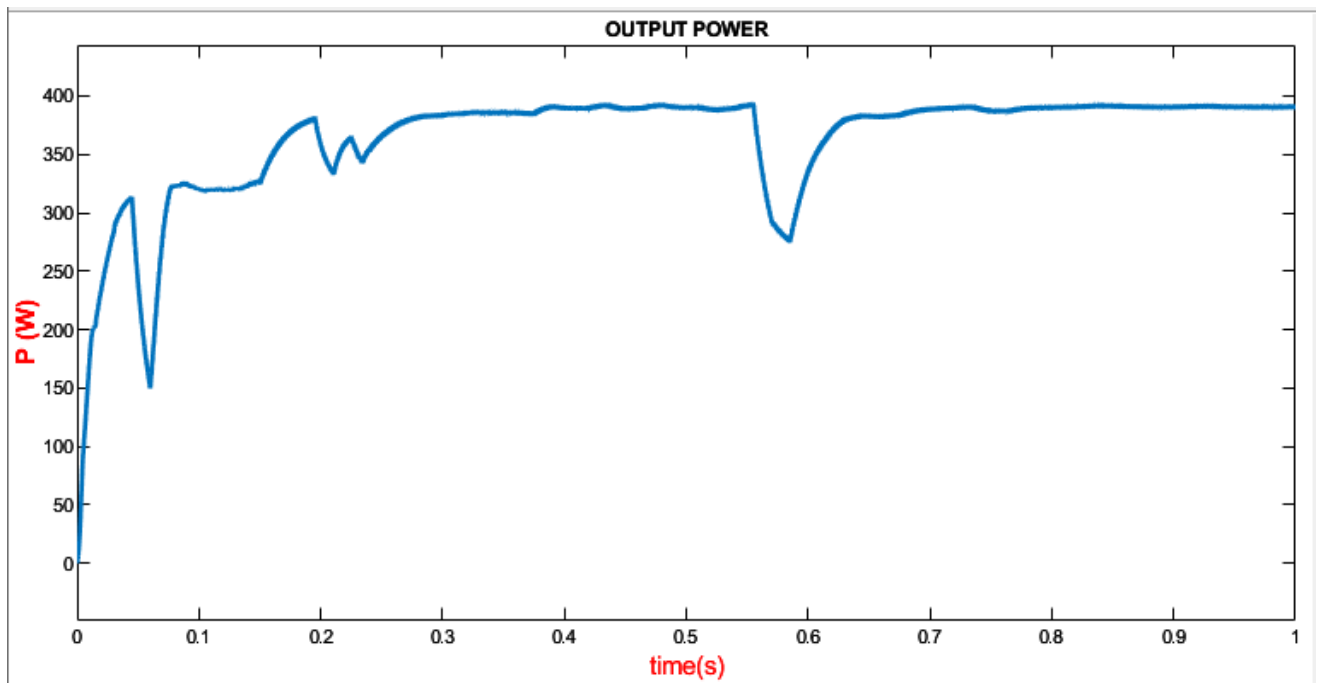


Figure IV.27 :The Output power value converges near the 400w GMPP of the pv system under partial shading

The Cuckoo search algorithm's inherent random walk behavior causes erratic current spikes

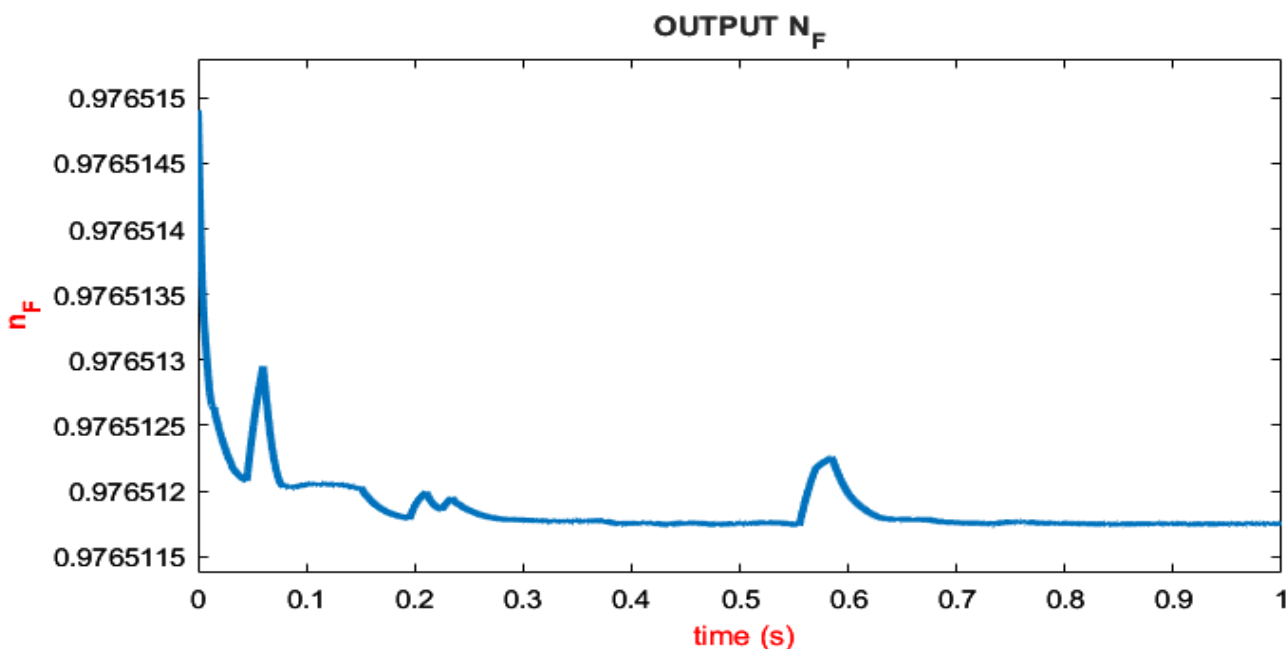


Figure IV.28 :The Output faraday efficiency n-F of the electrolyser system

We see that the output power current and hydrogen production rate converge to their GMPP point where the output power converges to the system MPP which is 400 bust is less smooth and has some spikes and we see the same look in it current and hydrogen production rate and faraday efficiency which is better and higher by over 20% than the traditional p&o algorithm that has lower power output LMPP not GMPP and shows more instability in it curve which will lead to worse hydrogen production and faster degradation of the electrolyser system due to that instability.

The CS output Current at around 2,78A

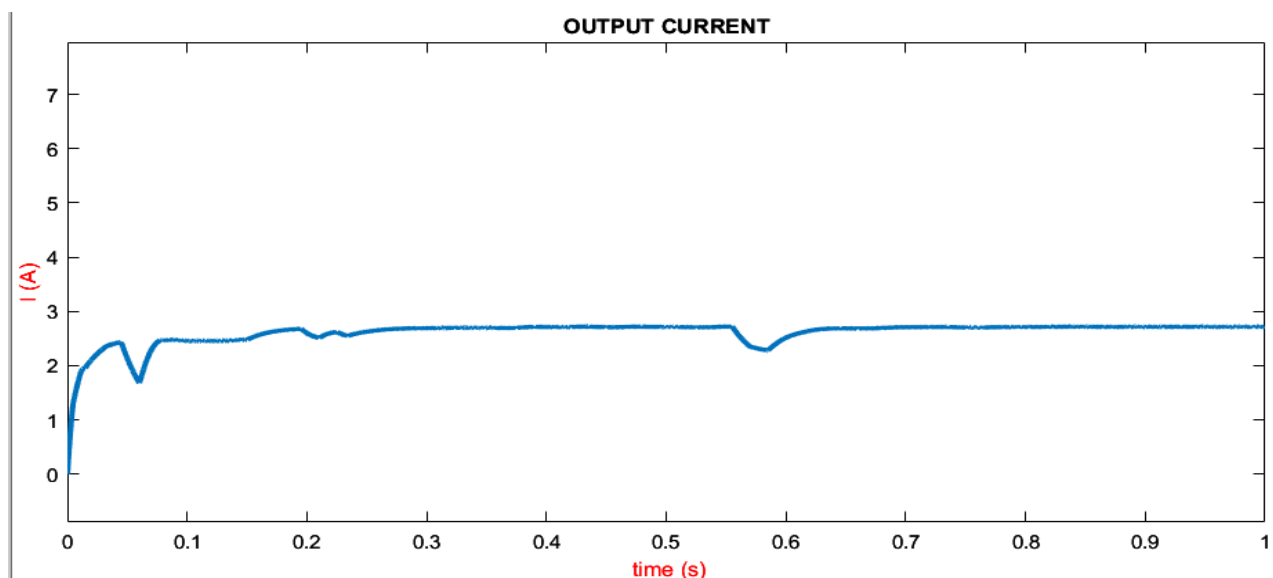


Figure IV.29 :The CS output Current

$N_{h_2} = 3,4 \times 10^{-4}$ same as FDB_TLABC value

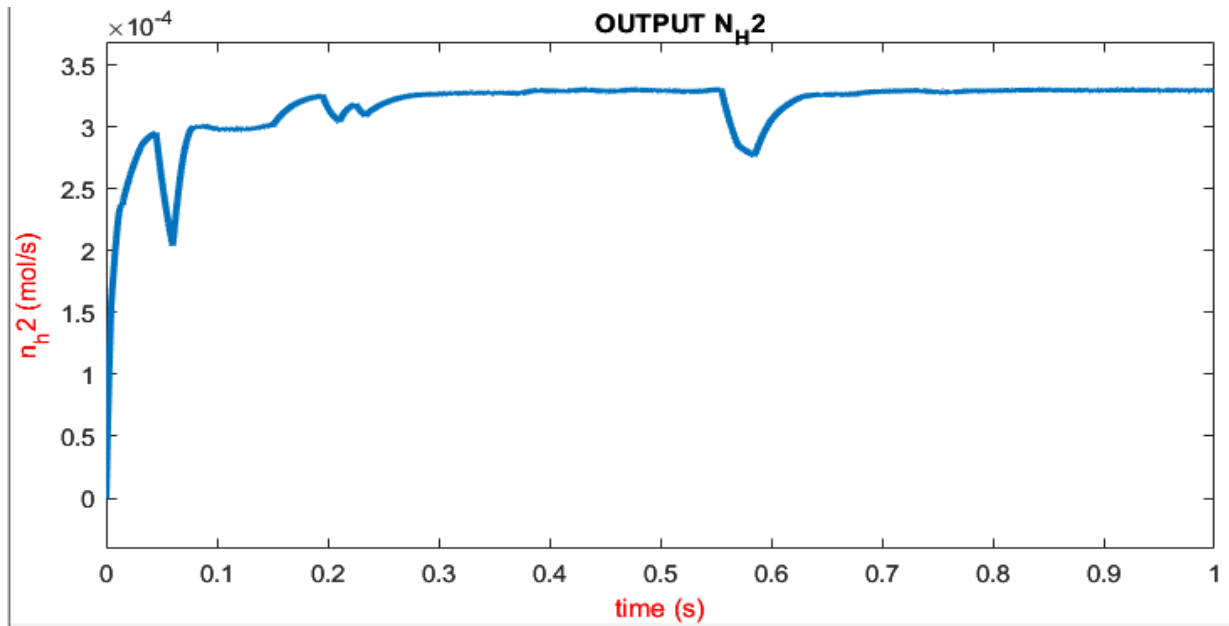


Figure IV.30 :The CS output hydrogen production rate

IV.7 Introduction to the FDB-TLABC Algorithm for PV Systems under Partial Shading :

The FDB-TLABC (Fitness-Distance Balance-based Teaching-Learning Artificial Bee Colony) algorithm is a hybrid optimization technique designed to address the challenges of maximum power point tracking (MPPT) in photovoltaic (PV) systems under partial shading conditions (PSC). Partial shading occurs when certain parts of a PV array receive different levels of sunlight due to obstructions like clouds, trees, or buildings. This leads to multiple local maxima in the power-voltage (P-V) curve, making it difficult for traditional MPPT algorithms to find the global maximum power point (GMPP)[55][56].

The FDB-TLABC algorithm combines the strengths of three key components:

- **Teaching-Learning-Based Optimization (TLBO)**: Enhances exploitation by simulating the teaching and learning process in a classroom.
- **Artificial Bee Colony (ABC)**: Provides robust exploration by mimicking the foraging behavior of honeybees.
- **Fitness-Distance Balance (FDB)**: Improves the selection process by balancing fitness and distance metrics to guide the search toward promising regions.

This hybrid approach ensures a balance between exploration (searching new regions) and exploitation (refining known solutions), making it highly effective for MPPT under partial shading[55][56].

IV.7.1 Teaching-Learning-based optimization (TLBO) in general use case:

→ Introduction:

Population-based algorithm inspired by classroom learning, with teacher (best solution) and learner (other solutions) phases.

→ Key Equations

Initialization: $x_{ij} = x_{jmin} + rand(0,1) \cdot (x_{jmax} - x_{jmin})$

Teacher Phase: $x_{new,ij} = x_{ij} + r_i \cdot (x_{teacher,j} - TF \cdot Mean_j)$ where $TF=1$ or 2 .

Learner Phase:

$x_{new,ij} = x_{ij} + r_i \cdot (x_{ij} - x_{kj})$ if $f(x_i) < f(x_k)$ otherwise $x_{new,ij} = x_{ij} + r_i \cdot (x_{kj} - x_{ij})$

→ Selection: Keep $x_{new,ij}$ if fitness improves.

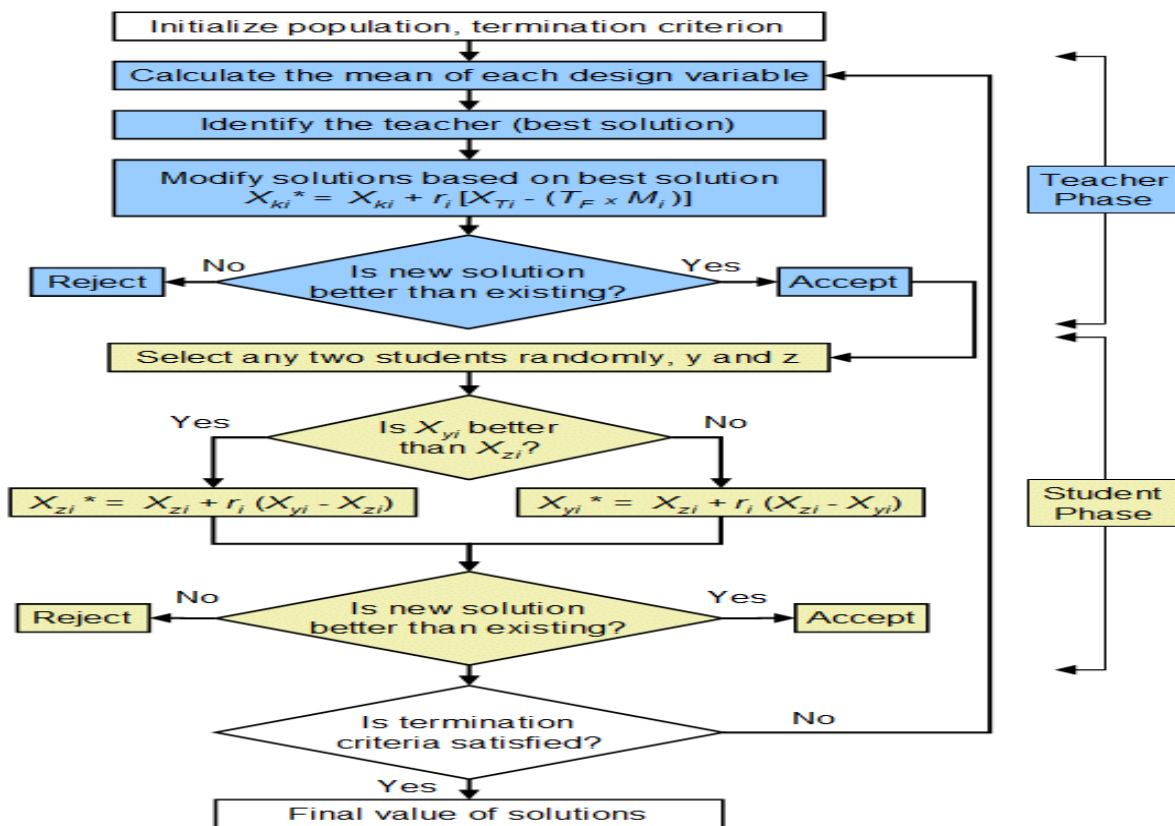


Figure IV.31 :The general structure of the TLBO algorithm in simulation[16]

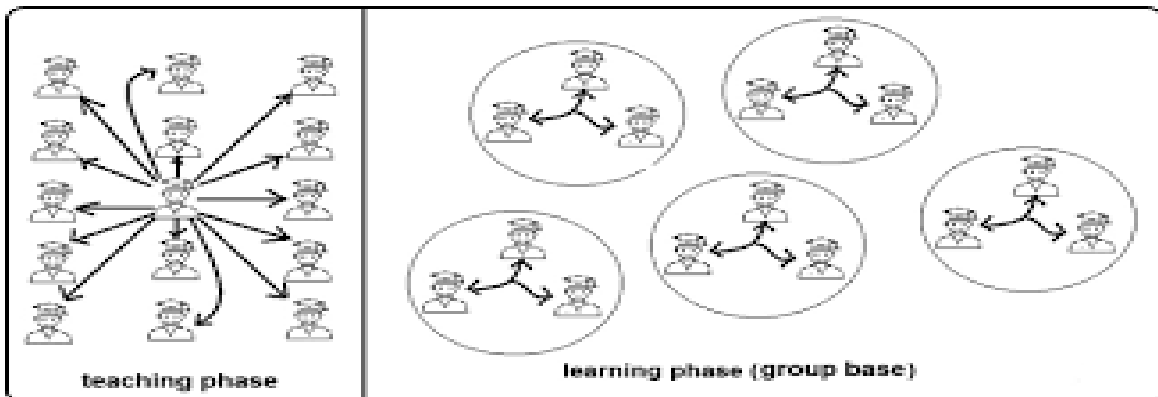


Figure IV.32 :The general structure of the TLBO algorithm in real life[17]

IV.7.2 Artificial Bee Colony (ABC) Algorithm in general use case:

→ Introduction

The Artificial Bee Colony (ABC) algorithm is a swarm intelligence-based optimization method inspired by the foraging behavior of honeybees. It mimics how employed bees, onlooker bees, and scout bees search for food sources (solutions) to find the best nectar (optimal solution).

→ What It Does

ABC is used for continuous optimization problems, balancing exploration (global search via scout bees) and exploitation (local search via employed/onlooker bees)[57].

→ ABC Algorithm Equations

→ Initialization

Randomly generate N food sources (solutions) x_i in the search space:

$$x_{ij} = x_{jmin} + \text{rand}(0,1) \cdot (x_{jmax} - x_{jmin}) \quad \text{where:}$$

x_{ij} = j -th parameter of solution i ,

x_{jmin}, x_{jmax} = bounds for parameter j . [57][58]

→ Employed Bee Phase (Local Search)

Each employed bee modifies its food source x_i to find a neighboring solution v_i :

$$v_{ij} = x_{ij} + \phi_{ij} \cdot (x_{ij} - x_{kj}) \quad \text{where:}$$

$k \neq i$ = random solution index,

$\phi_{ij} \in [-1, 1]$ = random step size [57][58].

→ Onlooker Bee Phase (Fitness-Based Selection)

Onlooker bees choose solutions probabilistically (better fitness = higher chance):

$$P_i = f(x_i) / \sum f(x_k) \quad \text{where } f(x_i) = \text{fitness of solution } x_i.$$

→ Scout Bee Phase (Abandonment & Replacement)

If a solution x_i doesn't improve after limit trials, it's abandoned, and a scout bee replaces it with a random solution: $x_i \leftarrow \text{random new solution}$ [57] [58].

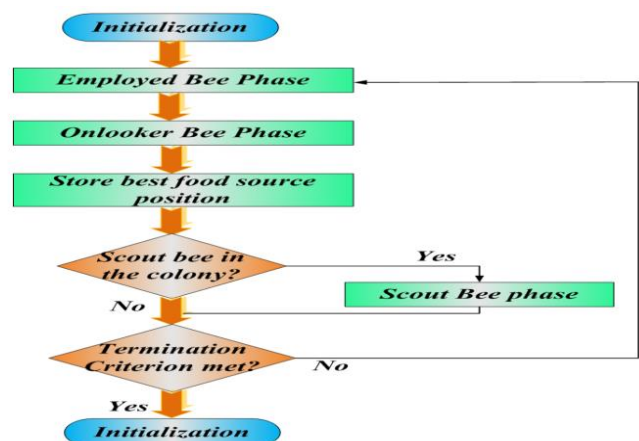
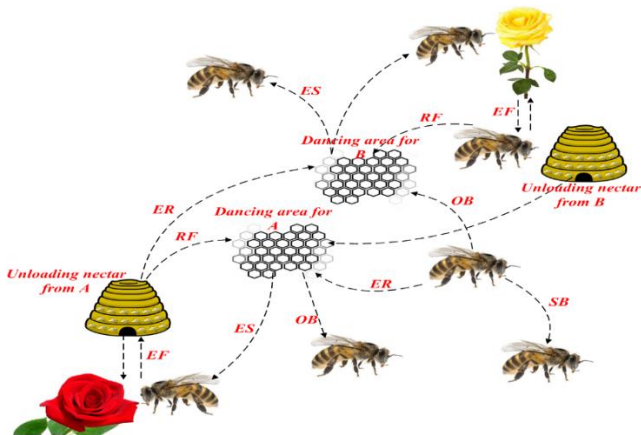


Figure IV.33 :The natural behavior and flow chart of the artificial bee algorithm[18]

IV.7.3 the FDB-TLABC Algorithm:

Teaching-Learning-Based Optimization (TLBO)

Concept: TLBO is inspired by the teaching-learning process in a classroom. It consists of two phases:

Teacher Phase: The "teacher" (best solution) improves the knowledge (fitness) of the "students" (other solutions).

Learner Phase: Students interact with each other to further improve their knowledge.

Role in FDB-TLABC: TLBO enhances the exploitation capability of the algorithm by refining solutions around the best-known solutions.

IV.7.4 Artificial Bee Colony (ABC):

Concept: ABC mimics the foraging behavior of honeybees. It consists of three types of bees:

Employed Bees: Explore the search space and share information about food sources (solutions).

Onlooker Bees: Select promising food sources based on the information shared by employed bees.

Scout Bees: Randomly search for new food sources to avoid stagnation.

Role in FDB-TLABC: ABC provides robust exploration by searching the entire solution space and avoiding local optima.

IV.7.4 Fitness-Distance Balance (FDB):

Concept: FDB is a selection mechanism that balances the fitness (quality) of a solution and its distance from the best solution. It ensures that solutions contributing to both diversity and convergence are prioritized.

Role in FDB-TLABC: FDB guides the selection process in both TLBO and ABC phases, ensuring that the algorithm focuses on promising regions of the search space.

IV.7.6 How FDB-TLABC Algorithm Works in PV Systems for MPPT:**→ Initialization:**

Initialize a population of solutions (voltage or duty cycle values) representing potential MPPs.

Evaluate the fitness (power output) of each solution.

→ Teacher Phase (TLBO):

Identify the best solution (teacher) and update other solutions (students) based on the teacher's knowledge.

This phase refines the solutions around the best-known MPP.

→ Learner Phase (TLBO):

Students interact with each other to improve their fitness.

This phase further refines the solutions and enhances exploitation.

→ **Employed Bee Phase (ABC):**

Employed bees explore the search space around their assigned solutions. New solutions are generated and evaluated.

→ **Onlooker Bee Phase (ABC):**

Onlooker bees select promising solutions based on their fitness and distance (using FDB). This phase ensures that the algorithm focuses on high-quality regions.

→ **Scout Bee Phase (ABC):**

If a solution stagnates (does not improve), scout bees randomly search for new solutions. This phase ensures exploration and avoids local optima.

→ **FDB-Based Selection:**

Throughout the algorithm, FDB is used to balance fitness and distance, ensuring a diverse and high-quality population.

→ **Termination:**

The algorithm terminates when a stopping criterion (e.g., maximum iterations or convergence) is met. The best solution represents the GMPP.

IV.7.7 Whole system:

This algorithm implements a Maximum Power Point Tracking (MPPT) technique for photovoltaic (PV) systems using Fitness-Distance Balance-based Teaching-Learning Artificial Bee Colony (FDB-TLABC). It dynamically adjusts the duty cycle of a DC-DC converter to maximize power extraction from the solar panel under varying conditions (e.g., shading, temperature changes).

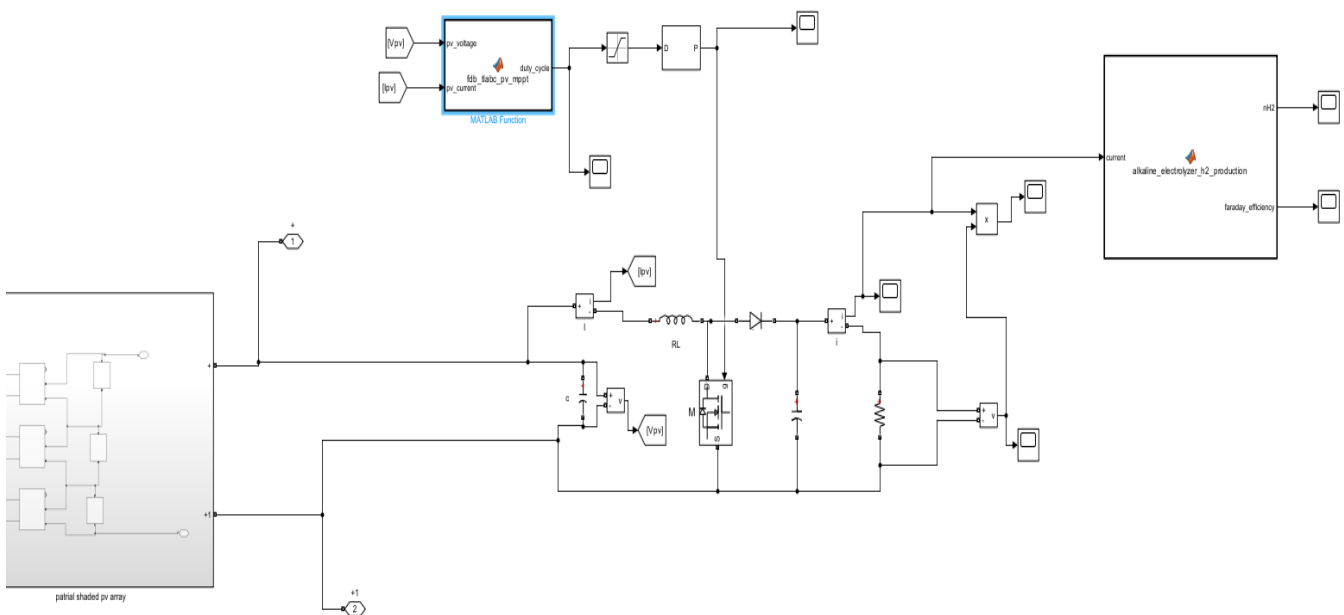


Figure IV.34 :the Whole simulated pv-electrolyser system when using FDB-TLABC algorithm under partial shading

```

function duty_cycle = fdb_tlabc_pv_mppt(pv_voltage, pv_current)
% FDB_TLABC_PV_MPPT - MPPT using FDB-TLABC
% Inputs/Outputs same as original

persistent X val_X trial FES gBest val_gBest

% constants
popsize = 8;           % population size
maxFES = 220;         % maximum number of Function Evaluations (FES)
limit = 6;            % abandonment limit
CR = 0.9;             % Crossover Rate

% Initialize persistent variables
if isempty(X)
    X = 0.65 + 0.15*rand(popsize, 1);
    val_X = zeros(popsize, 1);
    trial = zeros(popsize, 1);
    FES = 0;

    % Initial evaluation
    for i = 1:popsize
        val_X(i) = -pv_voltage*pv_current;
    end
    [val_gBest, idx] = min(val_X);
    gBest = X(idx);
end

% == == == == == Teaching-based Employed Bee Phase == == == == ==
for i = 1:popsize
    [~, sortIdx] = sort(val_X);
    teacher = X(sortIdx(1));
    mean_X = mean(X);
    TF = 1 + rand();
    Xi = X(i) + 0.5*(teacher - TF*mean_X)*rand();
    % Diversity learning
    r = generateR(popsize, i);
    F = 0.5 + 0.5*rand();
    V = X(r(1)) + F*(X(r(2)) - X(r(3)));
    if rand() < CR
        Xi = 0.5*Xi + 0.5*V;
    end

    Xi = max(0.1, min(0.9, Xi));
    new_power = pv_voltage*pv_current;
    val_Xi = -new_power;
    FES = FES + 1;

    if val_Xi < val_X(i)
        val_X(i) = val_Xi;
        X(i) = Xi;
        trial(i) = 0;
    end
end

% == == == == == Learning-based Onlooker Bee Phase == == == == ==
Fitness = calculateFitness(val_X);
for k = 1:popsize
    i = rouletteWheel(Fitness);
    j = randi(popsize);
    while j == i, j = randi(popsize); end

    if val_X(i) < val_X(j)
        Xi = X(i) + rand()*(X(i)-X(j));
    else
        Xi = X(i) + rand()*(X(j)-X(i));
    end

    Xi = max(0.1, min(0.9, Xi));
    new_power = pv_voltage*pv_current;
    val_Xi = -new_power;
    FES = FES + 1;

    if val_Xi < val_X(i)
        val_X(i) = val_Xi;
        X(i) = Xi;
    end
end

% == == == == == Scout Bee Phase == == == == ==
[max_trial, idx] = max(trial);
if max_trial > limit
    X(idx) = 0.65 + 0.15*rand(); |
    val_X(idx) = -pv_voltage*pv_current;
    trial(idx) = 0;
end

% Update global best
[current_min, idx] = min(val_X);
if current_min < val_gBest
    val_gBest = current_min;
    gBest = X(idx);
end

duty_cycle = gBest;
end

%% Helper Functions
function r = generateR(popsize, i)
    r1 = randi(popsize);
    while r1 == i, r1 = randi(popsize); end
    r2 = randi(popsize);
    while r2 == r1 || r2 == i, r2 = randi(popsize); end
    r3 = randi(popsize);
    while r3 == r2 || r3 == r1 || r3 == i, r3 = randi(popsize); end
    r = [r1 r2 r3];
end

function fFitness = calculateFitness(fObjV)
    fFitness = 1./(1 + abs(fObjV));
    fFitness = fFitness/sum(fFitness);
end

function index = rouletteWheel(Fitness)
    cumFitness = cumsum(Fitness);
    r = rand() * cumFitness(end);
    index = find(r <= cumFitness, 1);
end

```

Figure IV.35 :The FDB_TLABC algorithm mppt script

IV.7.8 Fitness-Distance Balance (FDB) in the Algorithm:

- **Core Principles** - Fitness = Solution quality (higher power output = better fitness).
 - Distance = Diversity between solutions (prevents clustering in one region).
 - Balance = Combines both to guide the search efficiently.

→ **Teaching-Based Employed Bee Phase (FDB)****Key Mechanics:**

Teacher Selection: The best solution (highest power) is chosen as the "teacher."

Population Mean: The average of all solutions represents the group's central tendency.

Update Rule: New solutions move toward the teacher but are balanced against the population mean.

FDB role :

Fitness Aspect: Teacher ensures exploitation of high-power regions.

Distance Aspect: Mean prevents over-convergence, maintaining diversity.

Teaching Factor (TF): Randomly adjusts the balance between the two.

→ **Diversity Learning Phase (FDB)****Key Mechanics:**

Random Partner Selection: Three distinct solutions are chosen randomly.

Mutation: Creates new solutions by combining traits from partners.

Blending: 50% weight on the teaching phase output, 50% on random exploration.

FDB role:

Balances deterministic (teaching) and stochastic (random) search.

Ensures exploration without abandoning fitness-driven progress.

→ **Onlooker Bee Phase (FDB Through Fitness)****Key Mechanics:**

Fitness-to-Probability: Converts power values to selection probabilities.

Roulette Wheel: Chooses solutions probabilistically (higher fitness = higher chance).

FDB Adaptation:

Indirectly embeds FDB by prioritizing fitter solutions while preserving diversity through randomness.

→ **Scout Bee Phase (FDB via Diversity)****Key Mechanics:**

Stagnation Check: Abandons solutions failing to improve after set iterations.

Focused Re-Initialization: Resets stagnant solutions near historically optimal ranges.

FDB Role:

Removes solutions "too far" from improving regions.

Reinjects diversity while respecting past performance.

IV.7.9 Key Steps & Working Principle:**→ Initialization**

Generates an initial population of 8 candidate duty cycles (between 0.1 and 0.9).

Evaluates each candidate by measuring the PV panel's voltage and current to compute power.

Identifies the best duty cycle (gBest) that maximizes power output.

→ Teaching-Based Employed Bee Phase (Exploitation)

Teacher Selection: The best-performing duty cycle ("teacher") guides others toward higher power regions.

Diversity Learning: Introduces random variations to avoid local optima using crossover (CR = 0.9).

Update Rule: Adjusts duty cycles based on the teacher's influence and random exploration.

Trial Counter: Tracks unsuccessful updates to trigger scouting if needed.

→ Learning-Based Onlooker Bee Phase (Exploration)

Fitness-Based Selection: Favors better-performing duty cycles via a roulette wheel mechanism.

Local Search: Refines duty cycles by comparing neighboring solutions.

Power Re-evaluation: Updates solutions if they improve power extraction.

→ Scout Bee Phase (Diversification)

Abandonment: If a duty cycle fails to improve after 6 trials (limit), it is replaced with a new random value.

Reinitialization: Ensures the algorithm escapes local optima and explores new regions.

→ Global Best Update

Continuously tracks the best duty cycle (gBest) across all phases.

Returns gBest as the optimal duty cycle for the DC-DC converter.

IV.7.10 Outputs of the system (power current hydrogen production rate N_{H_2}):

FDB-TLABC delivers superior performance over Cuckoo Search by achieving faster convergence to GMPP, resulting in higher and more stable PV output power. This translates to greater current delivery to the electrolyzer, maximizing hydrogen production rate (nH_2) with minimal fluctuations. Unlike Cuckoo Search's inherent oscillations, and lower production output FDB-TLABC's hybrid teaching-learning and bee colony mechanisms ensure smoother steady-state operation, preventing efficiency drops in the electrolyzer and normal working due to no unstable current. Its adaptive search strategy reacts quicker to shading changes, maintaining optimal current levels for consistent H_2 output. By reducing convergence time and eliminating power ripples, FDB-TLABC enhances both PV energy harvest and electrolyzer efficiency, making it ideal for real-world renewable hydrogen systems.

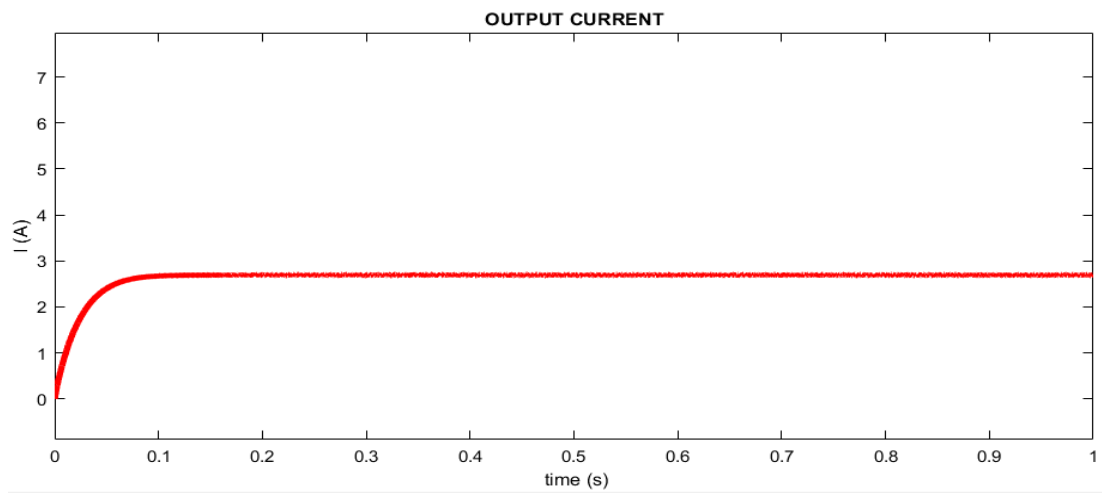


Figure IV.36 :The FDB-TLABC output current of around 2.8 A

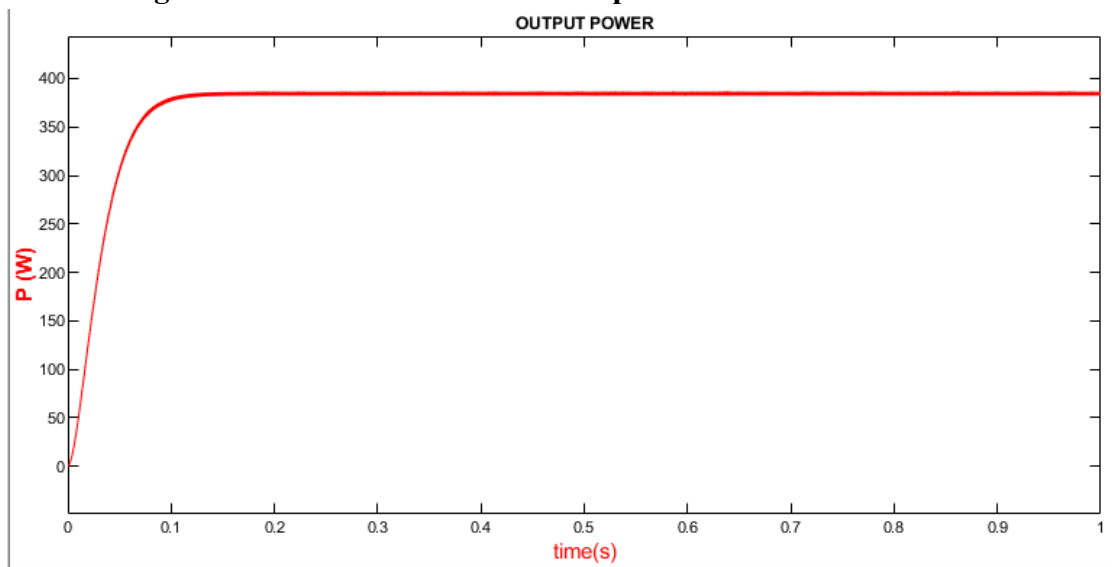


Figure IV.37 :The FDB-TLABC output power near the GMPP of the 400w

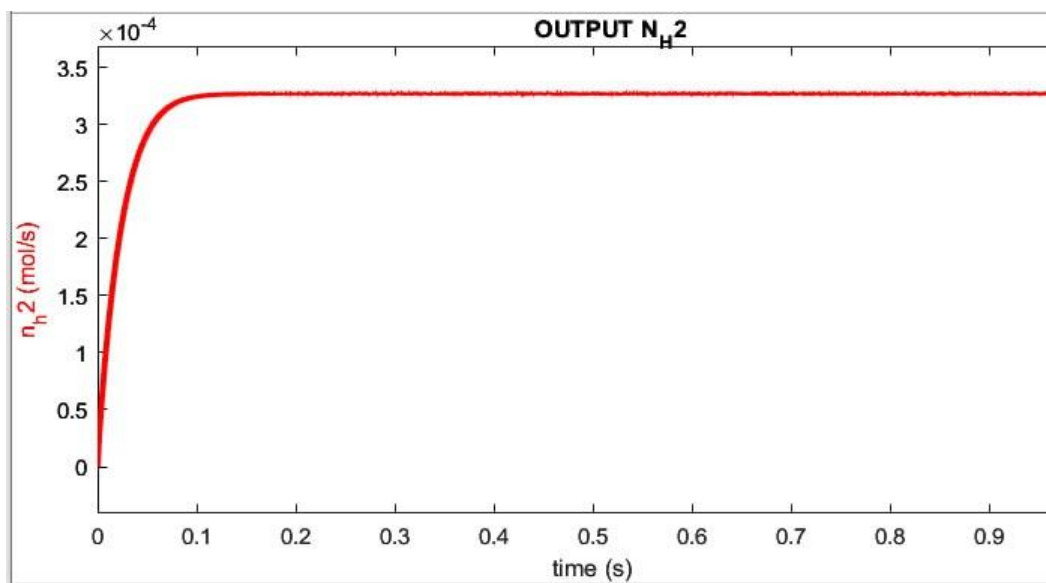


Figure IV.38 :the FDB-TLABC Hydrogen production rate n_{H_2} same value as CS algorithm

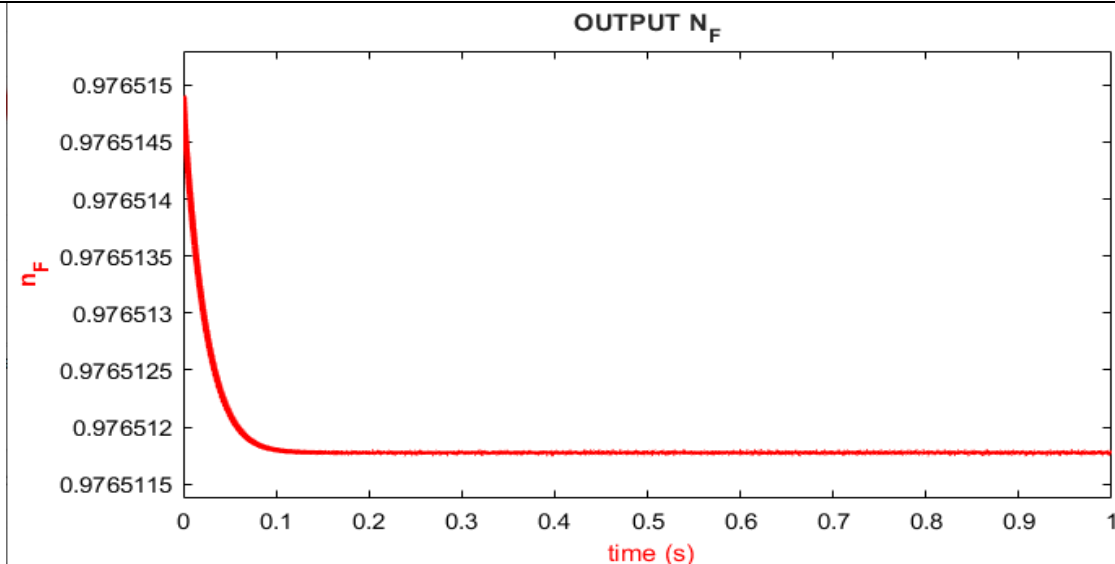


Figure IV.39 :The FDB-TLABC output value of N_F

From looking at the outputs of the pv-electrolyser system Figure IV.35 Figure IV.36 when using the hybrid intelligent MPPT algorithm FDB_TLABC we notice that the system power converges to near the GMPP of 400w we desire and higher current output compared to p&o and similar to the cuckoo search algorithm but also it convergence being much faster and smoother with oscillation compared to the cuckoo search algorithm which will lead to the same better electrolyser system outputs hydrogen production rate n_{H_2} and faraday efficiency n_F in Figure IV.37 and Figure IV.38 respectively

IV.8 Comparison of the Outputs of the Three MPPT Algorithms in the PV System Under PSC:

The three MPPT algorithms—Perturb & Observe (PO), Cuckoo Search (CS), and FDB-TLABC—are evaluated under partial shading conditions (PSC). While PO settles at a local MPP (LMPP) with lower power output, both CS and FDB-TLABC achieve the global MPP (GMPP). However, FDB-TLABC converges up to six times faster than CS, with smoother tracking and minimal oscillations. This superior dynamic response directly enhances hydrogen production rate (n_{H_2}) and maintains higher Faraday efficiency compared to the other methods. The results demonstrate FDB-TLABC's dominance in both speed and stability under PSC. where we see in the following 4 figures the comparison of the power and current and hydrogen production rate and faraday efficiency between the three mppt algorithms:

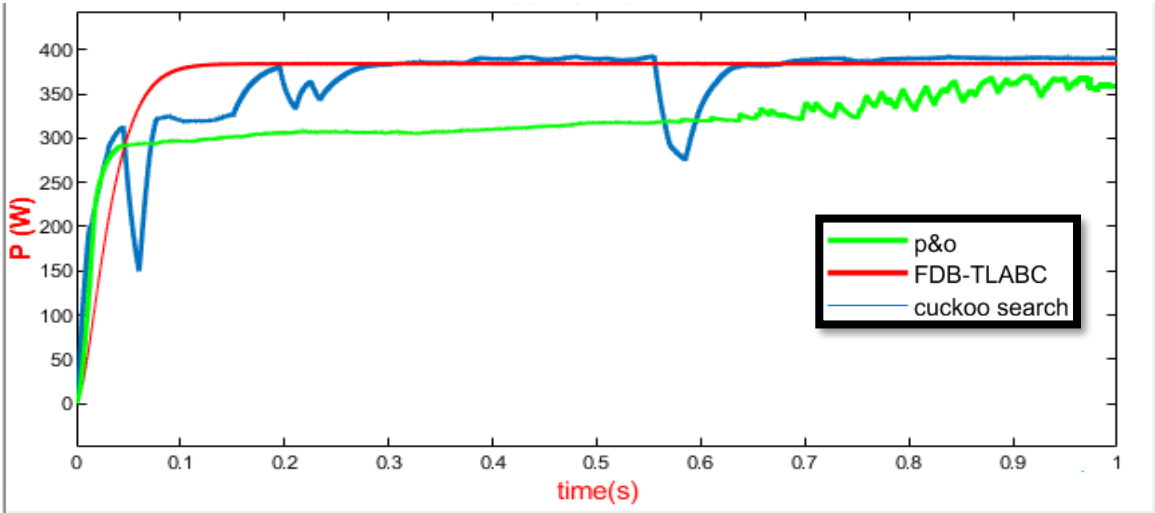


Figure IV.40 : output power comparison

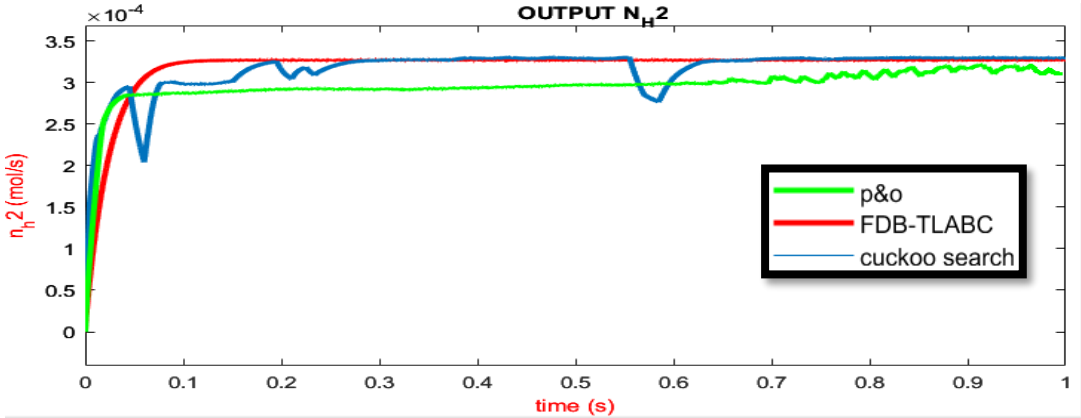


Figure IV.41 : output n_h2 comparison

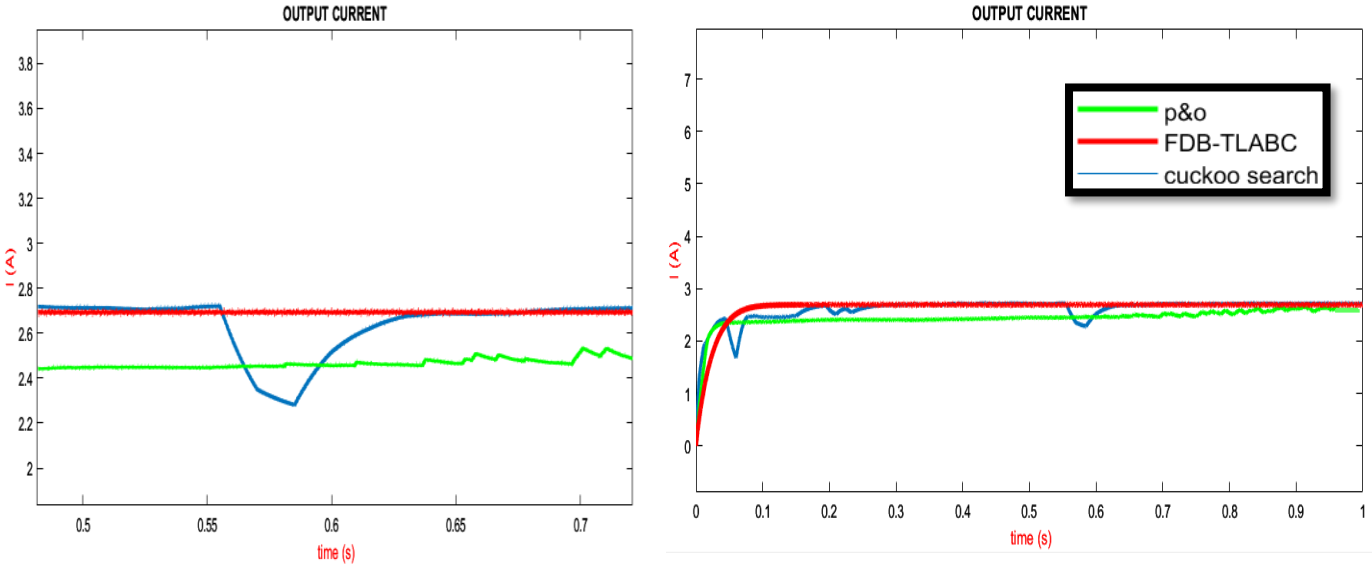


Figure IV.42 : output current comparison

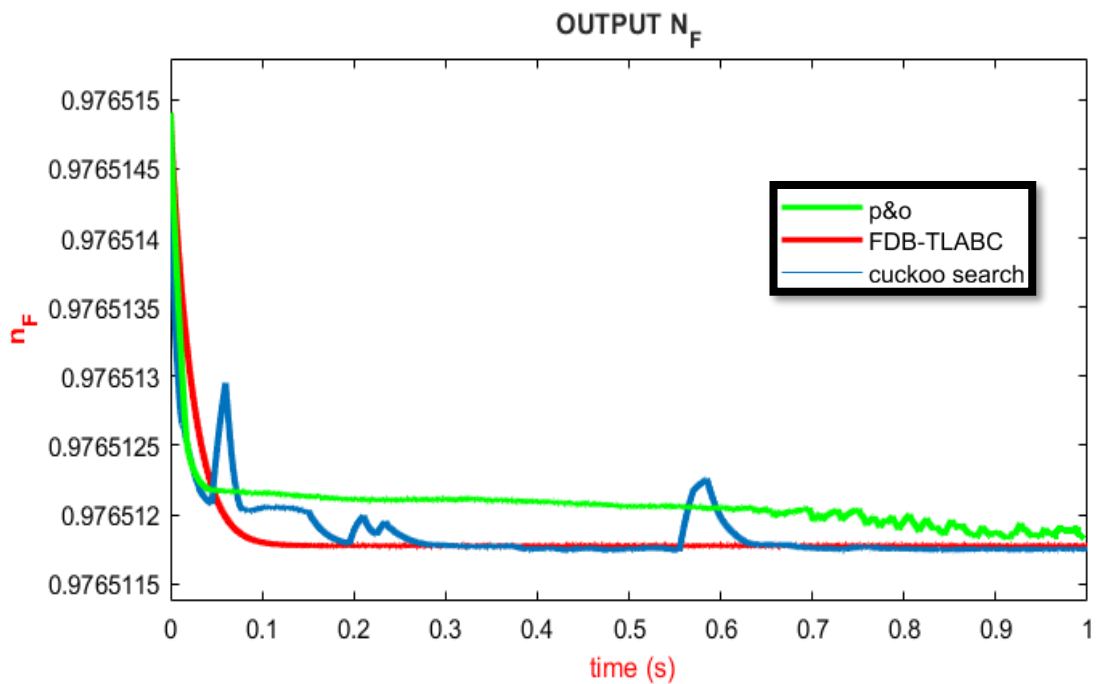


Figure IV.43 : output n_F comparison

from looking at the outputs valeus red for fdb-tlabc and bleu for the cuckoo search and green for the p&o across the three mppt algorithm under PSC we can see the lower performance with the p&o algorithm and the convergence to gmpp with both the cuckoo search and fdb-tlabc and the faster and smoother way that the hybrid mppt algorithm fdb-tlabc

Algorithm type	P&o	Cuckoo search	FDB-TLABC
Output power(W)	300 to 350 (no fixed point)	397	395
Output Current (A)	2,45	2,75	2,74
Hydrogen production rate n-H ₂ (mol/s)	3x10 ⁻⁴	3,4x10 ⁻⁴	3,4x10 ⁻⁴
Faraday efficiency	0.97	0,97	0.97
Conversion time(s)	Doesn't stay stable (no fixed point conversion)	0.6	0.1 (6 times faster than CS)
stability	unstable and doesn't stay at fixed Lmpp point	More stable but slower and less smooth conversion to Gmpp point	Very stable and faster and smoother conversion to Gmpp point

Figure IV.44 :Table comparing the three algorithms in the pv-electrolyser system under partial shading

IV.9 Comparison of P&O, Cuckoo Search, and FDBTLABC for Power Current Outputs & Hydrogen Production:

→ Power Current Output Stability

P&O:

Unstable and fluctuating due to premature convergence.

Often gets trapped in local maxima, leading to erratic power extraction.

Cuckoo Search (CS):

Better than PO but still noisy due to Lévy flights (random jumps).

Less stable than FDBTLABC but avoids some local optima like the p&o algorithm.

FDBTLABC:

Smoother and more stable output and faraday efficiency and hydrogen production rate output .

Avoids erratic movements, ensuring consistent power extraction and best hydrogen production .

→ Hydrogen Production Rate

P&O:

Lower and inconsistent due to unstable power output.

Frequent drops in current reduce electrolyzer efficiency.

Cuckoo Search:

Higher than PO but slower to stabilize.

Lévy flights help escape local optima but causes slower convergence and spikes .

FDBTLABC:

Highest and most consistent hydrogen production.

Fast convergence to GMPP ensures steady and stable power supply to the electrolyzer.

IV.10 Conclusion :

Partial shading in photovoltaic (PV) systems creates multiple power peaks, severely reducing efficiency and destabilizing hydrogen production when using traditional MPPT methods like Perturb & Observe (P&O). Conventional algorithms often get trapped in local maxima, causing power oscillations and suboptimal electrolyzer operation, which lowers hydrogen output. Intelligent and hybrid MPPT techniques—such as Fitness-Distance Balance-based Artificial Bee Colony (FDB-ABC) and Cuckoo Search Optimization—overcome these limitations by combining global search capabilities with adaptive learning. These methods efficiently track the Global Maximum Power Point (GMPP) even under dynamic shading, ensuring stable power delivery to electrolyzers and maximizing hydrogen production. By leveraging bio-inspired optimization and machine learning

the hybrid MPPT algorithms significantly outperform traditional approaches, offering faster convergence, smoother operation, and enhanced robustness in real-world conditions. And works better in hydrogen production than the standard intelligent MPPT algorithms like the cuckoo search and also others like the pso etc. that will require current smoothing and other stuff to deal with it problem's like the slower convergence and current spikes so it works as needed in hydrogen production and insures the smooth fast and stable production that the hybrid mppt algorithm fdb_tlabc does on its own

This makes the hybrid intelligent MPPT algorithms essential for reliable, high-efficiency solar-powered hydrogen generation in partially shaded environments.

General Conclusion:

This research focused on optimizing green hydrogen production using a photovoltaic (PV) system integrated with an alkaline electrolyzer, with particular attention to the role of Maximum Power Point Tracking (MPPT) algorithms. Given the global urgency to transition toward renewable and sustainable energy systems, green hydrogen—produced from water electrolysis powered by solar energy—represents a clean and promising alternative to fossil-fuel-based hydrogen production.

We developed a complete PV-electrolyzer system model and conducted simulations under various operating conditions, including standard irradiance and partial shading. The system's behavior was analyzed in terms of two main performance indicators: hydrogen production rate and Faraday efficiency. Our results confirmed that the performance of the electrolyzer is highly dependent on the consistency and magnitude of the power supplied by the PV array. Voltage and current fluctuations, especially those induced by shading or environmental variations, lead to a noticeable drop in hydrogen production.

To address these challenges, we tested and compared several MPPT algorithms:

Perturb & Observe (P&O): A traditional algorithm that performed well under stable conditions but experienced up to 25–30% power loss under partial shading due to its inability to escape local maxima.

Cuckoo Search (CS): A metaheuristic algorithm that improved tracking performance, showing a 15–25% increase in PV power output compared to P&O under fluctuating irradiance.

FDB-TLABC: The proposed hybrid algorithm, combining Fitness-Distance Balance (FDB), Teaching-Learning-Based Optimization (TLBO), and Artificial Bee Colony (ABC), achieved the best performance. It increased the PV output power as much as the cuckoo search algorithm but having much smoother and faster convergence toward the GMPP compared to Cuckoo Search in partial shading scenarios.

These gains translated directly into higher electrolyzer performance. In terms of hydrogen output:

Under standard conditions, the system using P&O produced a baseline hydrogen amount (normalized as 100%).

General Conclusion

When using Cuckoo Search, the hydrogen production increased by approximately 15 to 25%, while Faraday efficiency remained above 90% in moderate current ranges.

With FDB-TLABC, the hydrogen production improved by 15 to 25% compared to P&O, and Faraday efficiency remained consistently above 95%, even during current variations caused by partial shading.

This demonstrates that selecting an effective MPPT strategy is not only essential for solar energy harvesting but is directly linked to the efficiency and viability of green hydrogen production.

In conclusion, this thesis provides a comprehensive simulation and optimization framework for PV-electrolyzer systems. The proposed FDB-TLABC algorithm outperformed conventional and heuristic methods in power extraction and hydrogen yield. These findings support the integration of intelligent control techniques to ensure robust and efficient green hydrogen systems. By enhancing solar-to-hydrogen conversion by over 35%, this approach significantly contributes to sustainable energy solutions for applications in power grids, transport, and industry.

Perspective:

Hybridization of Renewable Energy Sources, The integration of complementary renewable energy sources, such as wind or hydropower, could mitigate the intermittency of solar power. This would ensure a more stable energy supply to the electrolyzer, improving the continuity of hydrogen production—especially at night or during periods of low sunlight.

Advanced Optimization via Artificial Intelligence, Although intelligent algorithms like Cuckoo Search and FDB-TLABC have shown promising results, the use of AI-based techniques (neural networks, machine learning, predictive control) would enable better real-time adaptation to rapid fluctuations in sunlight, further optimizing energy efficiency.

Experimental Implementation and Real-World Validation, Transitioning to an experimental model or real-world prototype is a crucial step. This would validate the performance observed in simulations, identify practical challenges related to control and maintenance, and demonstrate the system's feasibility in the field.

Techno-Economic and Environmental Study, A thorough analysis of costs, energy efficiency, and environmental impact (LCA) is essential. Evaluating the cost per kg of hydrogen and CO₂ savings will support large-scale deployment, particularly in Algeria, which has abundant solar potential.

Bibliographic References:

- [1] IEA, *The Future of Hydrogen*, 2019
- [2] REN21, *Renewables 2021 Global Status Report*, 2021.
- [3] IPCC, *Sixth Assessment Report*, 2021.
- [4] Staffell et al., *Energy Environ. Sci.*, 2019.
- [5] Boukhebouze et al., *Renewable Energy*, 2020.
- [6] Millet et al., *Int. J. Hydrogen Energy*, 2013.
- [7] Langins, Janis (8 Jun 1983). "Hydrogen production for ballooning during the French Revolution: An early example of chemical process development". *Annals of Science*. 40 (6). *Taylor & Francis*: 531–558. doi:[10.1080/00033798300200381](https://doi.org/10.1080/00033798300200381)
- [8] <https://impactful.ninja/the-history-of-hydrogen/>
- [9] Grimaldo, John & Barcelo, Juan & Rivera-Pacheco, Daniel & Ramos-Barrera, Luis & Martinez-Palacio, Ubaldo. (2021). A Review of History, Production and Storage of Hydrogen. *Journal of Engineering Science and Technology Review*. 14. 121-134. 10.25103/jestr.145.14.
- [10] Youssef Elaouzy, Abdellah El Fadar,
Water-energy-carbon-cost nexus in hydrogen production, storage, transportation and utilization,
International Journal of Hydrogen Energy,
- [11] Pavel Afanasev, Aysylu Askarova, Tatiana Alekhina, Evgeny Popov, Strahinja Markovic, Aliya Mukhametdinova, Alexey Cheremisin, Elena Mukhina,
An overview of hydrogen production methods: Focus on hydrocarbon feedstock,
International Journal of Hydrogen Energy,
- [12] S. Shiva Kumar, Hankwon Lim,
An overview of water electrolysis technologies for green hydrogen production,
Energy Reports,
- [13] B.A. Gyamfi, T.S. Adebayo, F.V. Bekun, E.B. Agyekum, N.M. Kumar, H.H. Alhelou, A. Al-Hinai
Beyond environmental Kuznets curve and policy implications to promote sustainable development in
Mediterranean
- [14] Kusoglu, A. (Re)Defining Clean Hydrogen: From Colors to Emissions. *Electrochemical Society Interface* 2022, 31 (4), 47, DOI: 10.1149/2.F08224IF
- [15] <https://www.southernlights.io/industry/what-is-green-hydrogen/>
- [16] F. Belaïd et al.
Balancing climate mitigation and energy security goals amid converging global energy crises: the role of
green investments
- [17] Budiyanto, E.; Salamon, S.; Wang, Y.; Wende, H.; Tüysüz, H. Phase Segregation in Cobalt Iron Oxide
Nanowires toward Enhanced Oxygen Evolution Reaction Activity. *JACS Au* 2022, 2, 697–710.
- [18] <https://www.eia.gov/energyexplained/solar/photovoltaics-and-electricity.php>
- [19] flickr. (May 10, 2018). Huston-Bursaw_000032_153515_492994_4578 [Online]. Available:
<https://www.flickr.com/photos/departmentofenergy/35941357930>
- [20] S. Islam et al.
Investigating performance, reliability and safety parameters of photovoltaic module inverter: test results
and compliances with the standards

Bibliographic References

- [21] B.D. Catumba et al.
Sustainability and challenges in hydrogen production: an advanced bibliometric analysis
COP28
- [22] Global renewables and energy efficiency pledge
[Online]. Available:
<https://www.cop28.com/en/global-renewables-and-energy-efficiency-pledge>, Accessed 18th Dec 2023
- [23] Olusola Bamisile, and all others The environmental factors affecting solar photovoltaic output,
Renewable and Sustainable Energy Reviews
- [24] Mirzayev, Abdulla & Tillahodjaev, Rustam. (2020). CALCULATION OF THE SOLAR ENERGY SYSTEM. International Journal of Scientific and Engineering Research. 54-57.
- [25] T. Logeswaran, A. SenthilKumar,
A Review of Maximum Power Point Tracking Algorithms for Photovoltaic Systems under Uniform and Non-uniform Irradiances,
Energy Procedia,
- [26] T. Logeswaran, A. SenthilKumar,
A Review of Maximum Power Point Tracking Algorithms for Photovoltaic Systems under Uniform and Non-uniform Irradiances,
Energy Procedia,
- [27] Long Zou, Qiuwan Shen, Guogang Yang, Shian Li, Naibao Huang,
Improved hydrogen production efficiency of a Photovoltaic-Electrolysis system with P&O Algorithm: A case study,
Chemical Physics Letters,
- [28] T. W. John Twidell, Renewable Energy Resources, New York: Routledge, 2015.
- [29] Ali M. Eltamaly,
Chapter 4 - Performance of MPPT Techniques of Photovoltaic Systems Under Normal and Partial Shading Conditions, 2018,
<https://www.mathworks.com/discovery/mppt-algorithm.html>
- [30] Mishra, Praveen Kumar & Tiwari, Prabhakar. (2021). Incremental conductance MPPT in grid connected PV system. International Journal of Engineering, Science and Technology. 13. 138-145. 10.4314/ijest.v13i1.21S.
<https://www.mdpi.com/2072-666X/12/10/1260>
- [31] MDPI and ACS Style
Villegas-Mier, C.G.; Rodriguez-Resendiz, J.; Álvarez-Alvarado, J.M.; Rodriguez-Resendiz, H.; Herrera-Navarro, A.M.; Rodríguez-Abreo, O. Artificial Neural Networks in MPPT Algorithms for Optimization of Photovoltaic Power Systems: A Review. Micromachines 2021, 12, 1260.
<https://doi.org/10.3390/mi12101260>
- [32] MDPI and ACS Style
Derbeli, M.; Napole, C.; Barambones, O. A Fuzzy Logic Control for Maximum Power Point Tracking Algorithm Validated in a Commercial PV System. Energies 2023, 16, 748.
<https://doi.org/10.3390/en16020748>
- [33] Noman, Abdullah & Addoweesh, Khaled & Mashaly, Hussein. (2012). A fuzzy logic control method for MPPT of PV systems. 10.1109/IECON.2012.6389174.
- [34] Tafticht, T., Agbossou, K. and Doumbia, M.L. (2007), "A new MPPT method for photovoltaic systems used for hydrogen production", COMPEL - The international journal for computation and mathematics in electrical and electronic engineering, Vol. 26 No. 1, pp. 62-74. <https://doi.org/10.1108/03321640710713976>
- [35] Martín David, Carlos Ocampo-Martínez, Ricardo Sánchez-Peña,
Advances in alkaline water electrolyzers: A review,
Journal of Energy Storage,

Bibliographic References

- [38] Snehasish Dash, and all others, Advances in green hydrogen production through alkaline water electrolysis: A comprehensive review, International Journal of Hydrogen Energy,
- [39] Wong SY, Li J. Enhancing efficiency in photovoltaic hydrogen production: A comparative analysis of MPPT and electrolysis control strategies. *MethodsX*. 2025 Feb 13;14:103220. doi: 10.1016/j.mex.2025.103220. PMID: 40093574; PMCID: PMC11910353.
- [40] V. Fulmali, S. Gupta and M. F. Khan, "Modeling and simulation of boost converter for solar-PV energy system to enhance its output," 2015 International Conference on Computer, Communication and Control
- [41] Saravanan, S. and Ramesh Babu, N. (2017) A Modified High Step-Up Non-Isolated DC-DC Converter for PV Application. *Journal of Applied Research and Technology*, 15, 242-249. <https://doi.org/10.1016/j.jart.2016.12.008>
- [42] Hayat, A.; Sibtain, and all others. Design and Analysis of Input Capacitor in DC–DC Boost Converter for Photovoltaic-Based Systems. *Sustainability* 2023, 15, 6321. <https://doi.org/10.3390/su15076321>
- [43] E. Figueres, G. Garcera, J. Sandia, F. Gonzalez-Espin, and J. C. Rubio, "Sensitivity study of the dynamics of three-phase photovoltaic inverters with an LCL grid filter," *IEEE Trans. Ind. Electron.*, vol. 56, no. 3, pp. 706–717, Mar. 2009.
- [44] <https://fr.mathworks.com/discovery/mppt-algorithm.html>
- [45] M. G. Villalva and E. R. F., "Analysis and simulation of the P&O MPPT algorithm using a linearized PV array model," 2009 35th Annual Conference of IEEE Industrial Electronics, Porto, Portugal, 2009,
- [46] A.Z. Arsad, A.W. Mahmood Zuhdi, A.D. Azhar, C.F. Chau, A. Ghazali, Advancements in maximum power point tracking for solar charge controllers, *Renewable and Sustainable Energy Reviews*,
- [47] <https://www.mathworks.com/help/sps/ug/solar-pv-system-maximum-power-point-tracking-using-boost-converter.html>
- [48] <https://www.mathworks.com/matlabcentral/fileexchange/39641-perturb-and-observe-p-o-algorithm-for-pv-mppt>
- [49] MDPI and ACS Style
Yodwong, B.; Guilbert, D.; Phattanasak, M.; Kaewmanee, W.; Hinaje, M.; Vitale, G. Faraday's Efficiency Modeling of a Proton Exchange Membrane Electrolyzer Based on Experimental Data. *Energies* 2020, 13, 4792. <https://doi.org/10.3390/en13184792>
- [50] Sushmita Sarkar, K. Uma Rao, Prema V., M.S. Bhaskar, Sanjeevikumar Padmanaban, Jayanth Bhargav, A model for effect of partial shading on PV panels with experimental validation, *Energy Reports*,
- [51] MDPI and ACS Style
Raza, M.A.; Zahra, S.; Raza, S.; Altimania, M.R.; Hassan, M.; Munir, H.M.; Zaitsev, I.; Kuchanskyy, V. Mitigating the Impact of Partial Shading Conditions on Photovoltaic Arrays Through Modified Bridge-Linked Configuration. *Sustainability* 2025, 17, 1263. <https://doi.org/10.3390/su17031263>
- [52] <https://www.mathworks.com/help/sps/ug/partial-shading-of-a-pv-module.html>
- [53] Alsadi, Samer. (2013). Partial Shading of PV System Simulation with Experimental Results. *Smart Grid and Renewable Energy*. 4.
- [54] X.-S. Yang; S. Deb (December 2009). Cuckoo search via Lévy flights. *World Congress on Nature & Biologically Inspired Computing (NaBIC 2009)*. IEEE Publications. pp. 210–214. arXiv:1003.1594v1.
- [55] R.V. Rao, V.J. Savsani, D.P. Vakharia, Teaching–learning-based optimization: A novel method for constrained mechanical design optimization problems, *Computer-Aided Design*,

Bibliographic References

- [56] D. Qu, S. Liu, D. Zhang, J. Wang and C. Gao, "Teaching-Learning Based Optimization Algorithm Based on Course by Course Improvement," 2015 11th International Conference on Computational Intelligence and Security (CIS), Shenzhen, China, 2015, pp. 48-52, doi: 10.1109/CIS.2015.20.
- [57] C. González-Castaño, C. Restrepo, S. Kouro and J. Rodriguez, "MPPT Algorithm Based on Artificial Bee Colony for PV System," in IEEE Access, vol. 9, pp. 43121-43133, 2021, doi: 10.1109/ACCESS.2021.3066281.
- [58] Karaboğa, Derviş (2005). "An Idea Based on Honey Bee Swarm For Numerical Optimization". S2CID 8215393. `{{cite journal}}: Cite journal requires |journal= (help)`

Figures:

- [1] <https://www.greenh2world.com/post/unleashing-clean-energy-the-alkaline-electrolyzer-revolution>
- [2] <https://www.linkedin.com/pulse/pem-proton-exchange-membrane-water-electrolysis-technology-guo-3ifhe>
- [3] <file:///C:/Users/GS%20STORE/Downloads/NMEOffprintfinal1.pdf>
- [4] https://www.researchgate.net/publication/304989151_Comparision_of_'perturb_observe'_and_'incremental_conductance'_maximum_power_point_tracking_algorithms_on_real_environmental_conditions
- [5] <https://www.scirp.org/journal/paperinformation?paperid=117510>
- [6] https://www.researchgate.net/publication/344363926_ANNBased_MPPT_Algorithm_for_Photovoltaic_Systems
- [7] https://www.researchgate.net/figure/e-The-rule-base-of-the-FLC-Change-in-PV-power-dP-dt_tbl1_315440501
- [8] https://en.wikipedia.org/wiki/Alkaline_water_electrolysis
- [9] https://www.researchgate.net/figure/P-V-curve-of-Conventional-P-O-MPPT_fig1_336012600
- [10] <https://www.nature.com/articles/s41598-023-46165-1>
- [11] <https://www.alternative-energy-tutorials.com/photovoltaics/bypass-diode.html>
- [12] https://www.researchgate.net/figure/The-multiple-peaks-effects-of-the-GMPP-a-I-V-and-b-P-V-curves-due-to-the-partial_fig2_349946903
- [13] https://www.researchgate.net/figure/Simulation-of-I-V-Curves-for-addition-of-shaded-PV-cells_fig7_324238205
- [14] <https://transpireonline.blog/2019/07/23/cuckoos-search-algorithm-to-solve-structural-optimization-problem/>
- [15] https://link.springer.com/chapter/10.1007/978-3-319-96002-9_8
- [16] https://www.researchgate.net/figure/Flowchart-for-the-TLBO-algorithm-Rao-et-al-2011_fig3_319943794
- [17] https://link.springer.com/chapter/10.1007/978-981-19-5403-0_25
- [18] <https://transpireonline.blog/2019/08/02/artificial-bee-colony-abc-algorithm-a-novel-method-motivated-from-the-behavior-of-bees-for-optimal-solution/>

تُعدّ الطاقة الشمسية خيارًا استراتيجيًا في مسار التحول نحو الطاقات المتجددة، خاصة في مجال إنتاج الهيدروجين الأخضر عبر التحليل الكهربائي. غير أن تحقيق مردودية عالية يتطلب إدارة فعالة للطاقة المولدة من الأنظمة الكهروضوئية، لاسيما عند تغذية محلل كهربائي مباشر. تهدف هذه الدراسة إلى تحسين أداء نظام كهروضوئي-محلل كهربائي من خلال تطبيق خوارزميات متقدمة لتتبع نقطة القدرة العظمى (MPPT). وقد تم نمذجة النظام بالكامل باستخدام بيئة MATLAB/Simulink، حيث يشمل المصفوفة الكهروضوئية، محول رافع للجهد، ومجموعة من خوارزميات (MPPT مثل P&O، Cuckoo Search، و FDB-TLABC، إلى جانب محلل كهربائي قلوي. وتم تقييم أداء النظام من خلال معدلات إنتاج الهيدروجين (nH_2) والأكسجين (nO_2) باعتبارها مؤشرات مباشرة على كفاءة التتبع والتحويل الطاقوي. أظهرت النتائج أن الخوارزميات التقليدية (مثل P&O و Incremental Conductance) تؤدي أداءً مقبولاً في ظروف الإشعاع الطبيعي، بينما تفوقت الخوارزميات الذكية (ك Cuckoo Search و FDB-TLABC) بشكل ملحوظ عند حدوث التظليل الجزئي، حيث ساهمت في تقليل الفاقد الطاقوي وتجاوز مشكلة الوقوع في نقاط عظمى محلية. تبرز هذه النتائج الأهمية البالغة لاختيار الخوارزمية المناسبة لضمان استقرار وكفاءة إنتاج الهيدروجين، خاصة في البيئات التي تعرف تذبذباً في الإشعاع الشمسي. وتقدم هذه الدراسة إطاراً عملياً موثقاً لتصميم أنظمة كهروضوئية متكاملة مع التحليل الكهربائي، تحقق التوازن بين تحسين استخلاص الطاقة الشمسية وتعزيز الأداء الكهروكيميائي.

الكلمات المفتاحية: الهيدروجين الأخضر، نظام كهروضوئي-محلل كهربائي، خوارزميات MPPT، التظليل الجزئي، MATLAB/Simulink، التحليل الكهربائي القلوي، Cuckoo Search، FDB-TLABC.

Abstract:

Green hydrogen production via photovoltaic (PV) systems represents a promising pathway toward sustainable energy. Maximizing the efficiency of such systems relies heavily on effective integration and control strategies, particularly under variable environmental conditions. This study presents an in-depth investigation into the optimization of a PV-powered alkaline electrolyzer using advanced Maximum Power Point Tracking (MPPT) algorithms. The system—comprising a PV array, boost converter, and various MPPT controllers (Perturb and Observe, Cuckoo Search, and FDB-TLABC)—was modeled and simulated in MATLAB/Simulink. Hydrogen (nH_2) and oxygen (nO_2) production rates were employed as key performance indicators of the electrolyzer, directly influenced by the stability and accuracy of power point tracking. Under standard irradiance, conventional MPPT methods (P&O, Incremental Conductance) demonstrated consistent operation. However, under partial shading conditions, intelligent optimization techniques such as Cuckoo Search and FDB-TLABC significantly outperformed traditional algorithms by effectively mitigating power losses and avoiding local maxima. These findings underscore the crucial role of algorithm selection in ensuring stable and efficient hydrogen production, particularly in scenarios characterized by intermittent solar irradiance. This work contributes a validated framework for the

Abstract

development of resilient and high-performance PV-electrolyzer systems, highlighting the interplay between solar energy optimization and electrochemical efficiency.

Keywords: green hydrogen, PV-electrolyzer system, MPPT algorithms, partial shading, MATLAB/Simulink, alkaline electrolysis, Cuckoo Search, FDB-TLABC.

Résumé :

La production d'hydrogène vert à partir de l'énergie solaire représente une solution stratégique dans le contexte de la transition énergétique. Pour en tirer un rendement optimal, il est essentiel d'assurer une gestion intelligente de l'énergie générée par les systèmes photovoltaïques (PV), en particulier lorsque ceux-ci alimentent directement un électrolyseur. Cette étude se concentre sur l'optimisation d'un système PV-électrolyseur en recourant à des algorithmes avancés de suivi du point de puissance maximale (MPPT). Le système étudié, modélisé sous MATLAB/Simulink, comprend un générateur PV, un convertisseur élévateur de tension, plusieurs algorithmes MPPT (Perturb & Observe, Cuckoo Search, FDB-TLABC), ainsi qu'un électrolyseur alcalin. Les performances du système ont été évaluées à travers les débits de production d'hydrogène (nH_2) et d'oxygène (nO_2), étroitement liés à la qualité du suivi énergétique. En conditions normales d'ensoleillement, les algorithmes classiques (P&O, Conductance Incrémentale) offrent une efficacité satisfaisante. Toutefois, en présence d'ombrages partiels, les méthodes intelligentes comme Cuckoo Search et FDB-TLABC s'avèrent plus robustes, permettant de minimiser les pertes de puissance et d'éviter les erreurs de convergence vers des maxima locaux. Ces résultats mettent en évidence l'impact déterminant du choix de l'algorithme MPPT sur la stabilité et l'efficacité de la production d'hydrogène, notamment dans des contextes climatiques à irradiance variable. L'étude propose ainsi un cadre de conception fiable pour les systèmes solaires dédiés à la production d'hydrogène, en valorisant l'interaction entre optimisation photovoltaïque et performance électrochimique.

Mots-clés : hydrogène vert, système photovoltaïque-électrolyseur, algorithmes MPPT, ombrage partiel, modélisation MATLAB/Simulink, électrolyse alcalin, Cuckoo Search, FDB-TLABC.

The Annexes:

The po algorithm MATLAB function script

```
1 function D = fcn(vpv,ipv)
2
3 Dinit=0.4;
4 Dmax=0.9;
5 Dmin=0.1;
6 deltaD=20e-6
7
8 persistent Vold Pold Dold;
9
10 dataType="double";
11
12 if isempty(Vold)
13     Vold=0;
14     Pold=0;
15     Dold=Dinit;
16 end
17
18 P=vpv*ipv;
19 dV=vpv-Vold;
20 dP=P-Pold;
21
22 if dP~=0
23     if dP<0
24         if dV<0
25             D=Dold-deltaD;
26         else
27             D=Dold+deltaD;
28         end
29     else
30         if dV<0
31             D=Dold+deltaD;
32         else
33             D=Dold-deltaD;
34         end
35     end
36 else D=Dold;
37 end
38 if D>=Dmax || D<=Dmin
39     D=Dold;
40 end
41
42 Dold=D;
43 Vold=vpv;
44 Pold=P;
```

The cuckoo search algorithm matlab function script

```

1  function D = Cuckoo(Vpv,Ipv)
2  %#codegen
3  persistent u;
4  persistent dcurrent;
5  persistent p;
6  persistent dc;
7  persistent dbest;
8  persistent counter;
9  persistent iworst;
10 persistent discover;
11 if isempty(discover)
12     discover=0;
13 end
14 if isempty(counter)
15     counter=0;
16 end
17 if isempty(dcurrent)
18     dcurrent=0.5;
19 end
20 if isempty(iworst)
21     iworst=0;
22 end
23
24
25
26 if isempty(dbest)
27     dbest=0;
28 end
29 if isempty(p)
30     p=zeros(4,1);
31 end
32 if isempty(u)
33     u=0;
34 end
35 if isempty(dc)
36     dc=zeros(4,1);
37     dc(1)=0;
38     dc(2)=0.3;
39     dc(3)=0.5;
40     dc(4)=0.9;
41 end
42 if counter>=1 && counter<150)
43     D=dcurrent;
44     counter=counter+1;
45     return;
46 end
47 counter=0;
48
49 if u>=1 && u<=4)
50     p(u)=Vpv*Ipv;
51 end
52 u=u+1;
53 if(u==7)
54     u=1;
55 end
56 if(u==1)
57     D=dc(u);
58     dcurrent=D;
59     counter=1;
60     return;
61 elseif(u==2)
62     D=dc(u);
63     dcurrent=D;
64     counter=1;
65     return;
66 elseif(u==3)
67     D=dc(u);
68     dcurrent=D;
69     counter=1;
70     return;
71 elseif(u==4)
72     D=dc(u);
73     dcurrent=D;
74     counter=1;
75     return;
76 elseif(u==5 || u==6 )
77     if(u==5)
78         if(rand(1)>0.25)
79             discover=1;
80             [m,i]=max(p)
81             dbest=dc(i);
82             %determine the worst nest
83             [m,iworst]=min(p);
84             %build new nest
85             %dc(iworst)=dbest;
86             dc(iworst)=levyflight(dbest,dc(iworst));
87             %dc(iworst)=withinlimits(dc(iworst));
88             D=dc(iworst);
89             dcurrent=D;
90             counter=1;
91             return;
92         else
93             u=u+1;
94             [m,i]=max(p)
95             dbest=dc(i);
96             D=dbest;
97             dcurrent=D;
98             counter=1;
99             dc(1)=levyflight(dbest,dc(1))
100            % dc(1)=withinlimits(dc(1))

```

```

100         % dc(1)=withinlimits(dc(1))
101         dc(2)=levyflight(dbest,dc(2))
102         %dc(2)=withinlimits(dc(2))
103         dc(3)=levyflight(dbest,dc(3))
104         % dc(3)=withinlimits(dc(3))
105         dc(4)=levyflight(dbest,dc(4))
106         % dc(4)=withinlimits(dc(4))
107         return;
108     end
109
110     else
111         %calculate new power of new nest
112         p(iworst)=Vpv*Ipv;
113         %determine the best nest
114         [m,i]=max(p);
115         dbest=dc(i);
116         D=dbest;
117         dcurrent=D;
118         counter=1;
119
120         dc(1)=levyflight(dbest,dc(1))
121         % dc(1)=withinlimits(dc(1))
122         dc(2)=levyflight(dbest,dc(2))
123         %dc(2)=withinlimits(dc(2))
124         dc(3)=levyflight(dbest,dc(3))
125         % dc(3)=withinlimits(dc(3))
126         dc(4)=levyflight(dbest,dc(4))
127         % dc(4)=withinlimits(dc(4))
128         discover=0;
129         return;
130     end
131
132     else
133         u
134         y='hello'
135         D=0.1
136
137     end
138
139
140 end
141 function dfinal=levyflight(dbest,d)
142 beta=3/2;
143 kcoeff=0.8;
144 sigmau=(gamma(1+beta)*sin(pi*beta/2)/(gamma((1+beta)/2)*beta*2^((beta-1)/2)))^(1/beta);
145 sigmav=1;
146 u=normrnd(0,(sigmau)^2);
147 v=normrnd(0,(sigmav)^2);
148 dup=d+(kcoeff*(abs(u)/((abs(v))^(1/beta)))*(dbest-d));

```

The FDB-TLABC algorithm matlab function script

```

1  function duty_cycle = fdb_tlabc_pv_mppt(pv_voltage, pv_current)
2  % FDB_TLABC
3
4  persistent X val_X trial FES gbest val_gbest
5
6  % constants
7  popsize = 8;      % population size
8  maxFES = 220;    % maximum number of function evaluations (FES)
9  limit = 6;       % abandonment limit
10 CR = 0.9;        % crossover rate
11
12 % initialize persistent variables
13 if isempty(X)
14     X = 0.65 + 0.15*rand(popsize, 1);
15     val_X = zeros(popsize, 1);
16     trial = zeros(popsize, 1);
17     FES = 0;
18
19     % initial evaluation
20     for i = 1:popsize
21         val_X(i) = -pv_voltage*pv_current;
22     end
23     [val_gbest, idx] = min(val_X);
24     gbest = X(idx);
25 end
26
27 % teaching based employed bee phase
28 for i = 1:popsize
29     [~, sortIdx] = sort(val_X);
30     teacher = X(sortIdx(1));
31     mean_X = mean(X);
32     TF = 1 + rand();
33     Xi = X(i) + 0.5*(teacher - TF*mean_X)*rand();
34     % diversity learning
35     r = generateR(popsize, i);
36     F = 0.5 + 0.5*rand();
37     V = X(r(1)) + F*(X(r(2)) - X(r(3)));
38     if rand() < CR
39         Xi = 0.5*Xi + 0.5*V;
40     end
41
42     Xi = max(0.1, min(0.9, Xi));
43     new_power = pv_voltage*pv_current;
44     val_Xi = -new_power;
45     FES = FES + 1;
46
47     if val_Xi < val_X(i)
48         val_X(i) = val_Xi;
49         X(i) = Xi;
50         trial(i) = 0;

```

Annexes

```
50         trial(i) = 0;
51     else
52         trial(i) = trial(i) + 1;
53     end
54 end
55
56 % learning based onlooker bee phase
57 Fitness = calculateFitness(val_X);
58 for K = 1:popsize
59     i = roulettewheel(Fitness);
60     j = randi(popsize);
61     while j == i, j = randi(popsize); end
62
63     if val_X(i) < val_X(j)
64         Xi = X(i) + rand()*(X(i)-X(j));
65     else
66         Xi = X(i) + rand()*(X(j)-X(i));
67     end
68
69     Xi = max(0.1, min(0.9, Xi));
70     new_power = pv_voltage*pv_current;
71     val_Xi = -new_power;
72     FES = FES + 1;
73
74     if val_Xi < val_X(i)
75         val_X(i) = val_Xi;
76         X(i) = Xi;
77     end
78 end
79
80 % scout bee phase
81 [max_trial, idx] = max(trial);
82 if max_trial > limit
83     X(idx) = 0.65 + 0.15*rand();
84     val_X(idx) = -pv_voltage*pv_current;
85     trial(idx) = 0;
86 end
87
88 % update the global best
89 [current_min, idx] = min(val_X);
90 if current_min < val_gbest
91     val_gbest = current_min;
92     gbest = X(idx);
93 end
94
95 duty_cycle = gbest;
96 end
97
98 %% fitness distance balance help ..
99
100 r1 = randi(popsize);
101 while r1 == i, r1 = randi(popsize); end
102 r2 = randi(popsize);
103 while r2 == r1 || r2 == i, r2 = randi(popsize); end
104 r3 = randi(popsize);
105 while r3 == r2 || r3 == r1 || r3 == i, r3 = randi(popsize); end
106 r = [r1 r2 r3];
107 end
108
109 function fFitness = calculateFitness(fObjV)
110 fFitness = 1./(1 + abs(fObjV));
111 fFitness = fFitness/sum(fFitness);
112 end
113
114 function index = roulettewheel(Fitness)
115 cumFitness = cumsum(Fitness);
116 r = rand()* cumFitness(end);
117 index = find(r <= cumFitness, 1);
118 end
```

The First National Conference on Renewable Energies and Advanced

Electrical Engineering (NC REAEE'25)

May 06-07th, 2025

University of M'Sila

Faculty of Technology

Electrical Engineering Laboratory (LGE)



CERTIFICATE OF PARTICIPATION

This Certificate is Awarded to:

chebli saber ayoub

for presenting a paper entitled: **Optimization of green hydrogen production using MPPT algorithms**

Authors: ***chebli saber ayoub , djaidja nazih , Zemmit Abderrahim***

at the First National Conference on Renewable Energies and Advanced Electrical Engineering (NC-REAEE'25),
held at M'Sila University- Algeria, on May 6-7th 2025.

Paper ID: 171



Conference Chair
Dr. Abderrahim ZEMMIT

